MONITORING AND ASSESSMENT OF THE 2010-2011 GRAVEL/COBBLE AUGMENTATION IN THE ENGLEBRIGHT DAM REACH OF THE LOWER YUBA RIVER, CA

(photo of a self-formed emergent gravel bar downstream of the gravel injection site)

Prepared for:
U.S. Army Corps of Engineers
Sacramento District
Englebright/Marlis Creek Lakes
PO Box 6
1296 Englebright Dam Road
Smartsville, CA 95977

Prepared by:
Rocko A. Brown, MS, EIT
Gregory B. Pasternack, PhD, AM. ASCE
University of California, Davis

December 15, 2012

Abstract

The USACE injected ~5,000 short tons of gravel and cobble into the Englebright Dam Reach of the lower Yuba River just downstream of the Narrows 1 powerhouse November 2010 to January 2011. The purpose of this study was to evaluate the status of the EDR and the efficacy of past gravel injections into the EDR with regard to making progress toward meeting the geomorphic and ecological goals stated in the GAIP. Gravel sluicing proved to be an effective and safe method of gravel addition and is recommended for continued use, with new enhancements made as opportunities arise. During and after injection was completed, there were several overbank floods including one that lasted for a month. Topographic change detection revealed that most sediment left the small injection zone, but all measurable amounts of sediment stayed within the reach. A myriad of topographic features were responsible for scale dependent sediment deposition and these mechanisms were investigated in detail in this study. Although a lot of sediment deposited as a blanket-fill down the reach, there were some notable alluvial landforms that were present when floods receded. Some of these landforms had the correct hydraulics to yield suitable Chinook spawning habitat. In Fall 2011, Chinook spawners heavily utilized these habitat patches and it was evident that more gravel addition will be able to create more usable habitat. Overall, gravel/cobble injection by gravel sluicing is working in that the sediment is getting added to the channel, it is moving downstream and creating landforms in the river, it is staying in the canyon for now (helping to reduce the sediment deficit), the hydraulics over the created landforms includes medium and high quality habitat that is preferred for spawning more than random likelihood, and Chinook spawners are making use of that habitat. Annual gravel/cobble addition should continue as permitted and the interim outcomes monitored until the sediment deficit is eradicated. At that point, the long-term plan in the GAIP should commence.

Citation: Brown, R.A. and Pasternack, G.B. 2012. Monitoring and assessment of the 2010-2011 gravel/cobble augmentation in the Englebright Dam Reach of the lower Yuba River, CA. Prepared for the U.S. Army Corps of Engineers, Sacramento District. University of California at Davis, Davis, CA.

Study Questions and Answers

- Q: Did the USACE add gravel and cobble to the lower Yuba River?
    - A: Yes. They added ~5,000 short tons just downstream of the Narrows 1 powerhouse in the bedrock canyon of the lower Yuba River in November 2010 to January 2011.
- Q: What was the method of gravel addition and were there any environmental impacts?
    - Sediment was trucked to the hilltop above Englebright Dam where a frontloader scooped it up and poured it into a hopper that blended it with water pumped from Englebright Lake and sluiced it down to the road and hillside to the river below. At the river end, a crew controlled how and where the sediment entered the river. Because the rate of addition was so slow and the ambient discharge so high, there was no significant water quality impact. In addition, because no heavy equipment was operated near the river, there was no chance for oil and gas spills or road-related impacts. Apart from some gravel/cobble left along the side of the road, there was no persistent impact from the gravel injection.
- Do you recommend this method be used in the future at this location?
    - Yes. The method is slower than others, but it worked and it was safe and harmless to the environment compared with other methods.
- Are there limitations to meeting the GAIP in using this method?
    - The size distribution of injected sediment is somewhat limited by the size of pipe used. At present, no particles > 5" (127 mm) may be added, due to the screen on the hopper.
- Do you recommend continued use of the sediment size distribution specified in the Gravel Augmentation Injection Plan (GAIP)?
    - No. That was based on early concepts drawn from the Stanislas River and by now there exists substantial evidence from the lower Yuba River demonstrating that a coarser mix is needed from both geomorphic and ecological perspectives. A new mix specific for this river was developed several and reviewed by stakeholders, including regulatory agencies

(USFWS, CDFG, and NMFS). Testing with the new mix in future projects will enable further evaluation of mix design.

- The Gravel Augmentation Implementation Plan has three geomorphic goals, how did the project perform relative to those goals?
  - o The first goal was to increase the cobble/gravel storage in the reach. That goal was met: ~8% of the minimum gravel deficit was filled. Despite multiple floods, all of the sediment injected into the river stayed in the reach.
  - o The second goal was to allow for downstream transport and deposition. That goal was met: most of the sediment was transported downstream of the small injection zone and it all deposited in the reach.
  - o The third goal was to provide morphologic unit diversity. Although the amount added was small, commensurately sized alluvial landforms were created by the deposits. See the photo on the cover of the report for an example. It is expected that it will take substantially more filling of the sediment deficit before large landforms will form.
- The Gravel Augmentation Implementation Plan has three ecological goals, how did the project perform relative to those goals?
  - o The first goal was to increase the quantity of high-quality habitat for spawning adult spring-run Chinook salmon. That goal was met. Although the amount of sediment added was small and it was eroded out of the injection zone, it did move downstream and create some high quality habitat that was utilized by Chinook spawners.
  - o The second goal was to provide adult and juvenile refugia in close proximity to spawning habitat. That goal was met. Analysis revealed an abundance of these habitat types within 10 m of the observed redds. Although not part of this study, subsequent RMT snorkel surveys observed juveniles using rearing habitat in the EDR.
  - o The third goal was to provide morphological diversity to support ecological diversity within the study reach. That goal was met, though the size and abundance of alluvial landforms remains small, commensurate with the small fraction of the total sediment deficit that was met by the injection.

- Based on the results so far, how much sediment do you recommend be injected annually?
    - The project is still in an early phase of rapid learning and adaptation. Several enhancements to the system and to the gravel mix are planned for the next project. It is necessary to determine how all the enhancements function to determine the final efficiency of the system with best practices.
    - Regulators will likely have to allow a longer period of injection than the common July and August window, and as demonstrated in 2010-2011, there is no reason why gravel can't be added to the bedrock/shotrock injection zone any time that site is devoid of previously injected gravel/cobble.

Acknowledgements

Table of Contents

List of Tables

List of Figures

1.0   Introduction

1.1.   Environmental Problem

Englebright Dam on the Yuba River blocks anadromous fish migration into the upper watershed, which has impacted the potential size of the spring-run Chinook salmon meta-population in the Sacramento River watershed, of which the Yuba is a major contributing subbasin. A substantial amount of the annual spring-run Chinook salmon individuals immigrating into the Yuba River each year attempt to spawn in September in the uppermost reach below the dam, which is also the most impacted and presently unsuitable for Chinook salmon reproduction. This reach, called the Englebright Dam Reach (EDR), was decimated by cumulative effects associated with (1) local mechanized channel disturbance by gold miners, (2) overabundance of large angular rock from dam construction and landsliding, and (3) a lack of river-rounded gravel/cobble supply (Pasternack et a., 2010). The last of those is a result of the sediment supply from upstream being ruined by hydraulic gold mining, which necessitated that Englebright Dam be built to hold back the excessive waste that is well mixed with the small beneficial fraction of gravel/cobble. In 2011, non-governmental organization plaintiffs suing the National Marine Fisheries Service et al. gave expert testimony in which they stated that spring-run Chinook salmon in the Yuba River face "irreparable injury" if measures are not taken right away to address problems in the EDR. Further, in the NMFS 2012 Biological Opinion, NMFS wrote that the "lack of spawning substrate limits spawning habitat and fish production." Note the use of the word "limits"- not that the lack of substrates is one of many stressors, but is the *limit* on habitat and fish production. NMFS went on to say that, "Lack of adequate spawning substrate presents a high risk to salmonids." As a result, there is a consensus among diverse stakeholders and experts that the most important need for sustaining and potentially recovering spring-run Chinook salmon abundance below the dam involves addressing the geomorphic deficiencies in the EDR reach.

The scientific foundations for understanding the hydrogeomorphology of the lower Yuba River have been laid out as well as any river in the region thus far in numerous scientific technical reports and journal articles (Gilbert, 1917; Pasternack, 2008a; James et al., 2009; Pasternack et al.; 2010; Sawyer et al., 2010; Escobar and Pasternack, 2010; White et al., 2010), culminating in a YCWA relicensing existing-information report on the (Pasternack, 2010b) and a review in the GAIP (Pasternack, 2010a). Meanwhile, the Yuba Accord River Management Team has nearly completed comprehensive suite of geomorphic studies for the entire LYR as part of its Monitoring and Evaluation Plan (YARMT, 2009), including associated reports addressing 2D hydrodynamic modeling (Barker et al., submitted; Abu-Aly et al., in prep), analysis of fluvial landforms (Wyrick

and Pasternack, 2011, 2012), and analysis of geomorphic change (Carley et al., submitted). Therefore, this study has a highly focused purpose to use and build on existing knowledge to facilitate science-based, transparent river rehabilitation in the EDR, which is where the dam's blockage of the gravel/cobble supply impacts the river (Pasternack, 2008a).

1.2. USACE Program to Address Problem

The United States Army Corps of Engineers (USACE) has been injecting a mixture of coarse sediment in the gravel (2-64 mm) and cobble (64-256 mm) size range into the lower Yuba River (LYR) below Englebright Dam, with an emphasis on fine gravel. The first effort occurred in November 2007 and consisted of ~500 short tons of gravel/cobble sediment being injected into the Narrows II powerhouse pool. The second effort occurred November 2010 through January 2011 and consisted of ~5000 short tons of gravel/cobble sediment being injected into the chute just downstream of the Narrows I powerhouse. Future gravel injections are anticipated as part of a long-term gravel augmentation program to mitigate negative impacts of Englebright Dam on the lower Yuba River.

The Gravel/Cobble Augmentation Implementation Plan for the Englebright Dam Reach (EDR) of the Lower Yuba River, CA (GAIP) describes present and proposed future efforts based on the data and information available at the time (Pasternack, 2010a). In brief, the long-term plan calls for continuing gravel/cobble injection into the EDR until the estimated coarse sediment storage deficit for the reach is eradicated, and then it calls for subsequent injections as needed to maintain the EDR sediment storage volume in the event that floods export material downstream of the reach. Monitoring is required to keep track of the sediment budget for the reach to know injections are needed and how much to add. Monitoring will also assess ecological outcomes.

Although the GAIP promotes a necessarily long-term effort to recover and sustain alluvial landforms and ecological functionality in the EDR, it does call for each year's gravel injection to try to yield a temporary riffle of value for spring-run Chinook spawning and embryo incubation in the subsequent autumn and winter. Figure 5.3 in the GAIP illustrates simple riffle design concepts for the temporary riffle to be built during gravel injection. In the upper section of EDR where the gravel is injected, the canyon is narrow and scour risk during floods is high. Pasternack (2008) reported that in the most constricted location upstream of the 2010-2011 injection point, a state of "partial transport" in which overrepresented finer gravels are scoured disproportionately begins at ~10,000cfs and full mobility of the riverbed begins at ~25,000 cfs (see figure 108 of Pasternack, 2008). Therefore, when the flows in the period

between gravel injection and Chinook spawning remain below ~10,000 cfs alluvial landforms built during injection will remain intact and usable for spawning.). Take note that these estimates and conclusions were based on an assumed coarser mixture than what the USACE subsequently injected. *Having such intact features at the injection site is not a primary goal of the GAIP*, as the sustainable alluvial deposition sites are further downstream in EDR where the river widens substantially (see Figure 122 of Pasternack, 2008). The GAIP makes this clear when it says:

> "If the gravel introduced in the first year washes downstream consistent with design objective #5, then that is fine, as the eroded material would still be serving the primary plan goal (design objective 1). Future injections would use the next amount of material purchased to rebuild as much of Area A, then Area B, and then Area C as possible. It is possible that frequent floods could preclude the complete design concept from ever being achieved, and that is an acceptable outcome consistent with the overall goals of the plan and the specific design objectives."

As a result, there is extra value possible when the river's hydrologic regime enables temporary riffle stability, but it is not an expectation or requirement.

To assess the outcome of each year's project and progress toward the long-term goal, the GAIP includes a formal experimental design with design objectives, hypotheses, methods, and tests (

Table 1). Following through on this experiment requires science-based monitoring and evaluation of the fate of previous injections. Notably, the initial injections are the first building blocks for ecological recovery in the reach, and the response to sequential injections is not expected to be linear (e.g Elkins et al., 2007). The outcome of hypothesis testing at incremental stages throughout the recovery of a normal volume of sediment storage will foster a better understanding of the linked physical-biological functionality of the reach, thereby enabling further improvement of the GAIP, including identification and development of potentially more detailed rehabilitation activities related to Englebright Dam impacts and the impacts of mechanized gold mining in the same reach.

2.0   Goals and Objectives

The overall goal of this report is to evaluate the status of the EDR and the efficacy of past gravel injections into the EDR with regard to making progress toward meeting the geomorphic and ecological goals stated in the GAIP. The GAIP says that the geomorphic goal of gravel/cobble augmentation is to reinstate interdecadal, sustainable sediment transport downstream of a dam during floods, which is necessary to support and maintain diverse morphological units, such as riffles, pools, point bars, and backwaters. It says that the ecological goal of gravel/cobble augmentation that yields self sustainable morphological units is to have the associated assemblages of physical attributes that are preferred for each of the freshwater life stages of salmonids. To achieve these goals, it lays out a long-term plan of gravel/cobble re-introduction and monitoring to track outcomes.

2.1.   GAIP Hypothesis Testing

The GAIP includes five specific design objectives to facilitate achieving these goals), and for each one there is a specific, transparent test that can answer whether (or to what degree) the injection projects are achieving the design objectives. Therefore, the specific objectives of this monitoring and evaluation project involve performing the tests stated in the GAIP and writing a report explaining the outcome.

Table 1. GAIP Study Hypotheses and Tests

Design objective	Design hypothesis	Approach	Test
1. Restore gravel/cobble storage	1A. Total sediment storage should be at least half of the volume of the wetted channel at a typical base flow under a heavily degraded state (Pasternack, 2008b).	Inject gravel into the river to fill up recommended volume of sediment storage space.	Use DEM differencing of bed topography over time to track changes in storage
2. Provide higher quantity of preferred-quality Chinook spawning habitat	2A. SRCS require deep, loose, river-rounded gravel/cobble for spawning (Kondolf, 2000).	Add river-rounded gravel/cobble.	Perform Wolman pebble counts of the delivered sediment stockpile and in the river after each gravel injection to insure that the mixture's distribution is in the required range.
	2B. Spawning habitat should be provided that is as close to GHSI-defined high-quality habitat as possible (Wheaton et al., 2004b)	Place and contour gravel to yield depths and velocities consistent with salmon spawning microhabitat suitability curves.	Measure and/or simulate the spatial pattern of GHSI after project construction to determine quantity of preferred-quality (GHSI>0.4) habitat present.
3. Provide adult and juvenile refugia in close proximity to spawning habitat.	3A. Structural refugia in close proximity to spawning habitat should provide resting zones for adult spawners and protection from predation and holding areas for juveniles.	Create spawning habitat in close (<10 m) proximity to pools, overhanging cover, bedrock outcrops, boulder complexes, and/or streamwood.	Measure distance from medium and high GHSI quality habitats to structural refugia and check to see that most spawning habitat is within reasonable proximity.
4. Provide morphological diversity to support ecological diversity, including behavoral choice by individuals.	4A. Designs should promote habitat heterogeneity to provide a mix of habitat patches that serve multiple species and lifestages.	Avoid GHSI optimization of excessively large contiguous areas of habitat; design for functional mosaic of geomorphic forms and habitat.	Large (>2 channel widths) patches of homogenized flow conditions in hydrodynamic model and homogenized habitat quality in GHSI model results should not be present at spawning flows.
5. Allow gravel/cobble to wash downstream	5A.Suitable mechanisms of riffle-pool maintenance are not present or realistically achievable in the upper section of the EDR	no specific action required	Conduct annual recon of EDR to track where injected gravel/cobble goes.
	5B. Flows that overtop Englebright Dam erode sediment off the placement area	no specific action required	Measure and/or simulate the spatial pattern of Shields stress and identify areas with values >0.06

2.1.1. GAIP Geomorphic Goals

Geomorphic goals for the GAIP include 1) increasing the cobble/gravel storage, 2) allowing for downstream transport and deposition, and 3) providing morphologic unit diversity. Depending on the size of any individual gravel injection and its timing in the progression of GAIP implementation, the third objective may not be suitable for interim evaluation. It is hypothesized that gravel/cobble storage will occur as both nested depositional features and through lateral and vertical bar growth when the supplied sediment is in excess of the spatially explicit transport capacity of specific locations in the river. Even as sediment storage increases in the reach, it is natural and expected

that over time added gravel/cobble will eventually migrate downstream out of the reach. The greater the storage, the greater likelihood that sediment will export and in higher quantity. This is an outcome of the general scientific principle of flux driven by concentration gradients (e.g analogous to Fick's, Fourier's, Darcy's, and Ohm's laws): the more of something there is in one area relative to another, the more of it will be in transport for any given flow condition.

Compared to the original conceptualization in Pasternack (2008), observations of the fate of the 2007 gravel injection have expanded the scope of sediment storage processes evident in EDR
). It is hypothesized that zones of sediment accumulation will fall into five categories tied to channel scale. First, at the smallest scale of bedrock fractures, small bedrock outcrops, individual boulders and large cobbles, it is hypothesized that selective deposition will occur as bedload in motion will get trapped by existing bed material larger than that in transport (Pasternack, 2009). This may account for a surprising amount of material, but it is impossible to quantify with modern technology. Second, at the hydraulic unit scale (10^{-1}-10^{0} channel widths) large bedrock outcrops and boulder clusters protrude into the flow creating obstructions that interrupt flow streamlines. Some amount of gravel and cobble cannot manage the deflection and end up trapped in the stagnation zone upstream of the obstruction. Third, these same features also create convective acceleration and flow convergence zones around them that focus and route sediment until it reaches an abrupt expansion eddy immediately downstream of the outcrop. Some of the gravel and cobble will get pushed and pulled into the eddy and deposit there. Fourth, morphologic unit scale (10^{0}-10^{1} channel widths) channel curvature can create positive feedbacks between the topographic steering of the flow field, secondary flow circulation, and inward (i.e. towards the origin of curvature) deposition due to variations in cross channel sediment competence and inward transport at the bed. Finally, as gravel accumulates locally and from curvature effects it is expected that valley scale ($>10^{1}$ channel widths) expansion zones will promote depositional features that may increase bed relief that can provide positive feedbacks with the prior scale dependent sediment deposition mechanisms mentioned earlier. These five mechanisms driven by different causes of topographic variation are the basis for the scientific expectation that gravel/cobble injected into the EDR will move downstream from the constricted injection zone and deposit within the reach.

Table 2. Scale dependent sediment storage mechanisms in the EDR.

Scale (Channel Widths)	Sediment Deposition Hypothesis	Dominant Topographic Elements	Detectable by TCD*?	Represented in 2D Model?
$<10^{-1}$	At the smallest scale of bedrock fractures, small bedrock outcrops, individual boulders and large cobbles, selective deposition will occur as bedload in motion will get trapped by existing bed material larger than that in transport.	Cobbles, small bedrock outcrops (<25 feet), boulders	No	No
10^{-1}-10^{0}	Large bedrock outcrops and boulder clusters protrude into the flow creating obstructions that create upstream backwater zones of preferential deposition.	Large bedrock outcrops (>25 feet), multiple boulders	Yes	Yes
10^{-1}-10^{0}	These same features also create convective acceleration and flow convergence zones around them that focus and route sediment until it reaches an abrupt expansion eddy immediately downstream of the outcrop where some of the gravel and cobble will get pushed and pulled into the eddy and deposit there.	Large bedrock outcrops (>25 feet), multiple boulders	Yes	Yes
10^{0}-10^{1}	Channel curvature can create positive feedbacks between the topographic steering of the flow field, secondary flow circulation, and inward (i.e. towards the origin of curvature) deposition due to variations in cross channel sediment competence and inward transport at the bed.	Gravel/Cobble Bars	Yes	Yes
$>10^{1}$	Finally, as gravel accumulates locally and from curvature effects it is expected that valley scale expansion zones will promote depositional features.	Valley scale curvature of reach	Yes	Yes

*TCD is topographic change detection.

2.1.2.   GAIP Ecological Goals

Ecological goals for the GAIP are to 1) increase the quantity of high-quality habitat for spawning adult spring-run Chinook salmon, 2) provide adult and juvenile refugia in close proximity to spawning habitat, and 3) provide morphological diversity to support ecological diversity within the study reach. On the basis of the explanation provided in section 1.2 above and depending on several factors (i.e. the size of any individual gravel injection, its timing relative to the timing of floods and that of the freshwater life stages of salmonids, and finally, its timing in the progression of GAIP implementation), these objectives may not be suitable for interim evaluation. To increase the quantity of high quality habitat for Chinook salmon, it is hypothesized that the augmented gravel riffle in the injection zone will be available as an ephemeral feature so long as flows are <

10,000 cfs and the median size of the injected material is ~60 mm. It is hypothesized that transported gravel/cobble will form spawning habitat downstream once there is sufficient deposition to yield suitable fluvial landforms. Similarly, it is hypothesized that self-formed spawning habitat will occur in close proximity to (e.g. < 10 m) structural refugia, such as deep pools, bedrock outcroppings, boulders, and large cobbles. These are common features of river canyons that the 2012 Biological Opinion also identifies as components of rearing habitat. To provide morphologic unit diversity it is hypothesized that floods will induce redistribution of injected gravel/cobble that will yield alluvial landforms at the scale of ~1-10 channel widths. These features in turn topographically steer in-channel flows to yield a diversity of micro- and meso-habitat conditions

2.2.   Iterative Learning and Improved Actions

The GAIP includes an initial, simple gravel placement design for the 2010-2011 project in an effort to obtain temporary riffle habitat, which is known to be the best morphological unit type for Chinook salmon spawning on the LYR (Pasternack, 2008a; Campos and Massa, 2011; Campos and Massa, 2012). However, there was high uncertainty about how gravel sluicing would perform in this setting and what its opportunities and limitations would be. Based on the experience in the 2010-2011 injection, most of those questions have been answered and it is now possible to develop project designs, design hypotheses, monitoring approaches, and long-term goals that are in line with the capabilities and limitations of gravel sluicing. With each subsequent project to meet the long-term goals of the GAIP, further lessons will arise and help guide future efforts.

3.0   2010-2011 EDR Gravel Augmentation Project

After the final environmental assessment for the 2010-2011 EDR gravel augmentation project was made public, the actual gravel/cobble injection began with gravel entering the river on November 19, 2010 and ended with the last gravel going in by January 17, 2011. It took a few days prior to that for the initial set up of the sluicing system according to the layout in the GAIP. During the first two weeks of injection additional safety measures and *ad hoc* system improvements were incrementally implemented to add layers of protection before any problems arose. Natural deposits of large wood in EDR made it feasible to construct sluice-pipe tripod supports, splints, and stands as well as a temporary lean-to shelter for participants (Figs. 1-2).

In practice the sluicing method went at a modest pace, which had benefits and detriments. In terms of benefits, the steady pace meant that the turbidity at the outlet was modest and easily diluted by the ambient river flow. Also, the steady pace kept everything under control, preventing any serious blowouts. On the other hand, the long run of sluicing pipe enabled several places where cobbles could jam at the couplings. Sometimes it would take a while before the jam was recognized, enabling more material to get stuck at the clog. Efforts to clear a jam involved first finding the clog if the pipe did not burst at the clog location, removing the debris, and then repairing or replacing the pipe. This process could take 30 minutes to several hours, depending on the severity of the clog. Some days were clog free, while other days had multiple clogs.

The key lesson from this for future efforts is that it could greatly improve the efficacy of the system and longevity of the pipes if the gravel/cobble hopper were re-located further down-pipe, so that as much of the run as possible would just carry water. One possible new location for the hopper would be at the switchback where the pipe abruptly changes slope as it leaves the roadside to go down the steep hill to the river. There is enough room to store 1-2 truckload of gravel/cobble at this location, so the idea would be to use a "just in time" method of deliver with little storage and trucks supplying material at the rate it is needed at the hopper.

As it turns out, the gravel/cobble injection took place during a particularly wet period, with a moderate flood of ~4 time bankfull discharge occurring in the middle of the procedure. According to Yuba County Water Agency, December 2010 was the 6th wettest month out of the 103-year precipitation record at the Colgate powerhouse upstream. The heavy precipitation resulted in uncontrolled spills over Englebright Dam for 16 days (Fig. 3), which delayed completion of injection. At the time injection began, flow into the injection site was ~800 cfs (Fig. 2). At this discharge, it was possible to build a partial riffle crest, but several factors limited the ability to fully span the channel with a riffle crest. First, there was a high abundance of fine gravel in the mixture that washed downstream out of the injection zone and promoted "equal mobility" of coarser gravel/cobble. Second, the more constricted the channel became, the higher the velocity in the remaining chute, so the lower the likelihood of fully blocking the channel with a riffle crest. Over time, additional aids for controlling the injection point were figured out using an overhead cable, rafts, floats, and tripods such that it was possible to inject gravel/cobble directly to the far bank. Then on 12/18 the discharge exceeded the reservoir's storage capacity and in a matter of four hours the flow rose from 4,000 to over 10,000 cfs. The peak occurred in the evening of 12/19 at ~19,000 cfs (Fig. 4, left). A second peak overspill of ~11,400 cfs occurred ten days later. According to the 2D model predictions for the injection riffle's design presented in the GAIP, this range of flood flows would be enough to cause full mobility of the

gravel/cobble mixture. However, riffle construction was not complete before flooding began, so the channel was not as constricted as in the model scenario. Visual observation during an EDR reconnaissance after the flood found that most of the injected material had in fact left the injection site. The material transported into the pool immediately downstream of the injection site and largely stayed there. A small amount made it beyond the rapid below the United States Geological Survey (USGS) gaging station where it was evident along the banks. No gravel was observed down at Sinoro Bar. Beginning on 1/1/2011, flow was back in the controlled range <4,500 cfs. Flow slowly declined from that flux down to ~3,000 cfs by the end of the injection. At these flows, injected material was observed to be transporting down from the injection site, so the decision was made to focus injection at two specific points- one just river-left of the middle of the channel where the flow's streamline carried the mixture to eddies on the left (i.e. east; Fig. 4, right) and one at the river-right (i.e. west) bank where the mixture was distributed along the right and middle sections of the channel. Given the high flows, there was no expectation that a riffle be constructed, in accordance with the quote from the GAIP provided above in section 1.2.

During gravel injection there was close communication between the gravel/cobble supplier, the construction contractor, USACE staff, and the GAIP's author who helped oversee the project and troubleshoot issues as they arose. USACE staff monitored turbidity downstream of the injection site and performed pebble counts on the delivered material. The GAIP's author assisted with injection activities at the sluice outlet. A few times, the staff of the UC Sierra Foothills Research and Extension Center helped out with machine shop tinkering of parts and receiving deliveries. The construction contractor did an excellent job of keeping everyone involved informed of the project's status. Periodic visits by observers were facilitated by the participants upon request.

Figure 1. Gravel/cobble sluice pipe and temporary lean-to. Photo courtesy Ralph Mullican.

Figure 2. EDR gravel/cobble injection site showing temporary alluvial crest, downstream alluvial tail, and sluice-pipe tripods made from natural large wood.
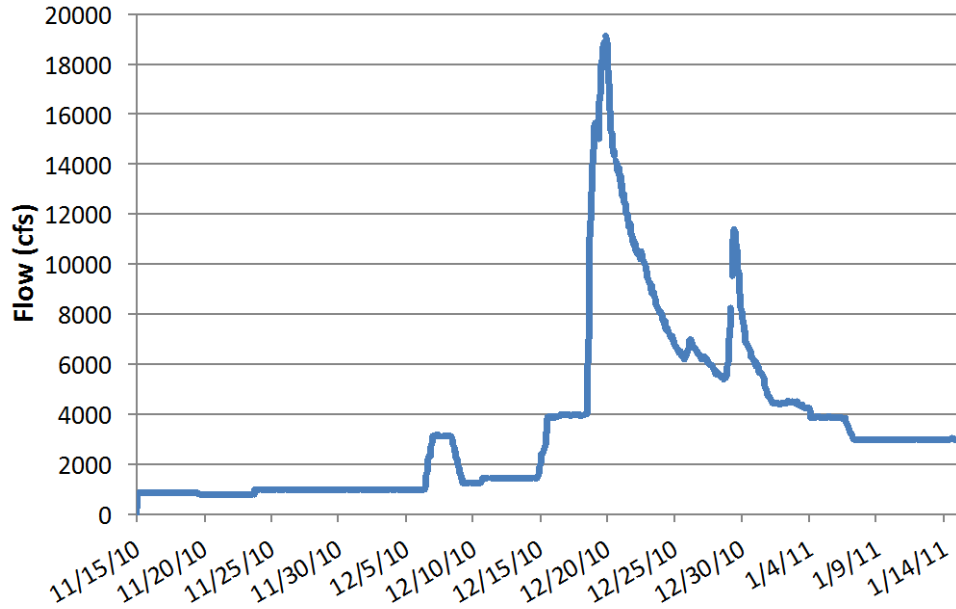
Figure 3. Discharge recorded at the Smartsville gage (_http://cdec.water.ca.gov_; YRS gage) during January 2011 injection.

Figure 4. December 20, 2010 flow of ~14,000 cfs on the falling limb of the first flood peak that caused an injection hiatus (left); January 10, 2011 gravel injection at ~3,000 cfs using rafts to get the mixture to east bank (right). The rafts are held in place by a tether attached to a cross-channel, overhead cable. In the foreground the steep descent of the sluice pipe down the hillside is shown.

3.1. Peak Flow Hydrology after Injection

During the period between the January 2011 injection and the October survey campaign for this report, the river had several floods, including peaks of 19,500, 13,700, 11,200, and 8,000 cfs (Fig. 5; rounded to the nearest hundredth). To put these flows into context, between 1942 and 2004, the long-term statistical bankfull discharge (Qb, 1.5 year recurrence interval) at the Smartsville gage was 11,596 cfs. In the period just post New Bullards Bar dam (1971-2004), the gage's Qb was 5,612 cfs. Wyrick and Pasternack (2011) pegged bankfull discharge at ~5,000 cfs, given that they found overbank stages to occur over a wide range of flows at different locations along the whole LYR. In addition, Pasternack (2008) suggested that partial transport of gravel occurs at flows > 10,000 cfs. Thus, it was expected that gravel transport occurred multiple times after injection and before the new monitoring in fall 2011 presented in this report.
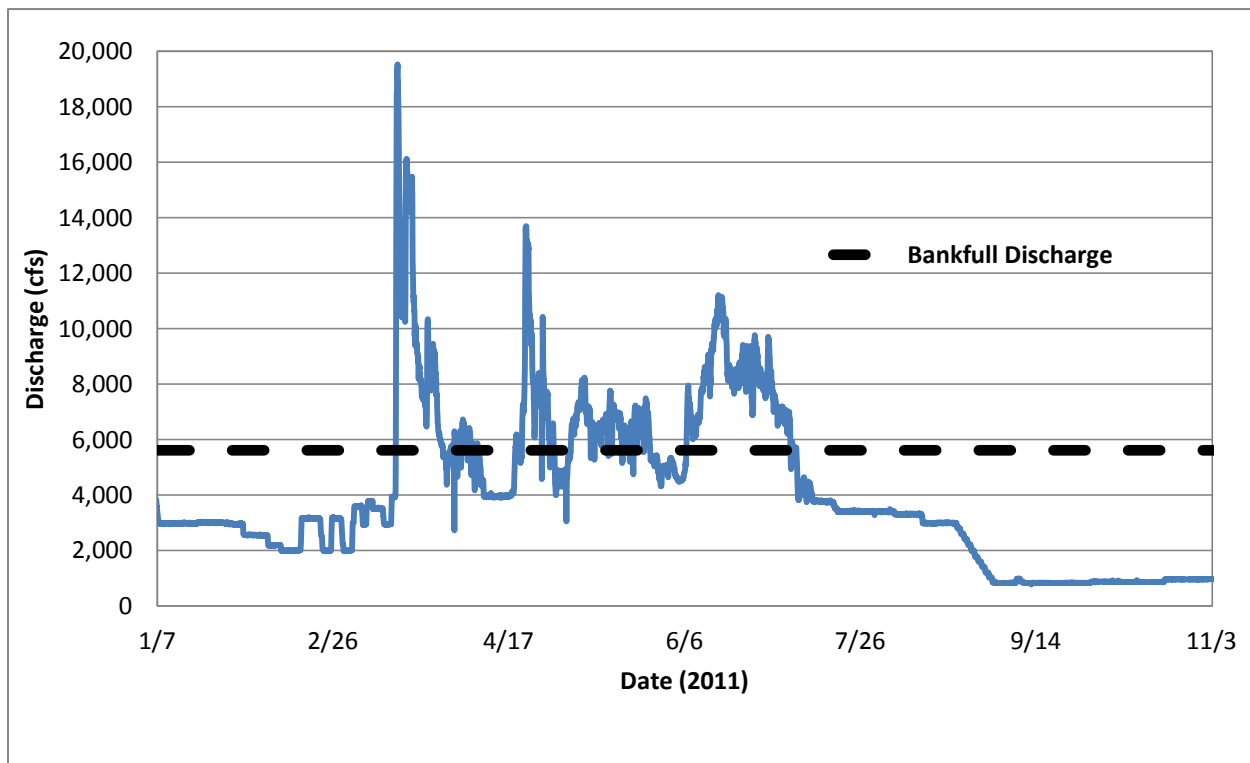
Figure 5. Discharge recorded at the Smartsville gage (http://cdec.water.ca.gov; YRS) during the period between the January 2011 injection and the October survey dates.

4.0   Post-Project Data Collection

Data collection and project monitoring began days after the 2010-2011 gravel/cobble injection was completed.   Activities were impacted by the sustained floods that occurred in 2011.   Of the 228 days between 1/15 – 9/1 that year, the mean daily discharge exceeded the 4,500 cfs maximum controlled release 46% of the time (105 days).   Nevertheless, the necessary topographic data was collected on two occasions, enabling evaluation of GAIP design hypotheses.   In addition, an independent weekly redd survey was undertaken and reported on by the Pacific States Marine Fisheries Commission with assistance from the Yuba Accord RMT.   The data from that effort was used in this report to address GAIP design hypotheses as well.

4.1.   Topography and Bathymetry

The baseline EDR topographic map for analysis of channel change and sediment-budget computation dates to a period from 2005-2007 when EDR was mapped (Pasternack, 2008).   New topographic and bathymetric surveys took place days after injection ended in January 2011 as well as over several weeks during October of 2011. Existing topographic ground control for the EDR was used that is tied into the State Plane California Zone 2 coordinate system in units of feet with NAD 1983 and NAVD88 horizontal and vertical datums, respectively.

Given the importance of having an "as-built" topographic map representing the condition of the injection area immediately after project completion, a bathymetric survey was undertaken on January 18-19, 2011 (Fig. 6).   The approach used involved a Sonarmite echosounder (Seafloor Systems, Inc., Folsom, CA) coupled with a Trimble R7 RTK_GPS for geographic positioning mounted onto a kayak (hereafter referred to as the "kayak method"; Fig. 7).   This is a common method for reservoir and channel mapping, with the modification of doing it using a kayak instead of a motor boat or cataraft due to the inaccessibility of EDR.   The flow of 3,000 cfs on those dates yielded a rapid at the top of the injection area, rendering that small area unmappable.   Similarly, the entrance to the large rapid at the USGS gaging station could not be safely mapped.   There appeared to be little reason to map downstream of the rapid, based on visual reconnaissance that indicated little deposition that far downstream at that time.   The total number of points collected was 8,473 over an area of 10,468 ft^2, yielding an overall point density of 8.1 points per 10 square feet (Fig. 6)   This is equivalent to an overall inter-point spacing of 0.9 feet, which would be considered "high-resolution" by present standards of ground or boat-based river mapping.

After flows were down to baseflow levels in autumn 2011, comprehensive bathymetric

mapping was done throughout EDR (Fig. 8). Terrestrial surveying was done in October 2011 and involved using a Leica TPS1200 total station and a Trimble R7 RTK GPS to map emergent gravel. Boat-based bathymetric mapping was done at the same time using the same kayak method as in January 2011. All areas within the study reach were surveyed with the exception of the center of the rapid downstream of the USGS gaging station due to safety reasons and problems with air bubbles confounding the echosounder (Fig. 8). For the October 2011 survey the total number of points collected was 24,287 of which 24,243 were used in the analyses over an area of 341,050 ft^2, yielding a point density of 0.07 points per square foot (Fig. 8).

During the survey dates the flow at the Smartsville gage ranged from 862 to 958 cfs (Table 3; Fig. 5). These flow values are important because they are used later in the report to validate the 2D model and subsequent spawning habitat predictions. Validating involves assessing the accuracy of 2D model predictions for the specific discharges at which depth, velocity, and water surface values are observed. Table 3 shows that for each survey period there was a standard deviation of 6-8 cfs (~1% of total discharge) as the river discharge fluctuated over these days. This is a small fraction, but it does cause some small uncertainty in comparing predictions against observations, because the predictions are for fixed discharge values and the observations are for ones with a little bit of fluctuation.

Table 3. YRS gage discharges during survey dates in October 2011.

October Dates	Average Discharge	Standard Deviation
6,7,8	870	8
13	862	6
20	951	7
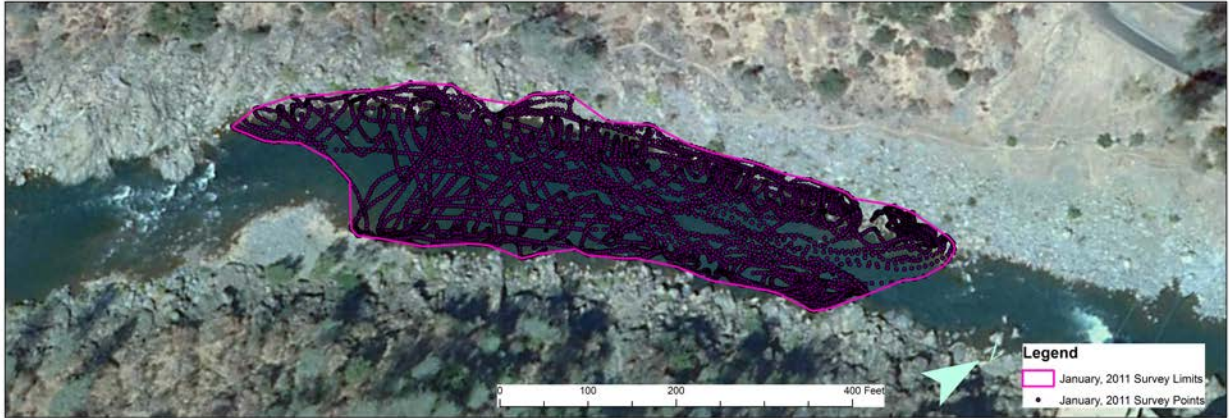
Figure 6. Survey limits and collected points in January 2011.

Figure 7. Photograph of kayak based bathymetric survey setup.
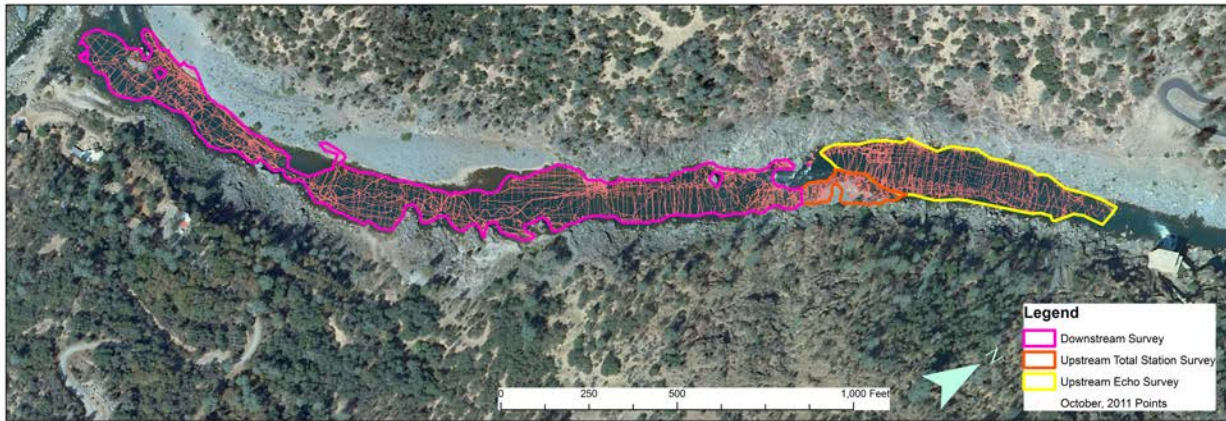
Figure 8. Survey limits and collected points in October 2011.

4.2. Water Depth & Surface Elevation Data

A benefit of using the kayak-based approach to bathymetric surveying is that each depth sounding may be combined with local bed elevation to obtain observed water surface elevation (WSE). Because the kayak bobs up and down in the water, the observed WSE value can deviate from the correct value (whereas this does not affect bed elevation mapping), suggesting that some averaging be used to smooth that out. A 2D model may be validated against either depth or WSE, since they contain the same information, but WSE is more useful for understanding model performance relative to topographic controls, so that was the approach in this study. Depth observations were collected at 0.2-1.0 Hz continuously, so the data was filtered to yield areal averages suitable for assessing the longitudinal pattern of WSE, which is a primary indicator of model performance, especially in terms of the suitability of the bed roughness parameter.

To obtain WSE areal averages, the data was averaged within 50'-spaced rectangles aligned down the river. First, the river was stationed with cross-sections in 50' intervals. Next, the cross-sections were buffered upstream and downstream by 25' to obtain rectangular polygons. Then the WSE point observations at each discharge within each polygon were averaged and the average value assigned to a field within the polygon attribute table. Similarly, the 2D-model-predicted WSEs at each discharge were averaged within each polygon and the average value assigned to a field within the polygon attribute table. Later, these values were compared against the 2D model for validation. For the October 13th date, no echosounding was done and only WSE observations were made using RTK GPS observations along the water's edge. Those WSE data turned out to be too few points to be of use for good-quality model evaluation.

4.3. Water Velocity Vector Data

As part of Yuba Accord RMT scientific investigations, Barker et al. (submitted) developed, tested, and applied a new kayak-based tracer method for validating 2D model performance in velocity prediction that not only tests water speed, but also tests flow direction. The ability to predict flow direction is what distinguishes 2D modeling, but prior to the development of this new method, measurement of flow direction was too time consuming and broadly ignored in 2D model studies. There are five key elements to this new method. First, a kayak is used as a tracer to move with the current along a selected streamline and an RTK GPS on the kayak records accurate positions on a fixed time interval (depending on velocity- high velocity gets high sampling frequency and low velocity gets low sampling frequency). Second, the kayaker is responsible for selecting diverse streamlines to sample the full range of velocities as equally as possible and the kayaker must keep the kayak moving at the same speed and direction as the ambient flow, as indicated by air bubbles, sticks, and other ambient debris that helps visualize the ambient velocity field. Third, the distance between two adjacent boat positions on a streamline is divided by the time between observations to obtain the surface speed and this value is assigned to the midpoint between the two boat positions. Also, the direction of velocity at each midpoint is computed based on the orientation of the line segment drawn between the two boat positions. Fourth, surface speed is correlated against 2D model prediction of depth-averaged speed and surface speed is adjusted to a depth-averaged value using a depth-average velocity constant (DAVC). By making detailed observations of the vertical velocity profile on the lower Mokelumne River, Pasternack et al. (2006) found a DAVC value of 0.71 by least squares regression. Note that the correlation coefficient (R) is insensitive to the DAVC, because multiplying all surface velocities by the DAVC results in a uniform shift that does not change the relative structure of the data for correlation analysis. Finally, because the method is capable of yielding an order of magnitude more observations spanning a wider range of ambient velocities than traditional methods (when done for an equal amount of time), statistical tests of 2D model performance end up having far higher confidence and adherence to statistical assumptions. By using the Barker et al. (submitted) method to evaluate 2D model performance, this study applied the broadest and strictest standards for determining if the model was valid or not.

4.4. Wolman Pebble Counts

Wolman pebble counting is a method for measuring and characterizing the grain size distribution of the surface of a river bed (Wolman, 1954). Studies have shown that for a homogenous mixture, a Wolman pebble count yields the same results as a weight-based

sieving procedure (Kellerhals and Bray, 1971). Such counts were performed regularly on the gravel/cobble injection supply at the holding pile adjacent to the hopper used in the 2010-2011 project, so there is a good characterization of the mixture as it was just before going into the river. Because the material was slowly sluiced into the river, it likely fractionated by size through the mechanism of hydraulic sorting in the sluice pipe, again as it trickled into the high-velocity flow of the river, and again during the late- December 2010 flood.

During the October 2011 data collection campaign, four locations of easily accessible deposition were identified and assayed for particle size distribution (Fig. 9). At each location, 100 particles were sampled using a standard gravel template (i.e., measuring b-axis dimensions of clasts) over a ~3x3-m^2 section of the bed. Less than 1% of particles within the ~3x3-m^2 area were removed from the bed during sampling; thus, there was negligible alteration to substrate texture as a result of sampling (Moir and Pasternack, 2010). From these data, the sediment sizes of which 50 and 90% of the samples are finer (i.e., D_{50}, D_{90}) were computed, among other metrics.
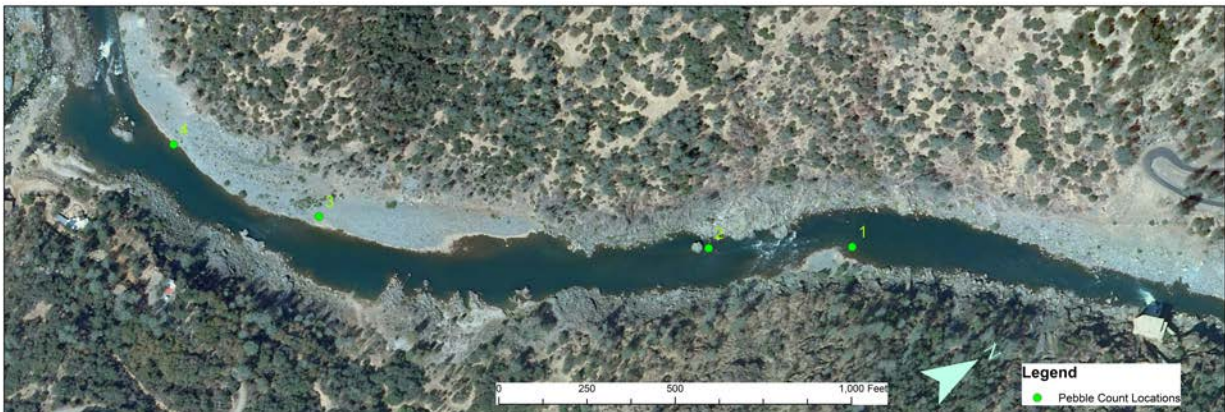
Figure 9. Locations where Wolman pebble counts were made in October 2011.

4.5. Blimp Aerial Imagery

Ultra-high-resolution (<5x5-cm^2 pixels) aerial imagery of the EDR was desired to facilitate gravel/cobble injection planning and to track gravels at transparent depths. The approach used in this study involved lofting a ~3'x6' (oblong ellipsoid) tethered helium kite-blimp with a 14.7 megapixel digital camera (Canon Powershot SD990 IS). Numbered plywood tiles were laid out on the river banks on both sides of the channel for the full reach at a spacing of approximately 50 feet for georeferencing.

Over three separate periods in October 2011 the kite-blimp was lofted above the river bed and moved up and down the reach to gather aerial images. Photos were later

examined to pick the best ones for use in creating a series with ~30% overlap between sequential images. Taking advantage of varying weather conditions, a "bright-light" set of photos was collected to image through the water to see bed conditions as well as possible and a "dark" set of photos was made to clearly see the positions of surveyed ground target and land features that could be used to aid georeferencing (Fig. 10).

The program Agisoft Photoscan was used to automatically mosaic blimp images. Each set of images was reduced into 2-4 mosaics to keep file sizes manageable, while retaining full resolution in the source images. The basic workflow is to add photos, match photos using scale invariant keypoint matching (Lowe, 2004), and mosaic. After a mosaic was constructed, the final image was georectified in ArcGIS with the aid of manually placed ground targets whose horizontal coordinates were surveyed with RTK GPS (Fig. 11). The bright-light images were taken in full sunlight and provided the best clarity through the water column to see the bed (Fig. 10, left). However, those images yield a white-out effect on land that precludes seeing or identifying the marks on the surveyed ground-control tiles due to the need to adjust the white balance to focus on the color temperature of the riverbed. Therefore, the dark set of images was used to locate and see the numbers on the surveyed ground-control tiles for georectification. Once the dark mosaics were rectified, then the bright-light mosaics were georeferenced to them by ArcGIS-based rubber-sheeting with numerous match points on visible features in both the bright-light and dark mosaics.

Figure 10. Illustration of mosaicked bright-light (left) and dark (right) blimp imagery collected at the same location for comparison.
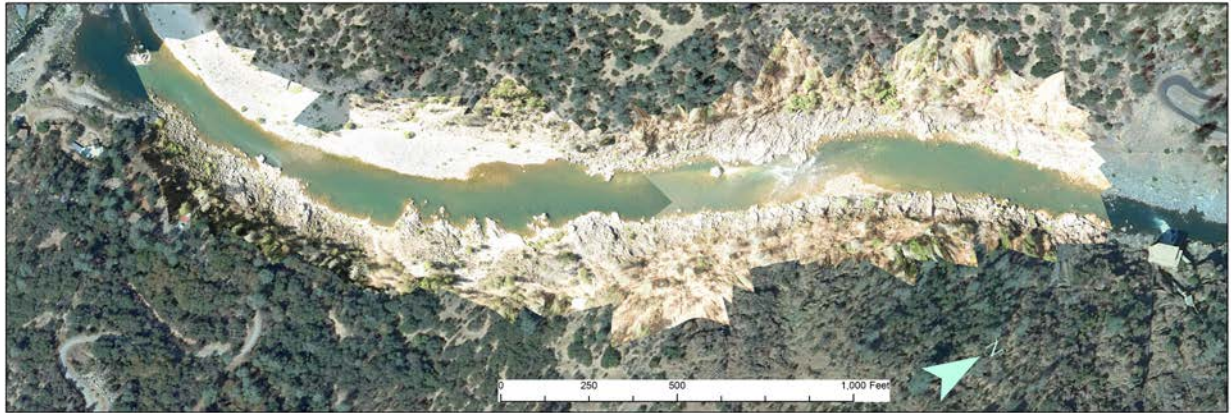
Figure 11. Final mosaic for the bright-light blimp imagery.

4.6. Topographic Map Construction

Because this study evaluated time-dependent changes in topography, it was necessary to create topographic maps for the three times considered. The times considered here are December 2007 (baseline reference map), January 2011 ("as-built" right after the gravel injection), and October 2011 (state after a winter and spring with floods). The data available from each time were used to map the surveyed areas, not to produce a complete map of the whole EDR for each time. The baseline map for December 2007 was previously produced and reported by Pasternack (2008); it is a complete map of EDR including hillsides. The mapped areas for January and October 2011 are shown in Figures 6 and 8. The partial maps from these recent times were the ones relevant for answering questions about channel change and gravel/cobble erosion and deposition.

In addition to these partial maps, a new comprehensive map for the whole EDR was made using the newest observations available. Areas that exhibited no change since 2007 (areas outside of polygons in Figure 8) required no new mapping, so the pre-existing data was retained for those areas. Areas that may have changed were all mapped in October 2011, so that new data was used in place of the older data for everywhere the new data was collected. This new complete map was used to make a new 2D model of the reach to assess physical process and fish habitat.

Topographic maps and associated digital elevation models (DEMs) were made in ArcGIS 10 using 3D Analyst. For each survey, boundary polygons were drawn around the new data collected at that time. Then a triangulated irregular network (TIN) was created using the points in the boundary polygons and the boundary itself as a hard clip. Finally, the TIN was converted to a 3'x3' raster. These rasters were the data used for evaluating topographic changes through time, which are indicative of gravel/cobble erosion and deposition as well as pre-existing channel change 2007-2011.

A similar procedure was used to create a TIN and 3'x3' raster of the new complete EDR map. This map was made using all the October 2011 points as well as the pre-existing observations outside of where the new data was collected. Because it was unfeasible to map the center of the rapid at the USGS gaging station (just as it was in previous years' efforts), it was necessary to use breaklines and artificial contours to create the best representation as possible for that small but important location that acts as a hydraulic control on channel upstream of it. The final 3'x3' EDR raster map was concerted to a uniform point grid and these point data were used to make the new 2D model.

4.7.   2D Numerical Model

A major tool used in this study to evaluate the design hypotheses was a 2D (depth-averaged) hydrodynamic model. These models are capable of simulating the spatial pattern of depth and velocity at points in a river. They are rapidly increasing in their use in private and academic settings as the necessary tool needed to assess geomorphic and ecological outcomes associated with river management and engineering (Pasternack et al., 2004; Brown and Pasternack, 2009; Pasternack, 2011). A 2D model solves the two dimensional equations for the conservation of water mass and momentum within a specified spatial domain. A downstream boundary of measured WSE is used along with an upstream boundary water inflow rate. Two model parameters (channel roughness and a turbulence closure parameter) must be specified as well.

The software used to perform 2D modeling was SRH-2D (with the aid of SMS 10.1 for computational mesh generation). SRH-2D was developed by the U.S. Bureau of Reclamation and is freely available to the public. This modeling software was used by the RMT to simulate 2D hydraulics for the entire LYR using the 2008-2009 topographic map for flows ranging from 300 to 110,400 cfs. It was also used for the 2D model simulations in the GAIP. The model uses a finite volume numerical scheme that can handle subcritical and supercritical flow. The algorithm is extremely efficient and stable for handling wetting and drying as well as steady or unsteady flows. Model outputs include water surface elevation, water depth, depth-averaged velocity components, depth-averaged water speed, Froude number, and shear stress. For more information, see http://www.usbr.gov/pmts/sediment/model/srh2d/index.html.

Based on lessons learned from previous modeling efforts and advances in the science of 2D modeling, a new computational mesh was created for EDR to go with the new topographic map. The mesh has 134,702 computational elements with ~3' inter-nodal spacing. The mesh extends up the canyon walls to enable it to be useful for future efforts to simulate a range of flows (Fig. 12). The location and alignment for the model's

exit flow boundary was shifted to be upstream of the crest of the Narrows Gateway rapid and to cross the channel where there is a more uniform cross-channel WSE. This remains an uncertainty, because the Narrows Gateway rapid appears to be eroding unevenly, making the WSE change somewhat through time. The new alignment is still consistent with the observational WSE data used to create the stage-discharge rating curve for this reach, but that curve is likely changing over time. Topographic points from the new complete EDR map on a 3'x3' grid were imported into SMS and used to interpolate the elevations of the new computational mesh nodes in the new 2D model.

SRH-2D requires the user to select a turbulence closure scheme. Traditionally, 2D models of the lower Yuba River were made using parabolic (Zero-Equation) closure with an eddy viscosity coefficient value of 0.6 (Moir and Pasternack, 2008; Sawyer et al., 2010; Barker et al. submitted). New research by co-author Pasternack suggests that 0.1 performs better by decreasing overpredicting of low velocities, so the RMT's flood models for flows ≥10,000 cfs use that value. In this study, both of those values as well as a completely different turbulence close scheme (k-ε model) were tested using the observational data for WSE and velocity vectors. This study eventually settled on the k-ε model due to its balanced performance across all indicators during the autumnal spawning flows that were evaluated, as explained later.
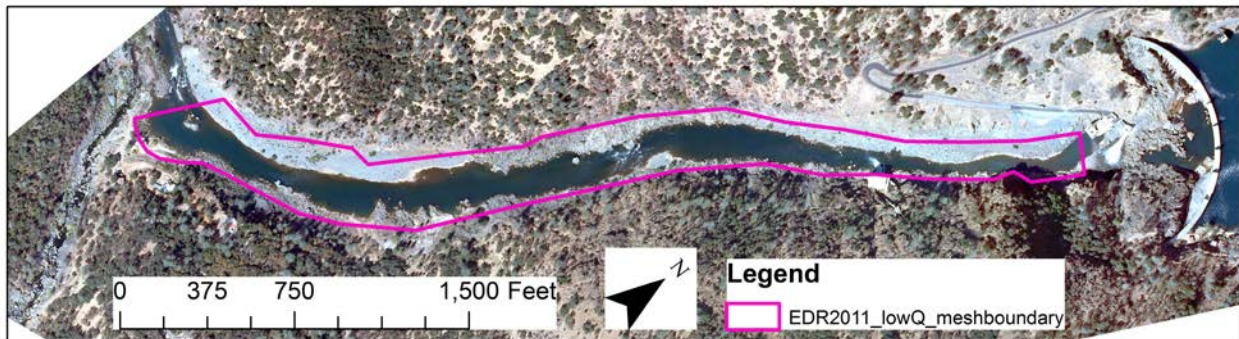
Figure 12. Extents of new EDR 2D model computational mesh.

4.8. Fish Observations

Ultimately, this study seeks to bioverify the habitat suitability modeling approach so that it can evaluate the design hypotheses presented in the GAIP. In order to do this, it is necessary to identify the flows that were present during redd observations. Flows present in the river during the spawning period where observations were recorded by the RMT ranged from 829 to 965 cfs (Table 4).

Table 4. Approximate Discharge during Spawning Observations.

Weekly Spawning Observation End Dates	Average Flow of Previous Week	Standard Deviation
9/26/2011	832	3
10/3/2011	852	23
10/13/2011	870	9
10/17/2011	861	4
10/25/2011	916	48
10/31/2011	958	3
11/7/2011	974	18
11/28/2011	957	8

Biological data was recorded by Campos and Massa (2012) from September 12 to December 19, 2012. They evaluated four aspects of physical habitat for Chinook salmon in the EDR including the number of redds, the spatial and temporal distribution of redds, the level of redd superimposition, and physical characterization of redds. In particular, substrate was visually characterized at each redd according to a protocol established by the RMT (Campos and Massa, 2012).

5.0   Data Analysis Methods

5.1.   Areal Extent of Gravel/Cobble Deposits From Blimp Imagery

A first step in assessing the spatial position of the gravel/cobble deposits was to determine areas of deposition of augmented gravels from the blimp imagery. To do this, the bright-light mosaic was processed in ArcGIS 10 using the image analysis toolbar to help visualize the deposits better. Adjustment of image brightness and contrast provided the best way to isolate patches of new gravel. Once areas were identified their spatial extents were mapped by creating a polygon shapefile. The final mosaic images had raster resolutions of 0.19 feet (5.8 cm).

5.2.   2D Model Validation

A necessary step in using any model is validating predicted outputs to real world observations. Two-dimensional models have inherent strengths and weaknesses, thus uncertainty in modeled results needs to be understood and accepted (Van Asselt and Rotmans, 2002). There are no agreed upon scientific standards for deciding whether a 2D model is accurate or not, so it is necessary to set transparent performance indicators and validation thresholds. Some examples of studies that have done 2D model validation include Lane (1998), Lane (1999), Gard (2003), Stewart (2000), Pasternack et al. (2004, 2006), Brown and Pasternack (2008), Moir and Pasternack (2008), and Pasternack and Senter (2011). In this study, more and stricter criteria for model performance were used to insure a rigorous analysis and characterization of model uncertainty.

Previous studies using 2D hydrodynamic models for gravel-bed rivers comparable to the lower Yuba River have validated the model for this application and provide valuable information regarding model utility and uncertainty (Pasternack et al., 2004, 2006; Wheaton et al., 2004a; MacWilliams et al., 2006; Elkins et al., 2007; Brown and Pasternack, 2008). However, in this study the canyon setting is far more topographically complex, so it was important to evaluate model performance. As part of model development, the model was first tested with a few different Manning's n channel roughness values and turbulence closure parameter values to evaluate the effects on deviation between the observed and predicted longitudinal profiles of water surface elevation. Then predicted and observed water speeds and velocity directions at independent locations were compared to provide an assessment of model accuracy and uncertainty.

In addition, past studies evaluating 2D model performance over a wide range of discharges (i.e. one to three orders of magnitude) found no systematic differences in model performance for velocity prediction associated with discharge (Pasternack and Senter, 2011; Barker et al., submitted). Discharges to be simulated in this study were all in a narrow range of baseflow conditions, so validation was done on a single day at a single flow.

Almost all published studies that included validation used some test of accuracy for depth or WSE (since they include the same information) as well as for water speed in the direction of flow. Velocity in a 2D model is a vector, not a scalar, so it has both magnitude and direction or two velocity components. Very few studies report mass conservation performance. Similarly, very few studies evaluate flow direction or the velocity components independently, despite this being the unique identifying aspect of a 2D model. Some exceptions are Lane (1999), Barker et al. (submitted), and now this study.

5.2.1. Mass Conservation Standard

Surprisingly few studies evaluate mass conservation performance, especially for long, complex model reaches where mass loss can be significant. By comparison, discharge gaging at USGS gaging stations is normally within ~5-10% of the actual value, so having substantially higher accuracy than that hardly matters. A mass loss > ~2-3% of the flow input for a long segment is a sign of poor model performance (Pasternack and Senter, 2011). For a short reach such as EDR, mass loss should be < ~0.1-0.5 % based on simple reasoning. For example, for an input of 1000 cfs, a mass loss of 0.1-0.5 % would correspond with ~1-5 cfs.

5.2.2. Types of Variables Assessed

Error! Reference source not found. shows which variables were tested at which discharges. For each variable, some tests are done on the raw values, some on the raw (i.e. signed) deviations between observed and predicted, some on the absolute value (i.e. unsigned) deviations, and some on the signed or unsigned percent errors. WSE has to be analyzed in terms of deviations, not percent error. The reason is that WSE values are generally high numbers when a river is far from the ocean, so a small water surface deviation is a minuscule fraction of WSE. For example, a WSE deviation of 2 ft would yield a percent error of 0.1 % if the WSE happens to be 2000 ft high on a mountain for the datum and coordinate system used in a given study. That creates the false impression that the error is small (0.1%), but in fact a WSE deviation of 2 ft is usually considered unacceptably high. In contrast, for depth and speed validation, percent error is a meaningful number, because the deviations are a substantial fraction of the observed values. Percent error is a variable that is easily recognized and interpreted by most readers. Sometimes percent error is not evaluated for low values of depth or velocity, because the difference between a depth of 0.01' and 0.1' is usually not meaningful, but it does yield an enormous numerical error. That is why some studies report deviations instead of percent errors.

Table 5. Flows at which different 2D model variables were evaluated for their accuracy.

Discharge (cfs)	Mass Conservation	WSE	Velocity Magnitude	Velocity Direction
832	X			
862	X		X (n=532)	X (n=525)
870	X	X (n=136)		
916	X			
951	X	X (n=147)		
974	X			

5.2.3.   Validation Tests and Performance Standards

For each of the variables, there are different tests to assess model performance. One approach is to make a cross-sectional or longitudinal plot of observed and predicted conditions, which allow for visual inspection of the lateral pattern of accuracy, which can reveal the cause of inaccuracy (e.g. Pasternack, et al., 2004, 2006). However, statistical tests provide a more robust and objective basis for evaluation, so sectional plots should only be used as a secondary basis for evaluation. In hydrological modeling (i.e. rainfall to runoff), it is very rare for modelers to show head-to-head scatter plots, and in hydraulic modeling it is only sometimes done. One argument against analysis of a scatter plot is that it does not convey an understanding as to why individual points are deviating from a one-to-one line. Instead, cross-sectional comparisons show the role of eddy viscosity limitations and patterns of topographic variability. On the other hand, a scatter plot provides the most rigorous quantitative evaluation.

Statistics for signed and unsigned variables can be generated and compared against reference data and past studies. For all signed variables, statistics and plots should show that the data are centered on zero, which means there is no bias in the model predictions. There is no standard as to how much bias is permitted before a model is invalid, but the closer to zero, the better. Statistical distributions of depth and WSE deviations should be compared to that from topographic deviations obtained from testing of different survey methods to make sure that model prediction deviations are no noisier than topographic uncertainty. For example, if topographic error is biased, then it could prove difficult for 2D model predictions to avoid bias as well. Also, if the underlying map is accurate to within 0.5 ft, then it cannot be expected that 2D model depth predictions should be accurate to much better than that, because topographic error is the predominant factor explaining 2D model error in depth prediction (Pasternack et al., 2006). There is no standard for how accurate depth prediction has to be relative to topographic uncertainty before the model is invalid, but as a starting point one could use the standard that the metrics for topographic deviations should not be

exceeded by those for depth or WSE deviations.

Correlation and regression analyses are highly useful for evaluating 2D model performance. Some studies report R-values, but that can be misleading and it is fairer to report R^2 values. R^2 is always higher for depth (~0.7-0.8) and lower for water speed, as the later is highly sensitive to the nonlinear terms of the momentum equation. Based on a review of the literature, people have deemed their models valid even with R^2 values as low as ~0.4 for water speed. Many 2D models yield R^2 values of ~0.6 for water speed, with the best performing models for natural rivers being in the ~0.7-0.85 range. Barker et al. (submitted) found that the for RMT's 2D model of the alluvial LYR, the R^2 value for velocity was 0.79. Note that 2D models of flumes with bed undulations and porous beds have R^2-values of 0.9-1.0, indicating that topographic accuracy and channel complexity are key factors explaining why 2D models of natural rivers are not as good as 2D models are capable of predicting.

A major drawback of relying only on R^2 as a model test is that it only indicates the degree to which one variable is predictive of another, but that is not the same as testing accuracy. Given the linear regression equation between predicted vs. observed velocity, the slope of the equation indicates whether the model is biased or not. Several studies have reported a bias toward over predicting low velocities and under predicting high velocities. This has been attributed to excessive lateral mixing caused by the parabolic turbulence close scheme using an eddy viscosity coefficient value of ~0.5-0.8 (MacWilliams et al., 2006; Pasternack et al., 2006). Meanwhile, the y-intercept of the regression equation indicates whether the model has an overall shift of over- or under-prediction, which might be due to an inappropriate Manning's n value. There are no standards for these metrics, but as a starting point we propose that the slope be >0.8 and the intercept be <10% of V_{max}. Once there are more studies using these metrics, these thresholds can be revisited.

Another important set of measures of model accuracy comes from statistical analysis of unsigned percent error of depth and velocity. Commonly 2D models yield a mean error of ~10-15% for depth and ~20-30% for velocity. Median error is usually lower than mean error, due to the influence of a few outliers on the mean value. There are no set standards, but if the mean velocity error >40%, then that would be unusually poor performance compared to past studies. Another test that is sometimes done is to break up velocity tests for low and high values, recognizing that a small deviation in velocity at low velocity can yield an unusually high percent error. There is no specified cut-off, but some studies have used 2 or 3 ft/s to differentiate the performance at lower and higher velocities.

Finally, there are no proposed metrics for accuracy in prediction of velocity direction. Only two previous studies have ever tested the 2D flow pattern at velocity observations

(Lane, 1999; Barker et al., submitted). Lane (1999) analyzed 3D velocity components and used similar metrics as commonly used for water speed in the direction of flow. Barker et al. (submitted) tested flow direction based on particle tracking with RTK GPS. For observations generally made in the mean flow direction, that study reported an unsigned direction angle deviation of -0.11°, a mean signed deviation of 5.5°, an R^2 between observed and predicted direction angle of 0.80, and a linear regression slope for that comparison of 0.90. For unsigned deviation, an average of 10° is proposed as the cutoff above which a model is not validated. In addition, Barker et al. (submitted) illustrated locations of poor model performance at some large eddies and explained why those problems occurred.

5.3.   Topographic Change Detection By DEM Differencing

Per the GAIP, the test for design hypothesis one is an evaluation of topographic change from difference of DEMs (Wheaton et al, 2010a,b; Carley et al., submitted). In simplest terms, a DEM difference is just the subtraction of one topographic map (i.e. a raster map) from another with the resulting difference indicating the locations and magnitudes of landform change. The map of topographic change itself may be represented by a DEM, so it is termed the DEM of Difference (DoD). However, topographic maps have uncertainties in them that people normally do not think much about. When a DoD is produced, it not only has the errors from each source map, but also the errors of propagation through the mathematics. As a result, it is crucial to characterize DoD uncertainty instead of relying on analysis of a raw DoD. Topographic change detection (TCD) by DoD analysis including uncertainty is a rapidly progressing technique for monitoring and understanding rivers (Wheaton et al., 2010a,b; Carley et al., submitted). For this study, three sets of topographic data were used in four topographic change scenarios to evaluate changes in topography using the method developed by the RMT for use on the lower Yuba River (Carley et al., submitted).

5.3.1.   TCD Components

Because of the significant role of the rapid downstream of the USGS gaging station in serving as a topographic control on channel hydraulics, EDR was divided into two sections for TCD by DOD analysis at this location. The upstream area (injection zone to crest of rapid) was isolated to assess sequential fill and scour periods that occurred before the January 2011 survey and between the January and October 2001 surveys. The downstream area (rapid crest to Narrows Gateway entrance) was isolated to analyze the overall net change in the river between December 2007 and October 2001 surveys. These areas are segregated by a red line in the results figures.

A list of the TCD components is shown below in bulleted form:

- Upstream Area
  - December 2007 to January 2011
    - The first TCD component quantified the volume of augmented gravel that can be detected in the as-built survey, recognizing the uncertainty due to the inability to map the very top of the injection zone.
  - January 2011 to October 2011
    - The second TCD component evaluated gravel/cobble redistribution within the upstream area and export to the downstream area in the 2011 water year after injection.
  - December 2007 to October 2011
    - This net TCD component characterized the overall change from the baseline December 2007 state in the upstream area.
- Downstream Area
  - December 2007 to October 2011
    - This net TCD component characterized the overall change from the baseline December 2007 state in the downstream area.

5.3.2. TCD Production Workflow

The Carley et al. (submitted) method of accounting for uncertainty with geomorphic change detection was utilized to perform topographic change detection and analysis. This method is based on the idea that locations where there is a lot of topographic variation in the raw point data for a topographic map are the ones that are most uncertain (Heritage et al., 2009). Consequently, the more variation a location has, the higher the bar has to be to consider raw DoD values as real as opposed to an artifact of map errors. Topographic variation stems from measurement error as well as natural sharp features (e.g. steep banks, boulder clusters, and sedimentary bars). By focusing on the existence of topographic variation regardless of its cause, the method is less sensitive to expert-based decisions as to potential native sources of topographic error.

Implementation of the Carley et al. (submitted) method used in this study involved the following steps in ArcGIS 10:

a. Create a uniform {x,y} point grid with 1' point spacing.

b. Elevate the 1' point grid using the topographic data for each map to create oversampled topographic point datasets for $\{x,y,z)_{time1}$ and $\{x,y,z)_{time2}$ that capture all available topographic information in the source DEMs.

c. For each 1' $\{x,y,z\}$ topographic dataset, create a raster of standard deviation (SD) of point elevation with a 3'x3' cell size (yielding nine points per cell in the statistical computation).

d. Apply the appropriate survey and instrument error (SIE) empirical equation from Heritage et al. (2009) to the SD rasters to obtain the SIE raster for each topographic map. For this application with a point density comparable to that obtained using airborne LiDAR mapping, the Aerial Lidar equation was used for triangulation with linear interpolation:

$$SIE = 0.4432{\cdot}SD + 0.0434$$

e. Produce a Level of Detection (LoD) grid that combines the two SIE rasters into a single error raster using the t-value for 95 % confidence (1.96) and the statistical equation for error propagation given by:

$$LoD = t\sqrt{(SIE_{time1})^2 + (SIE_{time2})^2}$$

f. Create the raw DoD raster with a 3'x3' cell size.

g. Create separate deposition and erosion rasters using the "Con" function in the ArcGIS raster calculator.

h. Remove the LoD from each raster by subtracting it from the deposition-only raw DoD and adding it to the erosion-only raw DoD.

i. Create spatial coherence polygons to clip deposition and erosion rasters.

    a. Con statements were used to turn deposition and erosion rasters into presence/absence polygons.

    b. The area of each erosion and deposition polygon was calculated.

    c. A minimum threshold of 100 ft² (~9 raster cells) was used to distinguish coherent change.

    d. The original deposition and erosion rasters were clipped to exclude the areas of change below the size threshold.

j. Clip to lowest extent of data set survey limits.

k. Exclude a uniform threshold for all surveys of +/- 0.16 ft to account for a presumed uniform uncertainty in topographic surveying.

5.3.3. Volume and Weight Gravel/Cobble Budgeting

Once a final DoD raster with a 95% confidence was developed it was necessary to quantify erosion and deposition volumetrically and by weight. To do this, the volume of topographic change for each raster cell was determined by multiplying each cell's change value by the cell's area (3'x3'). This was performed separately for erosion and deposition.

Converting volume to mass required an estimate of gravel/cobble bulk density as present in the river. For this study, we used a value of 110 lbs/ft^3 that came from five experimental bucket tests on gravel density performed at a quarry as material was stockpiled for a gravel augmentation on the Mokelumne River (Merz et al., 2006). Sawyer et al. (2009) analyzed full-scale bulk density at gravel placement sites on the Mokelumne River and found that the actual values varied around this one depending on how much front loaders had driven over the material. Given that the EDR sediment was not driven over and was recently redistributed and deposited by flow, it has been found to be loosely packed. When a person walks on one of these deposits, one feels the material slides down and away from each footfall. Therefore, its bulk density is probably similar to that from the bucket tests. Given this bulk density value, the conversion from ft^3 to short tons involved multiplying the volume by the bulk density and dividing by the conversion factor of 2,000 lbs per short ton.

5.3.4. Evaluating TCD with Channel Geometry

Beyond mapping patterns of erosion and deposition and computing volumetric change, a key analysis in this study involved evaluating the geomorphic processes responsible for those observations. Potential mechanisms were described in section 2.1.1 and. To understand erosional and depositional controls at the morphological unit and reach scales, analyses were conducted relating TCD variables to channel geometry variables.

The simplest test involved looking for a relation between detrended bed elevation (with water depth as a surrogate for that) and deposition (or erosion) based on the notion that deeper areas tend to be slower and thus zones of deposition, while shallower areas tend to be faster and thus zones of erosion. However, this simple assumption is not always valid, as velocity is conditional on all aspects of cross-sectional area, not just depth; the locations of maximum and minimum cross-sectional area change as a function of discharge (MacWilliams et al., 2006).

To conduct this simple test, scatter plots and regression analyses were done between water depth at 862 cfs (since that identifies troughs and ridges in the bed) and amount

of deposition as well as water depth and amount of erosion. Because there are so many points in the scatter plots, an additional analysis was done to compute and plot the histogram of water depth at 862 cfs was made for depositional pixels only, to see if there was a trend of increasing deposition with increasing depth. The same thing was done for erosional pixels to see if an inverse relation was evident.

One problem with the basic analysis is that deposition and erosion may depend on the longitudinal organization of shallow and deep areas as well as narrow and wide areas. As a result, the next level of sophistication in the analysis involved evaluating whether scale dependent and longitudinal positional aspects of channel geometry controlled topographic change. To do this, a suite of covariance analyses were performed on the flow width from 2D model outputs at 862, 5,000, and 21,100 cfs, with the cumulative volume of TCD along a channel centerline, termed Volume Per Node (VPN). The same exact analyses were done between detrended, standardized bed elevation (Z11std) and VPN as well as between flow width at the different discharges and Z11std. Finally, the bivariate coefficient of determination (R^2) of covariances was calculated to find out if any of them were interdependent.

The serial covariance between paired series was calculated from the detrended and standardized series residuals by the product $x_{std} * y_{std}$ where the subscript *std* refers to standardized values. To extract series first a linear reference within the river was established using the thalweg path. This was done in ArcGIS by taking the product of depth and velocity at 5,000 cfs and tracing a path along the path of the maximum of this product (Pasternack and Senter, 2011). Next, the thalweg series was stationed by creating points at 3 ft intervals to be consistent with both the model and TCD rasters. To develop a spatial series of volume of topographic change for each stationing node (i.e. VPN), an existing algorithm in ArcGIS was used that determines the nearest object for a pair of data sets. Using this algorithm after converting rasters of topographic change to points spaced every 3 ft allows each of these points to be associated with the thalweg stationing. For flow width series, transects are created at each station node that extend to the limits of flow width. The length of each transect associated with the thalweg stationing gives a series of flow width per node. Significance was assessed as covariances that exceed at least one standard deviation (68th percentile), which for the covariance plots here is simply any value above one. Stronger significances may also be assessed by looking at two or more standard deviations, as desired.

5.4. Evaluating Habitat Quality and Spawning Use

The GAIP states that a design objective (Design Objective 2) for gravel augmentation is to provide a higher quantity of preferred-quality Chinook salmon spawning habitat in

the injection zone until the sediment moves downstream. For the 2010-2011 project the injected material started washing downstream of the injection zone in the floods that occurred during and after injection. As a result, it is not possible to strictly apply the GAIP's habitat tests. However, the sediment did wash downstream and form some alluvial features, even though the injected volume was only a small percent of the total deficit for the reach. Therefore, this study chose to apply the tests to the self-formed downstream deposits.

Hypothesis 2A posits that SRCS require deep, loose, river rounded gravel/cobble for spawning. The test for this involves performing Wolman pebble counts and checking to see if the deposits match the size specifications for spawning presented in the GAIP. This test was performed using the results from grain size data described in section 4.4. Hypothesis 2B posits that spawning habitat should be provided that is as close to GHSI defined high-quality habitat as possible. The test for this requires performing 2D modeling of the reach and applying LYR Chinook salmon spawning habitat suitability curves to obtain the GHSI pattern for representative flows at which spawning occurred in fall 2011. The GHSI patterns were then checked to quantify the amount of preferred habitat available on the new downstream deposits.

In addition, the RMT conducted weekly redd surveys through the spawning season (section 4.8), so that made it possible to do testing beyond the explicit GAIP hypotheses. First, the red data were analyzed to see how many were present on the deposited sediment. Second, post injection surveys and subsequent change detection analyses were used to infer whether or not redds corresponded with newly injected gravel and at what sediment thickness. Finally, a bioverification procedure was used to find out if the fish were showing a higher utilization of model-predicted preferred spawning habitat than would be expected from the availability of the habitat (e.g. Elkins et al., 2007).

5.4.1. Comparing Observed Redds with Deposition

The GPS redd data were compared against the final adjusted DoD from TCD analysis for the 2007 to October, 2011 scenario for both upstream and downstream sections. This was performed in ARCGIS 10 by joining the final adjusted DoD grid values of the deposition raster to the redd data shapefile. This was not performed for erosion because there were no redds located in those areas for this scenario.

5.4.2. Spawning GHSI Modeling

Simulated patterns of Chinook salmon spawning physical habitat were needed to assess

design hypotheses 2, 3 and 4. In the emerging discipline of ecohydraulics, physical habitat quality predictions are often made by extrapolating depth and velocity observations or predictions through independent habitat suitability curves (HSC) for depth and velocity that are developed locally or regionally to obtain a univariate habitat suitability index (HSI) for each flow variable (Leclerc, 1995). These are then geometrically averaged (sometimes often along with HSI for cover and substrate) to obtain a global (aka combined) habitat suitability index (GHSI). Some studies refer to GHSI as hydraulic habitat suitability index (HHSI), because it only considers depth and velocity. To account for uncertainty when hydraulics are obtained from 2D model predictions, Pasternack (2008) lumped GHSI values into broad classes, with GHSI = 0 as non habitat, 0 < GHSI < 0.2 as very poor habitat, 0.2 < GHSI < 0.4 as low quality, 0.4 < GHSI < 0.6 as medium quality, and 0.6 < GHSI < 1.0 as high quality habitat.

Recognizing that the channel in the EDR is unsuitable for spawning in the absence of injected gravel/cobble, the channel was first segregated into potential and non-potential spawning habitat on the basis of substrate alone. The area of potential spawning habitat was defined as a polygon containing the areas determined by the DoD analysis to be fill (within the thresholded DoD between December 2007 and October 2011) (section 5.3.2) plus the areas identified from the blimp imagery as containing new gravel deposits (section 5.1). All areas not included in this polygon were by default given an HSI value of 0, meaning they are "non-habitat".

LYR hydraulic habitat suitability curves developed by Beak Consultants, Inc. (1989) for SRCS based on utilization data using the method of non-parametric tolerance limits were bioverified in this study and then applied to address the design hypotheses. Depth and velocity 3'x3' rasters were produced using the 2D model for the representative discharges for fall 2011. Combining the Beak HSCs and the hydraulic rasters, 3'x3' HSI rasters were computed for depth and velocity (DHSI and VHSI, respectively). As already explained, substrate was modeled as a presence-absence phenomenon where a value of 1 was assigned to suitable substrate and a value of 0 was assigned to non-suitable substrate. The final global habitat suitability index applied to the areas where gravel/cobble was present was calculated as GHSI = $(DHSI*VHSI)^{0.5}$.

5.4.3. Bioverification of Chinook Spawning GHSI

The first step in habitat suitability analysis is to determine if the HSC's utilized in the study capture the selection of "good" habitat over "poor". Following the work of Ivlev (1961) and Elkins et al. (2007), an electivity index (EI) based on the classic forage ratio was utilized to evaluate the HSC's ability to capture observed habitat preferences. The forage ratio in this context is the ratio of the proportion of redds observed in a region to

the proportion of channel area within that region. The regions used in bioverification testing can be anything, but in this case they are the areas within the specified ranges of GHSI values associated with different levels of habitat quality (e.g. 0.4 < GHSI < 0.6 as medium quality habitat). A "preferred" region is one with EI > 1.2 (i.e. occurrence is significantly greater than random), a "tolerated" region is one with 0.5 <EI < 1.2 (i.e. occurrence is similar as random), and an "avoided" region is one with 0 < EI < 0.5. (i.e. occurrence is significantly less than random). The forage ratio has been heavily scrutinized over the decades (e.g. Lechowicz, 1982), but no consensus has ever emerged that a different metric works better for the type of assessment undertaken in this study. Although EI values based on the forage ratio could theoretically go to infinity, in practice they are typically <10 in this usage. The primary concern in applying the forage ratio is when there is such a small number of observations or such a low area of a test region that the EI becomes spuriously high simply due to inadequate numbers. Care was used to avoid that problem in this study.

To achieve bioverification, two criteria have to be met using the EI. First, predictions must include areas that are "preferred" and "avoided". A trivial prediction is one that says the whole channel is preferred, and then utilization is observed somewhere in the river, so presumably the prediction is correct. However, a prediction must have specificity. The higher the EI value of preferred regions, the riskier and more specific the predictions are. Second, the EI metric must result in higher EI values for higher GHSI regions and lower EI values for lower GHSI regions. In other words, if the prediction shows that there is disproportionately high utilization in a region, but the region was thought to be poor quality habitat, then the understanding of what constitutes high quality habitat is wrong and needs to be re-conceived. Utilization should be highest where the habitat quality is highest. If not, then the predictions are not bioverified.

The procedure for this analysis involved the following steps. First, GHSI rasters were made for all modeled flows representing fall 2011 spawning conditions. Second, the rasters were reclassified according to the habitat quality bins defined earlier and the reclassified raster was converted into polygons. Third, the area of each GHSI bin was determined and divided by the calculated total wetted area for that discharge to arrive at the % available habitat for each bin. Fourth, the GHSI at each redd location was determined from the GHSI raster. Fifth, the number of redds in each GHSI bin was computed and divided by the total number of redds to arrive at the % utilization for each bin. Finally, EI was computed as the ratio of % utilization to % available habitat.

5.4.4. Proximity Analysis of Observed Redds to Refugia

Hypothesis 3b of the GAIP states that structural refugia in close proximity (assumed to be < 10 m) to spawning habitat should provide resting zones and refugia from predators. To test this hypothesis each redd cluster was buffered by 10 m in ArcGIS creating a bounding polygon that encloses all observations. Next, visual inferences were made as to whether this area had structural elements such as proximity to deep pools, bedrock outcrops, boulders, large cobble, and large streamwood.

6.0 Results

6.1. Wolman Pebble Counts

During the 2010-2011 injection 27 Wolman pebble counts were done to evaluate the particle-size distribution in the gravel supply pile. Most counts had a D_{50} between 20-50 mm and a D_{90} between 50-80 mm (Fig. 13). During the October 2011 data collection campaign four Wolman pebble counts were done on the redistributed sedimentary deposits downstream of the injection site. Most of these counts collected had a D_{50} between 10-20mm; no particles were present in the counts coarser than 80 mm (Fig. 14). Particle sizes diminished in the downstream direction, with sites 3 and 4 finer than sites 1 and 2. The figure shows that these deposits were substantially finer than the injected source material, which in turn was finer than what is commonly observed as the spawning sediment sized used by Chinook on the LYR (Moir and Pasternack, 2010).
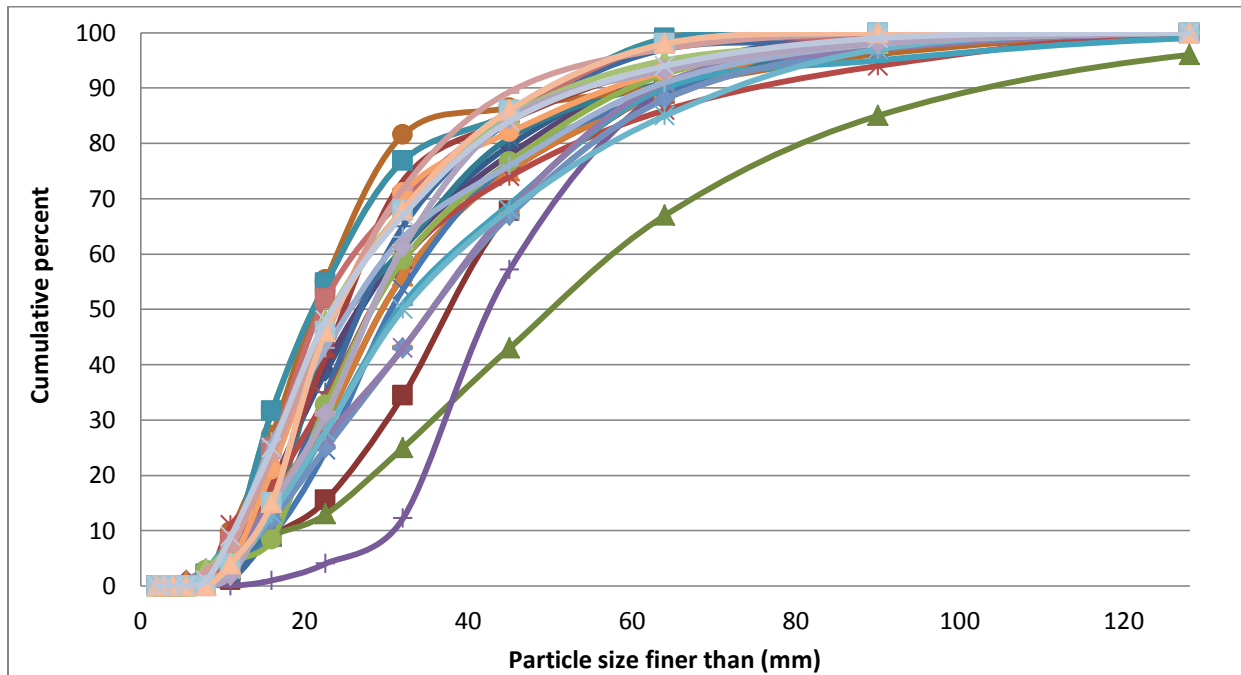
Figure 13. Cumulative particle-size distribution of injected sediment during the 2010-2011 injection.
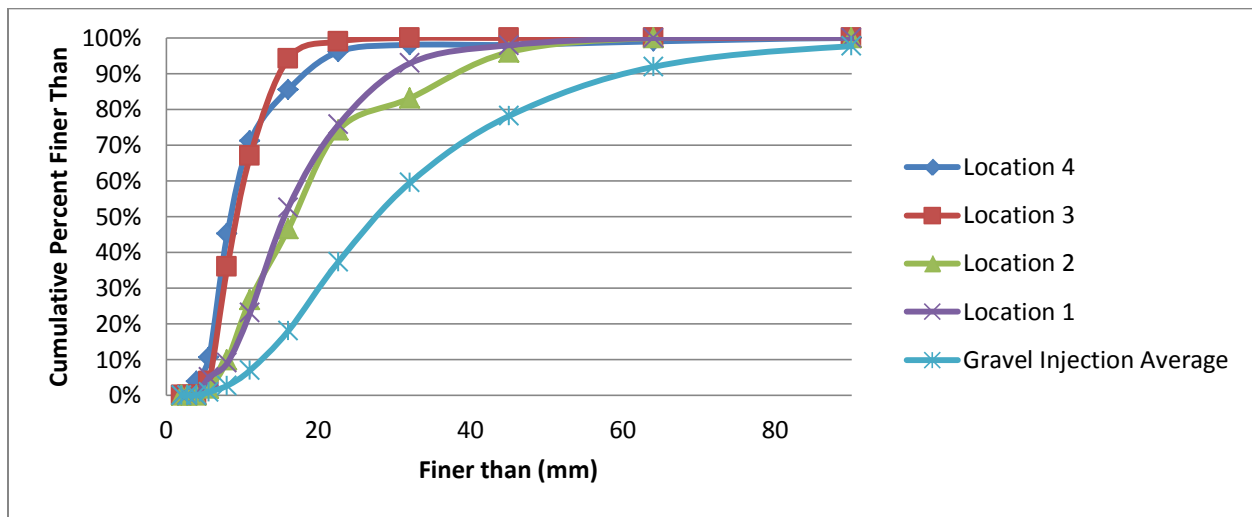
Figure 14. Cumulative distributions of four sedimentary deposits relative to that from the gravel injection material stockpiled at the hopper.

Table 6 compares the percent abundances of the Wolman counts against the specification in the GAIP and what was actually added to the river during the January, 2011 injection. Apparent in the data is that the specification and actual injection are reasonably close for gravel sizes, but there is a notable deficiency of particles in the 32-90 mm range. In addition, Wolman counts indicated that downstream fining is occurring. This is likely the result of sediment transport mechanisms such as selective transport of smaller fractions over larger fractions. Another possible mechanism is simple trapping of materials behind larger obstructions on the bed of the channel. Regardless of which mechanism is more dominant the trend of fining is consistent with theoretical and empirical explanations of sediment transport dynamics. Size fractionation was anecdotally reported for the 2007 injection (Pasternack, 2009) and now it is quantitatively documented.

Table 6. Tabular data for Wolman counts comparing GAIP specification, January 2011 injection, and October 2011 downstream observations.

	Specified Gravel Mixture	Gravel Injection	Location 1	Location 2	Location 3	Location 4
Size (mm)	Cumulative Percent Finer					
2						
2.8						0.00%
4		0.00%	0.00%	0.00%	0.00%	3.85%
15.6	0.00%	0.97%	5.05%	1.98%	3.88%	10.58%
8	3.97%	2.76%	9.09%	9.90%	35.92%	45.19%
11	11.36%	7.06%	23.23%	26.73%	66.99%	71.15%
16	22.81%	18.05%	52.53%	46.53%	94.17%	85.58%
22.6	36.33%	37.40%	75.76%	74.26%	99.03%	96.15%
32	52.64%	59.55%	92.93%	83.17%	100.00%	98.08%
45	70.14%	78.18%	97.98%	96.04%		98.08%
64	86.87%	91.93%	100.00%	100.00%		99.04%
90	97.51%	97.71%				100.00%
128	100.00%	100.00%				
180						
300						

6.2. Blimp Image Analysis

A very low-resolution version of the final bright-light mosaic is shown in Figure 15 with areas of visually discernible gravel deposits enclosed in red. A larger map is available upon request. The areas shown were what could be visually identified as new gravel deposits that matched the composition of the injected gravels. The total area of the polygons is 72,020 square feet, which is 17% of the wetted area at 855 cfs from Narrows 1 to the confluence of Deer Creek at the study limit.

Figure 15. Areas of gravel deposition from the January 2011 Injection that were discernible using blimp imagery and visual inspection in ArcGIS.

Recall that this analysis used iterative image filters adjusting the contrast and brightness as needed to identify patches of injected gravel. Because depth is spatially variable the effect of using this filters is also variable in deep and shallow parts of the river. This makes it difficult to show one image that shows all deposits of gravel discerned from the analysis. To illustrate the type of result gained from the technique, Figure 16 shows a zoom of an area that illustrates how the image filters were able to make visual deposits more discernible relative to the raw bright image.
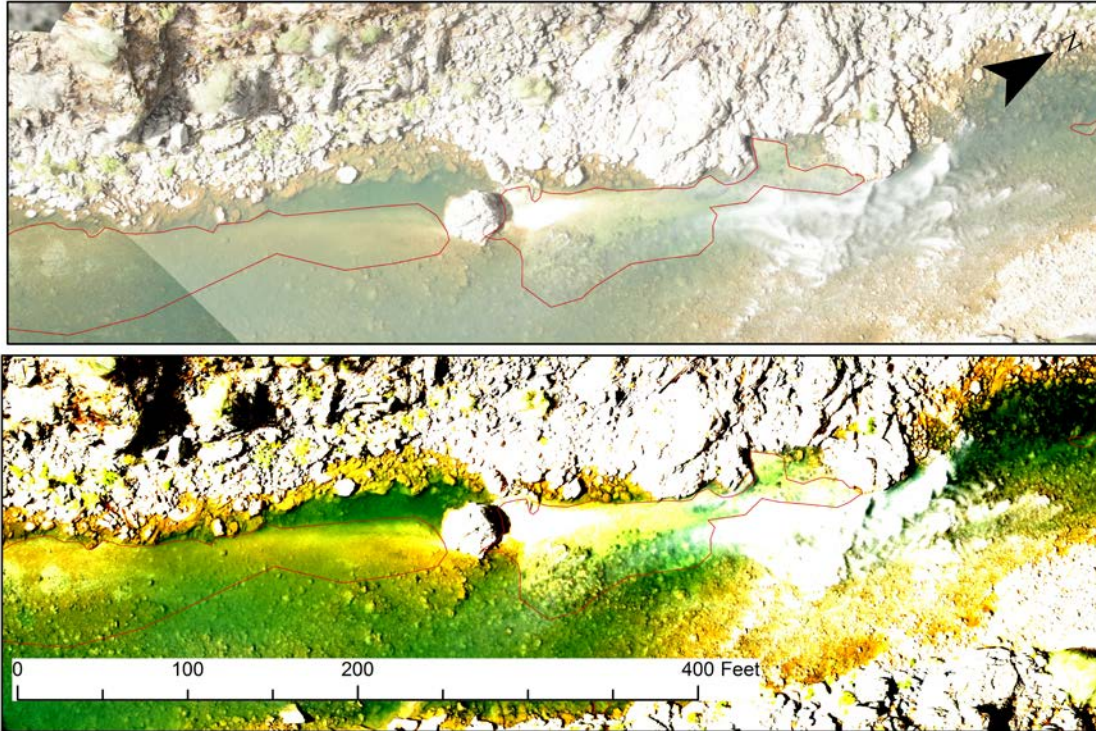
Figure 16. Comparison of bright image (top) and an example of using image filters to identify gravel deposits (bottom).

6.3. 2D Model Validation

6.3.1. Mass Conservation Checks

In a river with a highly complex terrain, there is a risk of poor model performance with mass conservation, especially at low flows. For each simulation, mass conservation error was computed between the specified inflow and the model-predicted outflow. Table 7 shows that flow losses between cross-sections was extremely low and well within accepted standard.

Table 7. EDR 2D model mass conservation performance in this study.

Inflow (cfs)	Outflow (cfs)	% Error
832	831.90	0.01%
862	861.90	0.01%
870	869.91	0.01%
916	915.90	0.01%
951	950.91	0.01%
974	973.95	0.01%

6.3.2. WSE Validation

The first key test that reveals a lot about model performance is the test of the ability of the 2D model to match measured WSE collected during the field campaign. In this test, we utilized data collected via kayak with an echo sounder for 870 and 951 cfs. For the 862 cfs simulation we tried to compare model results against water edge shots collected near the downstream end of the model with an RTK GPS, but the number of observations was too few to make a reasonable analysis of model performance. Given the abundance of WSE data at the other two discharges, it was deemed unnecessary. For reference, the accuracy of bathymetric mapping with the method used in this study is usually in the 0.2-0.5 ft range, but the high variability of the bed roughness in the boulder-bedrock channel can yield larger uncertainties. Further, any slight adjustment of the echosounder below the level of visible detection while portaging the boat around rapids or an adjustment in boat buoyancy (e.g. boat bobbing up and down) could easily yield an observational offset of ~0.01-0.03 ft data gathering periods. Therefore, WSE deviations should fall within the range of topographic uncertainty and not exceed that.

For 870 cfs, the histogram of WSE deviations shows a small tendency toward underprediction, but not enough to warrant adjusting the Manning's n value (Fig. 17, left). The mean signed deviation between observed and 2D-model predicted WSE was –0.07 ft (slight average underprediction by the model), with the mean of the absolute value of deviations 0.10 ft (representing a nonexceedence probability of 54%). Under-predictions were mostly within the -0.05 to -0.15 range, while over-predictions tailed off rapidly after the 0.05-0.01 bin. No deviations exceeded 0.25 ft.

To understand why there are underpredictions and where they are occurring, the longitudinal profiles of observed and predicted WSEs at 870 cfs were evaluated (Fig.

18).   Beginning in the downstream-most section of the model, WSE is slightly overpredicted (0.05 ft on average) until a major hydraulic control is reached where the channel constricts between Sinoro Bar and a bedrock outcrop forming a small bed step with a high-velocity chute. Upstream of that, the model underpredicts WSE by 0.13 ft on average. Similarly, upstream of the major rapid at the USGS gaging station, the model also underpredicts WSE, but only slightly (0.07 ft on average).

For 951 cfs, the histogram of deviations shows a very slight tendency for the model to overpredict (Fig. 17, right).   The mean signed deviation between measured and predicted WSE was 0.04 ft, with the mean of the absolute value of deviations 0.07 ft. Eighty-three percent of deviations were within 0.1 ft and 97% were within 0.25 ft, which is substantially higher performance than for 870 cfs, except for a few outlier points (Table 8).   Over-predictions were mostly within the 0-0.05 ft bin, while under-predictions tailed off rapidly after the 0-0.05 ft bin.   The longitudinal profiles of observed and predicted WSEs for 951 cfs do not show the same pattern of systematic WSE deviation associated with bed steps, but appear more randomly distributed (Fig. 19).

Overall, model-predicted WSE deviations for the EDR 2D model turned out to be significantly smaller than observed bed topographic variability, indicating that the model is valid across a suite of WSE performance indicators. The lack of systematic error in WSE longitudinal profiles between 870 cfs and 951 cfs precludes the existence of a problem in the underlying topographic map or chosen Manning's n values. Instead, the underpredictions in the 0.05-0.25 ft range at 870 cfs may point toward measurable differences in performance of the GPS satellite constellation on the days of WSE data collection. Observational WSE data had some noise, requiring averaging to enable comparison against model predictions.

Table 8. Nonexceedence probabilities for 870 cfs WSE deviations meeting different thresholds of performance.

870 cfs		951 cfs	
WSE Deviation (ft)	Nonexceedence probability*	WSE Deviation (ft)	Nonexceedence probability*
0.025	14%	0.025	24%
0.05	27%	0.05	53%
0.1	54%	0.1	83%
0.25	100%	0.25	97%
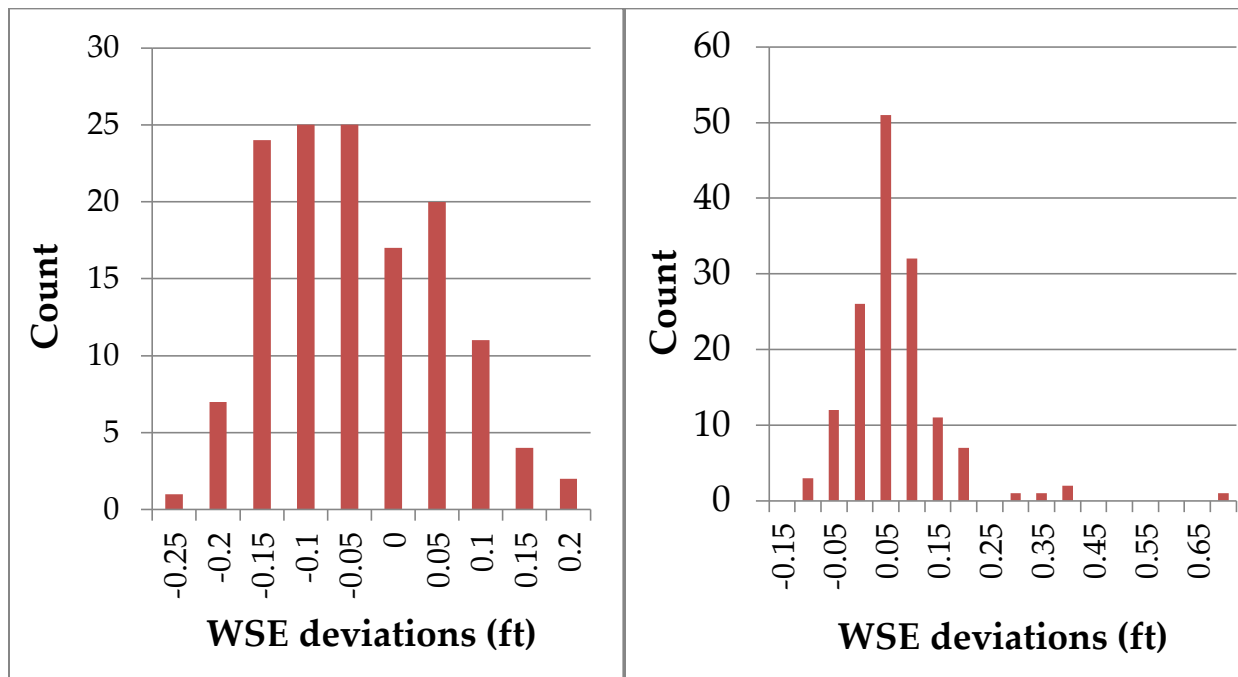
Figure 17. Histograms evaluating 2D model WSE performance at (left) 870 cfs and (right) 950 cfs. Numbers shown are the lower bin values. Negative numbers mean the 2D model underpredicted WSE.
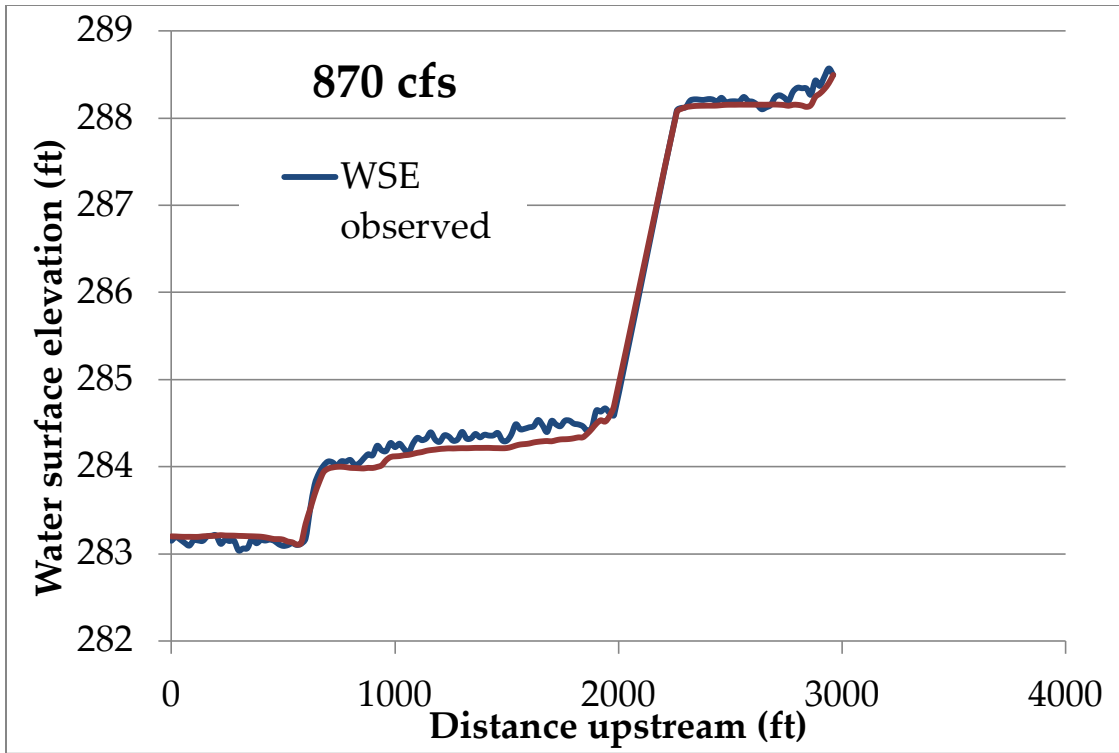
Figure 18. Longitudinal profile of observed and predicted WSEs at 870 cfs.
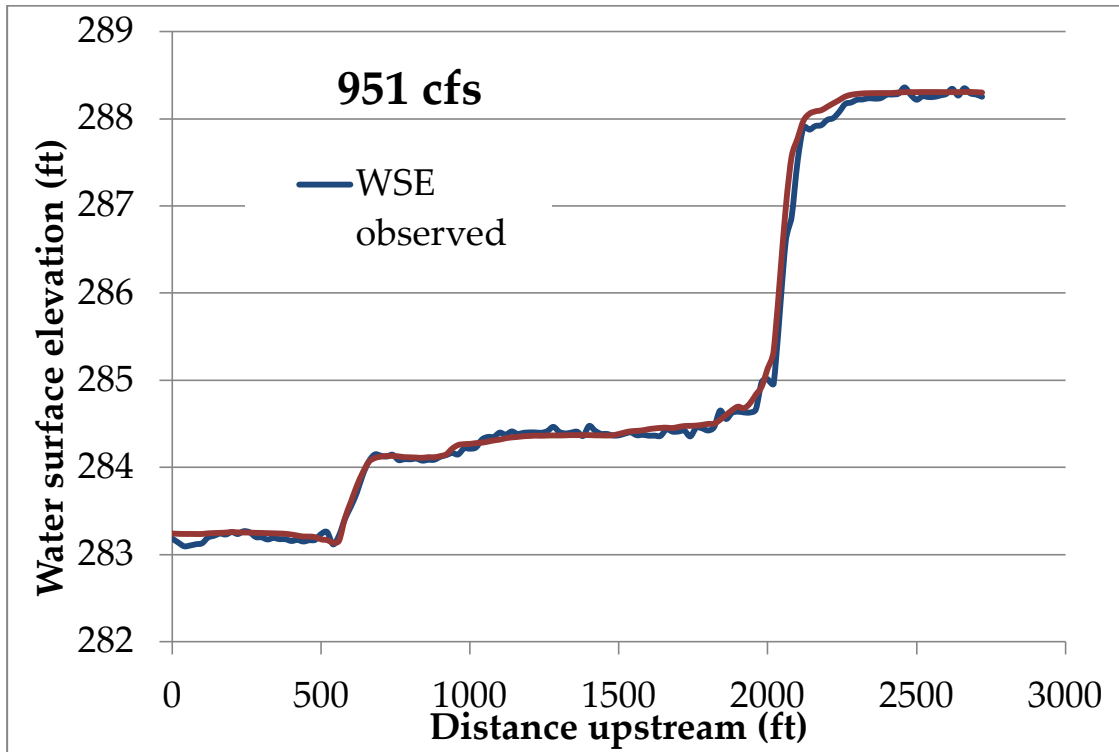
Figure 19. Longitudinal profile of observed and predicted WSEs at 951 cfs.

6.3.3.   Water Speed Validation for 862 cfs

After the determination of WSE validation for 870 and 951 cfs, the next step was to evaluate 2D model performance with predicting velocity magnitude in the direction of flow (i.e. water speed). For this suite of tests, statistical analyses were done comparing observed point velocities using the kayak-based positional tracking method and the 2D-model predicted velocities at the same locations for 862 cfs, which was the flow at which validation data was collected.   This flow is representative of spring-run spawning conditions in September in EDR.   Comparisons between observed and predicted values were done on signed and unsigned percent error, as explained in section 5.2.

Beginning with the analogous tests presented for WSE, velocity was checked for the balance of the statistical distribution of signed percent error around zero (Fig. 20). For all velocity observations, the 2D model overpredicted speed by a signed average of 13% (signed median of 8%). Comparing signed error below and above 2 ft/s, the former was overpredicted by an average of 20 %, while the latter was slightly underpredicted by an average of 0.7 %. The signed analyses suggest the model is yielding velocities that are somewhat too fast for velocities <2 ft/s, whereas the model is pretty much spot on for velocities > 2ft/s. This is a common occurrence in 2D model performance.

For the unsigned percent velocity error, the means for all data, below 2 ft/s, and above 2 ft/s were 26%, 32% and 14%, respectively.   Recall that the standard performance reported in most studies is ~20-30% error on average, so these values are right on par with that. The corresponding medians were lower at 17%, 21% and 11%, respectively. Considering all observations, 58.5 % were within 20% error and 89% were within 50% error (Table 9).

In terms of correlation analysis, the R^2 value for the scatter plot was 0.76 (i.e. R = 0.87 for those who prefer to view the correlation coefficient) for all observations (Fig 21), while for the segregated data on either side of 2 ft/s it was 0.6-0.62 (Fig. 22). The value for all observations is notably higher than most values from previous studies and is on par with that reported by Barker et al. (submitted) for the alluvial LYR. The values for the segregated data are on par with literature values.

Looking at the linear regression relations, the slopes were within 0.82-0.92 and the y-intercepts were within 0.3-0.43. The latter range scales to 5.4-7.7% of the observed maximum depth-averaged velocity. There are no standards specified in previous studies, but these values are within the acceptable validation ranges suggested in section 5.2. Still, the slopes and y-intercepts all indicate a bias of overpredicting low velocities. The observed low velocities tend to occur along the banks, so it is likely that there is additional bank roughness associated with the jumble of shot rock and

fractured bedrock lining the channel. It is unclear what roughness value might be assigned to represent this in the model, since this variability is at a scale finer than a 2D model can legitimately represent. Also, the exact water's edge position varies with discharge, so a strip of high roughness placed at the edge would have to be shifted for each flow simulation, and that seems somewhat arbitrary to apply. Recall that the channel does not require a systematically higher Manning's n value, because the WSE deviations are not uniformly underpredicted at the observed flows.

Overall, the tests of 2D model performance in predicting point-scale water speed in the direction of flow were mostly on par with previous studies, except that the coefficient of determination was notably higher (0.76) and high velocities were predicted with unusual accuracy (median signed and unsigned errors of just 3% and 11%, respectively). Like other models, this one was found to overpredict velocities < 2 ft/s, but this time it cannot be attributed to the turbulence closure scheme, because this time a higher order k-e scheme was used instead of an eddy viscosity scheme. As a result, the error is interpreted to be due to the extremely high complexity of bank roughness that cannot be captured with standard topographic surveying and 2D modeling. Interestingly the overprediction in velocities < 2 ft/s did not result in an underprediction of high velocities (Fig. 22), which is what commonly happens. Instead, velocities > 2 ft/s were predicted much more accurately than reported in the literature.

Table 9. Percent of 2D model velocity predictions meeting different thresholds of performance for all data as well as above and below the 2 ft/s threshold.

All Data		Below 2 ft/s		Above 2 ft/s	
% velocity error	Non-exceedence (%)	% velocity error	Non-exceedence (%)	% velocity error	Non-exceedence (%)
5	15	5	11	5	21
10	30	10	21	10	46
20	59	20	48	15	61
25	69	25	60	25	86
50	89	50	83	45	99
75	93	75	89		
100	96	100	94		
150	99	150	99		
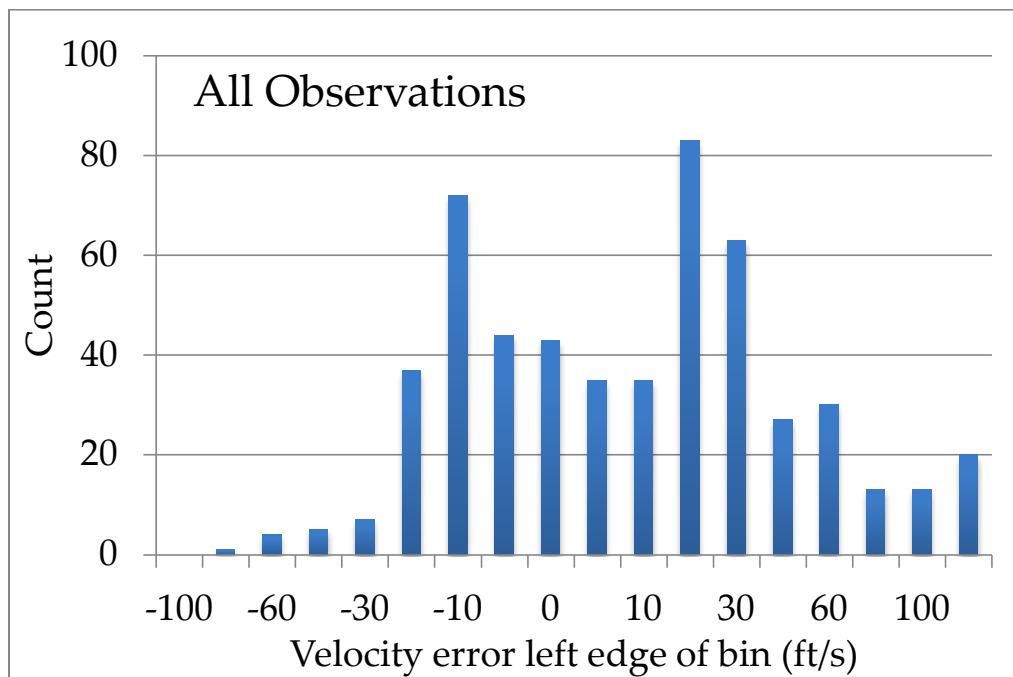
Figure 20. Histogram of percent velocity error.
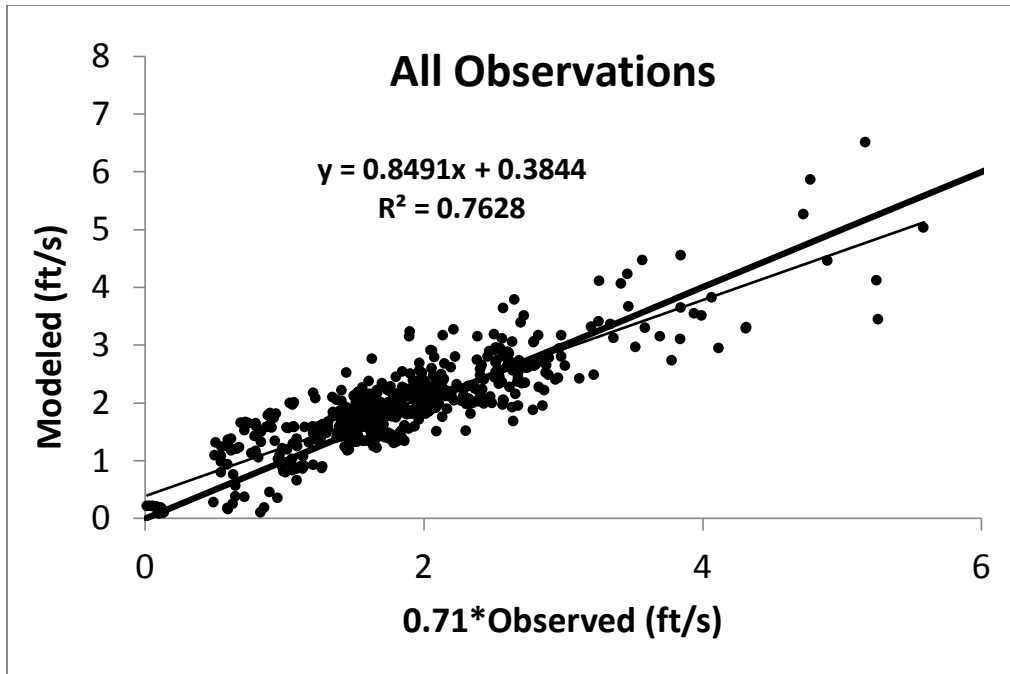
Figure 21. Scatter plot of 2D model predicted water speed versus observations showing linear regression equation and coefficient of variation.
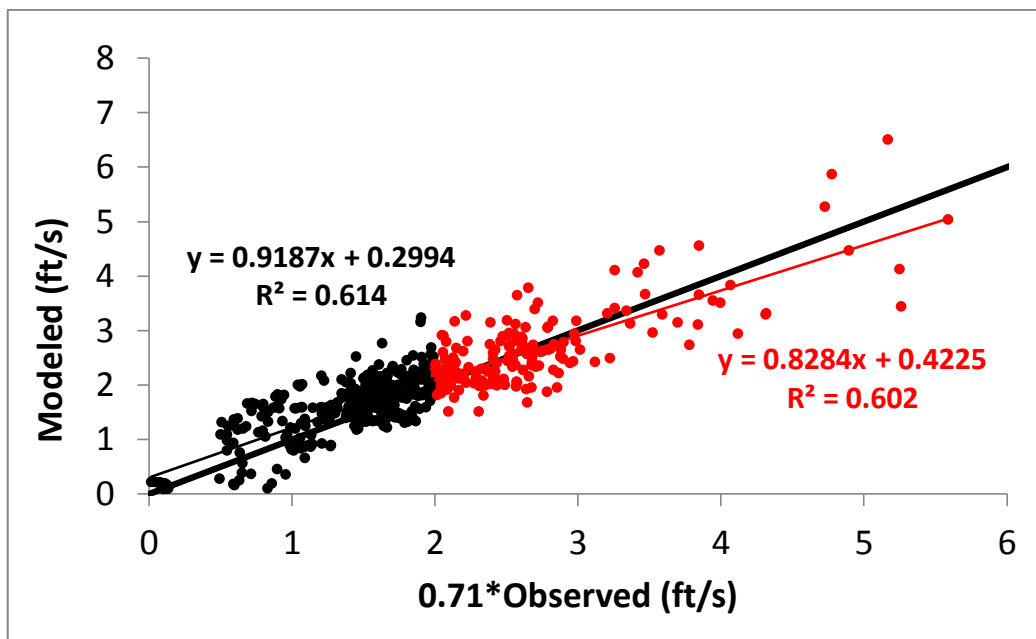
Figure 22. Scatter plot of 2D model predicted water speed versus observations showing linear regression equation and coefficient of variation when the data is segregated at 2 ft/s.

6.3.4. Velocity Direction Validation for 862 cfs

An additional test to validate the 2D model was to compare the observed and predicted velocity direction. The average and median signed angle deviations were 1.3° and 1.1°, respectively, while the same values for unsigned deviations were 5.9 and 4.8 degrees. The histogram of unsigned angle deviations shows that there is a tendency for the model to over-predict the direction of velocity, with the errors appearing to be normally distributed around the mean (Fig. 23). The minimum and maximum raw deviations were -29 and 25 degrees, respectively. The signed mean is higher than reported in Barker et al. (submitted), but still very low, and the unsigned deviation is close to the same. Eighty-three percent of angle deviations were within the 10° threshold desired for good model performance (Table 10). In terms of correlation and regression analyses, the EDR 2D model performed worse than that reported by Barker et al. (submitted). The R^2 was 0.65 (R = 0.81), which is good, but the regression slope was only 0.6 (Fig. 24). Overall, the angle deviations show good performance of the model in predicting direction, but there does appear to be a systematic bias in flow direction in the model where low directions are overpredicted and high directions are underpredicted. The cause of this is unknown and this is only the second study to evaluate flow direction quantitatively, so more studies may be needed before an understanding of the controls on direction error are understood.

Table 10. Percent rank of 862 cfs absolute velocity direction deviations meeting different thresholds of performance for the main flow (e.g. no eddies).

Angle deviation (deg)	Non-exceedance
1	0.115
5	0.516
10	0.833
15	0.938
20	0.99
25	0.998
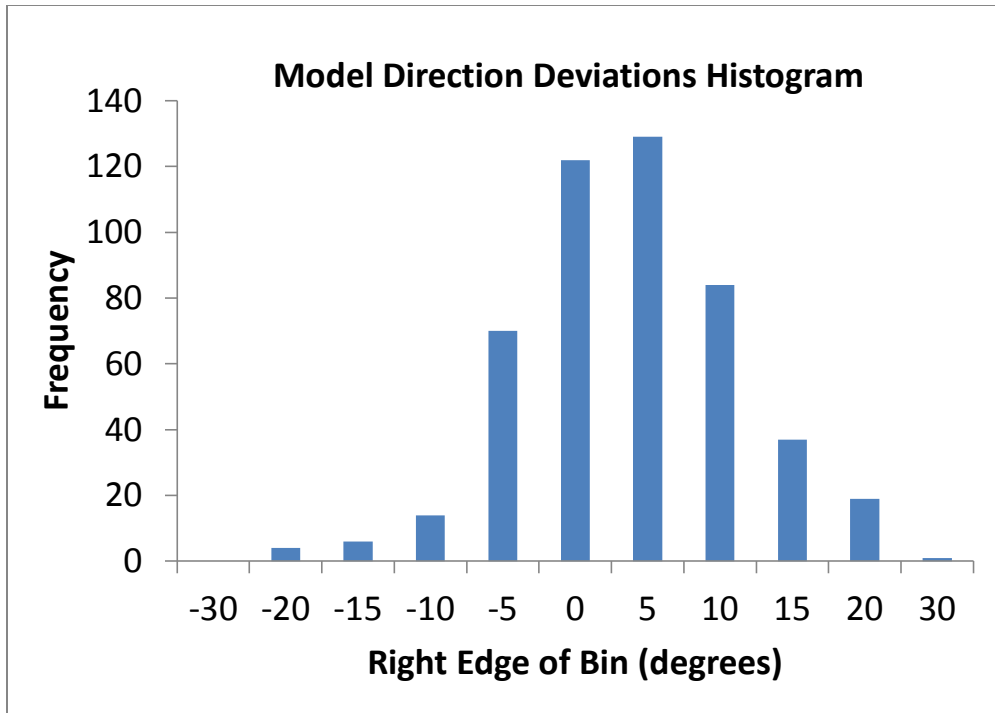
Figure 23. Histogram evaluating 2D model velocity direction performance at 862 cfs, with deviations centered on -5 to 5.
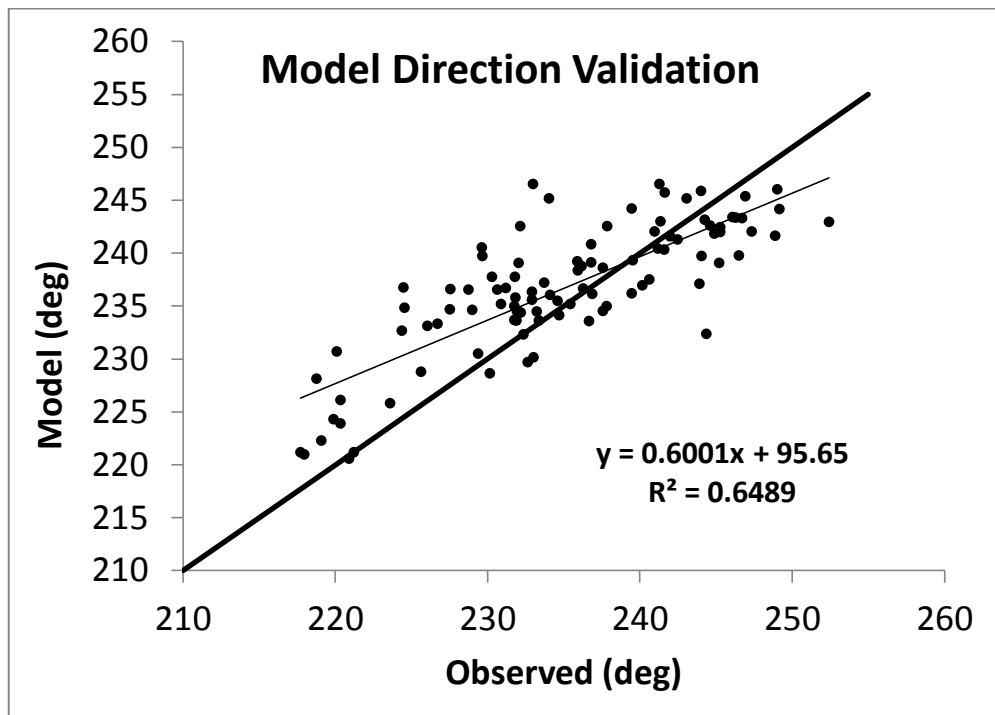
Figure 24. Scatterplot evaluating 2D model velocity direction performance at 862 cfs for the main flow (e.g. no eddies).

6.3.5.   Successes and Challenges with Eddy Prediction

Due to the presence of high topographic complexity on the channel edges from bedrock and large shot rock, eddies of all sizes are found throughout EDR at the simulated baseflows. Similar to the approach of Barker et al. (submitted), this study evaluated model performance at eddies. The two eddies investigated had substantially different hydraulics. The topography and bathymetry of the river was surveyed in great detail throughout these regions (Fig. 25). The tightest point spacing was where the echosounding system was set to record observations at 1 Hz, yielding sub-foot resolution. Emergent bedrock outcrops were intensively surveyed along their sharp facets to accurately represent breaks. Given that in both cases the eddies were ~100 ft long, the amount of topographic points and computational mesh nodes were highly dense compared to the amount necessary to resolve them. Consequently, problems with eddies cannot be due to inadequate mapping of channel topography at the scale of ~1- to 3-foot resolution. Although it was not possible to fully explain the observed differences that were found, it does help to appreciate the inherent uncertainty in use of a 2D model, no matter how detailed the topographic survey may be.

In one instance, there was a large slow eddy behind a large bedrock outcrop that constricted the channel width by more than half the width in an area where the water was relatively slow (Fig. 26, left), so kayak-based particle tracking was used to see how the model would perform at simulating the size and shape of that eddy. The circulation pattern was also filmed using a video camera taking advantage of the abundance of floating plant debris revealing the pattern. Beneath the eddy there was a bedrock outcrop protruding up out of the bed midway down the river, so there was a significant chance this feature would impact velocity when floating over it. The circulation pattern present (as mapped with RTK GPS, videography, and kayaker experience) was a double vortex in which the bank outcrop did indeed push the flow away from the bank and back upstream to the tip of the larger outcrop that creates the eddy; then the flow turns both inward and outward, with the inward flow going along the outcrop back to shore and then downstream along the bank until it gets to the small bank outcrop where it completes the circle. The presence of the double vortex eddy in reality is illustrated in Figure 26 (right) by the red arrows. Videos are available from the authors on request. The arrows point in the direction the water was flowing. As it turns out, water recirculating up the eddy in the 2D model was also deflected toward channel center by the bed protrusion (no matter whether the k-e or eddy viscosity turbulence closure scheme was used), which then caused a second recirculation cell to emerge upstream of that. The 2D model predicted flow pattern is illustrated in Figure 26 (right) by the black arrows. There is a remarkably close match of red and black arrows in both the eddy as

well as in the thalweg in the top left of the image away from the eddy. This highlights model sensitivity to topography that has not been reported before and also shows that a 2D model can capture a large, complex eddy correctly.

The second instance involved a long, narrow recirculation on river left caused by the second bed step (see Fig. 19) and the associated hydraulic constriction (Fig. 27). This time the water was shallow and flowing over a highly rough bed. The observer experience floating in the eddy was that the water moved swiftly upstream along the bank, despite the roughness. The GPS data indicated velocities of ~0.5-1.0 ft/s. This time the model also did very well at predicting the upstream velocity speed and presence of the eddy, but in the model the eddy attached to the bank sooner than it did in reality. Given how localized this effect is, it is difficult to provide a specific mechanistic explanation.

The overall conclusion from the evaluation of these two eddies is that having a very high point density from the topographic/bathymetric survey density (point spacing of ~ 1-3 ft) goes a long way toward helping there be a good match between real and predicted 2D flow field. Nevertheless, in both case there are small details that are not exactly matched.
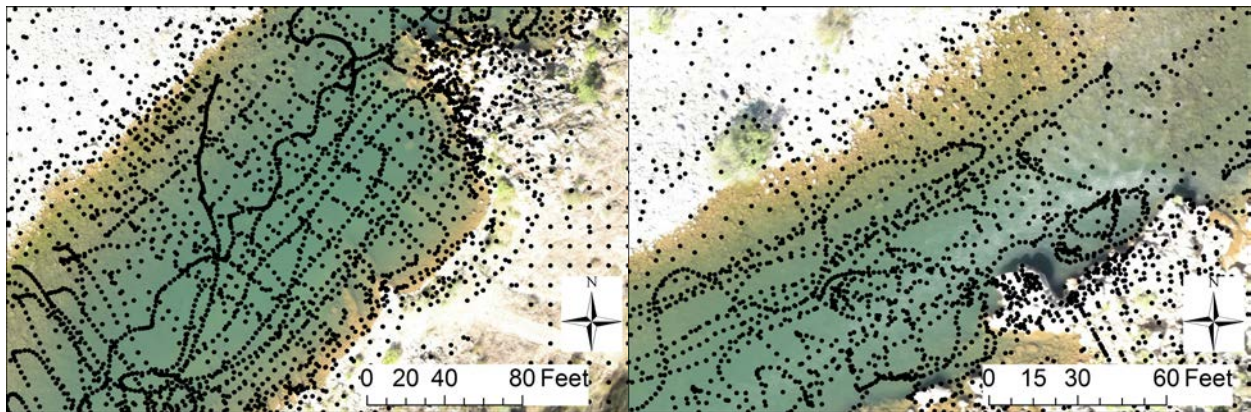
Figure 25. Elevation survey points in the region of two different eddies investigated to understand model performance with these features.
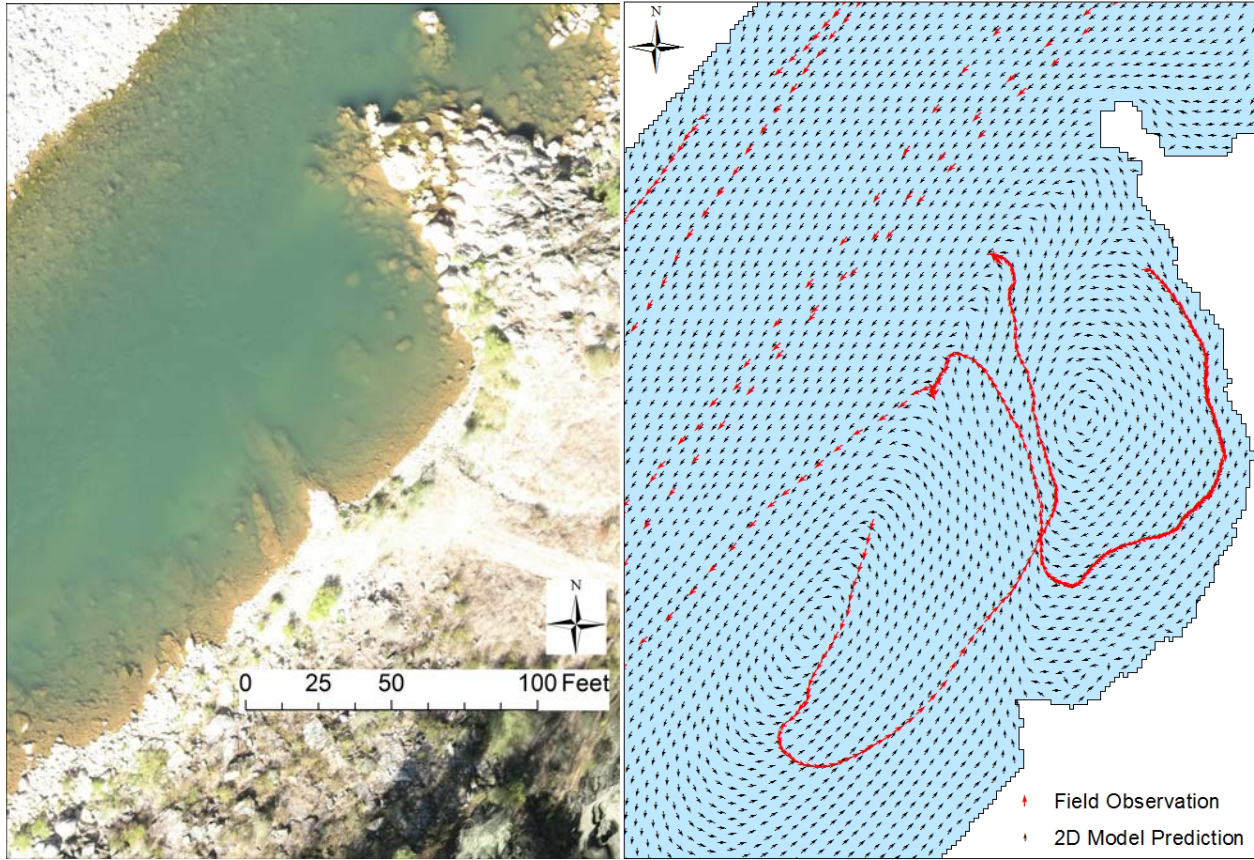
Figure 26. Blimp image, flow direction observations, and 2D model predicted flow directions for a two-cell eddy on river left near the beginning of Sinoro Bar ~700 feet upstream of Narrows Gateway. Red arrows show observed directions and black arrows show model-predicted directions.
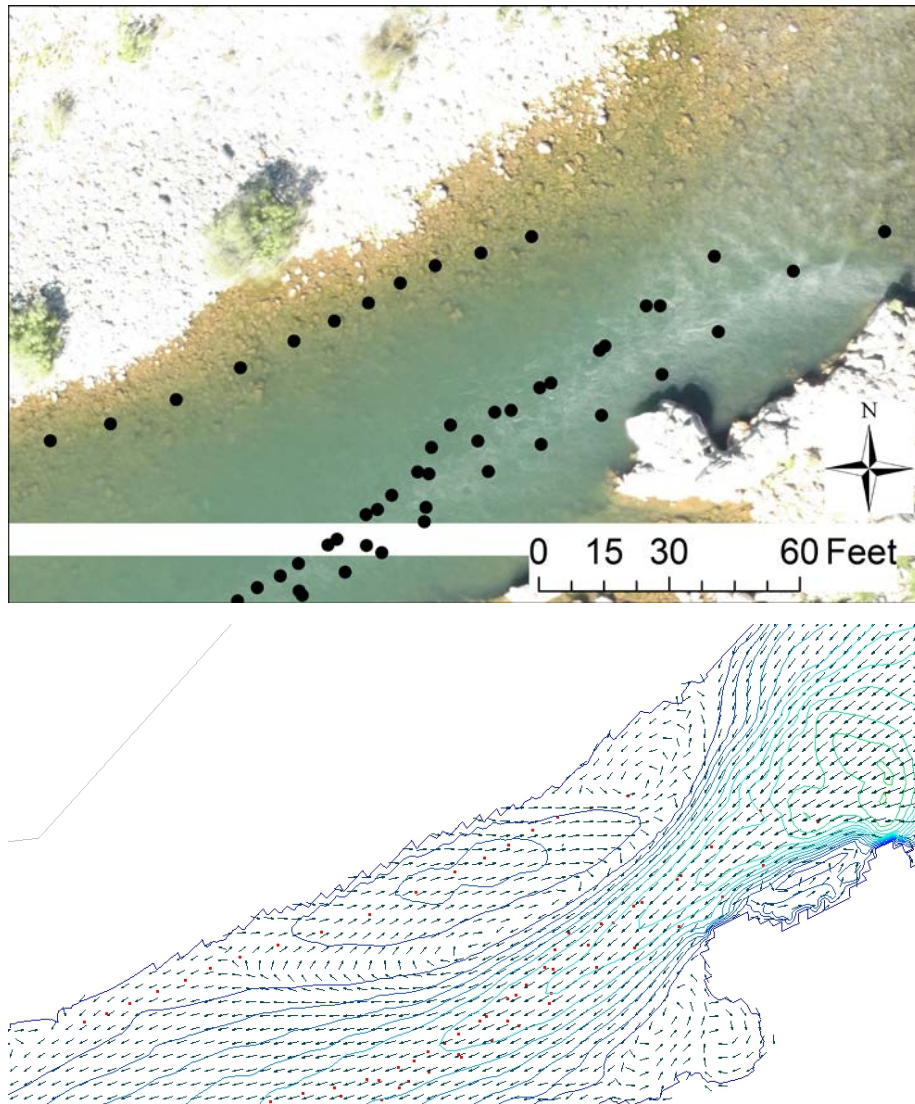
Figure 27. Blimp image and 2D model simulation of an eddy on river right below the bed step opposite Sinoro Bar. The model matches it well, but the eddy reattaches to the bank too soon downstream.

6.4.   Redd Observations

The first step in assessing redd use was overlaying the observed data with the visually identified sediment deposits. All observed redds were located in areas of new gravel deposition, as identified from blimp- image analysis (Fig. 28). Considering how little of the total sediment deficit this initial injection addressed (~8 %), it is remarkable that any habitat was created downstream at all. Further, spawning was focused in three distinct clusters (Fig. 29), and not necessarily where there was the most deposition. Notably two of the clusters were in association with pre-existing, excessively coarse alluvial bars

(Fig. 29, left and right), while the third was upstream of a bedrock outcrop that promoted deposition there (Fig. 29, middle), but no so much as to yield an emergent bar, as occurred just below the main rapid and above a house-sized boulder (Fig. 28, middle). The upper cluster had approximately 24 redds, while the other two had 12 redds each. All redds were relatively close to the water's edge, because there is no channel-spanning alluvial riffle landform in the EDR.

The visual sediment data collected by Campos and Massa (2012) were averaged for each cluster of observed redds, with cluster 1 being the most upstream area and cluster 3 being the last in the study site. Clusters 1 and 2 had the finest distribution with D_{50} and D_{84} values of approximately 20 and 90 mm. The most downstream cluster (3) was coarser as expected with D_{50} and D_{84} values of approximately 90 and 150 mm. Cumulatively, redds were associated with finer material in that 36 of the 48 redds were in clusters 1 and 2. Cluster 1 corresponds with site 1 of the pebble count observations (Fig. 9) and the results were fairly similar. In contrast, Cluster 3 was in the water adjacent to terrestrial pebble-count site 4. As a result of the higher velocities where fish spawn compared to on the bank, the sediment is coarser in the spawning cluster than on the bank. Overall, the results confirm the wide range of sediment sizes that Chinook spawners in the LYR will use, as previously documented by Moir and Pasternack (2010). If the velocity is higher, then adults are content to spawn in beds with sizes of 150 mm and if it is lower, then they will use sizes down to 20 mm.

Figure 28. Observed redds and polygon boundaries of visually identified gravel deposits.
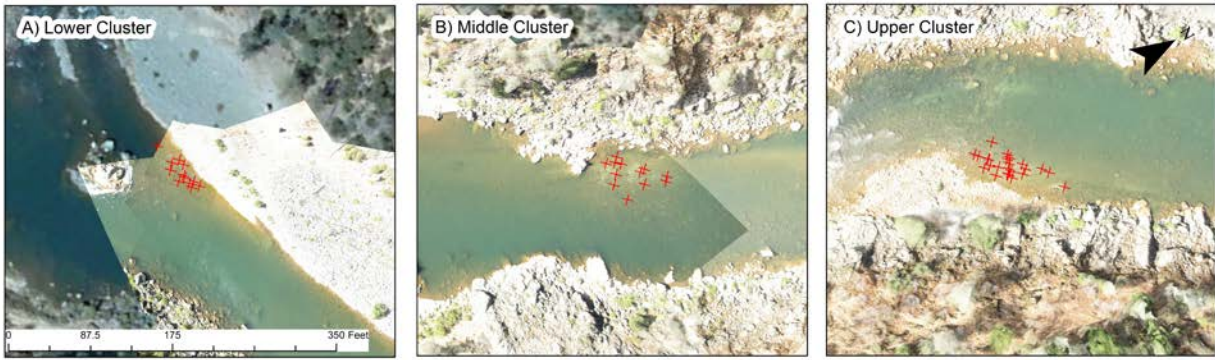
Figure 29. Zoomed in views of the three spawning clusters observed showing that they occurred on deposits fomr the gravel injection, though fill depth was variable.
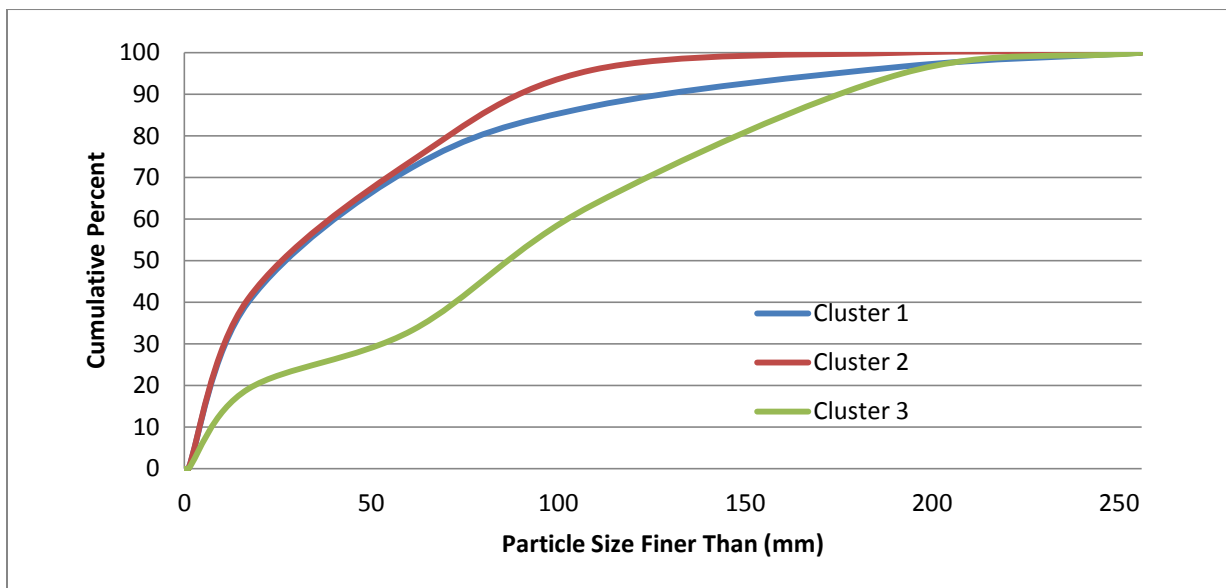
Figure 30. Average sediment size distributions recorded at observed redd clusters. Cluster 1 is the most upstream and cluster 3 is the most downstream.

6.5. TCD and Sediment Budget Analyses

Results of topographic change detection come in the form of final adjusted DoD rasters where the LoD for each pixel was subtracted out and any pixels with changes within 0.16′ were excluded. The final DoD rasters exist for upstream and downstream areas as well as for three different epochs (December 2007 - January 2011, January – October 2011, and December 2007 – October 2011). Summaries of the results were in the form of

tabular amounts, spatial plots, and elevation change distributions for erosion and deposition.

6.5.1. Upstream TCD

For the injection period, the spatial patterns of gravel deposition are consistent with the overall riffle design in the GAIP (Pasternack, 2010) with a large central bar in the middle of the river with two chutes on both sides (Fig. 31, left). Downstream of the bar the gravel was arranged in more of blanket fill, with subtle variations in topography. For the post injection period, the spatial pattern of erosion (Fig. 31, middle) conformed well with the overall patterns of Shields stress shown in the GAIP for 10,000 and 15,000 cfs (Pasternack, 2010), demonstrating that these flows are sufficient to move the size mixture specified in the GAIP. Despite erosion occurring during the time between the gravel injection and the 2011 fall survey campaign some gravel did persist in the upstream injection area (Fig. 31, right).

A quantitative perspective can now be gleamed from analysis of tabular data (Table 11). From December 2007 to January 2011 TCD analysis predicted 4,010 tons of deposition. For the 2010-2011 injection there was ~5,000 tons of gravel added into the river (with slightly more than 5,000 tons delivered to insure that contractual obligations were met, but no exact accounting of what went into the river possible in light of some losses after delivery as a result of left-overs in the delivery area, rejections at the hoper, and spillage at pipe clogs), leaving ~990 tons unaccounted for. It is inferred that this material was stored in the as-built state of the project in the unmappable rapid at the entrance of the injection site and ~10 tons never made it into the river and/or washed downstream beyond the mapped as-built survey. This is consistent with the high fill depth where mapping was able to begin, as the onset of fill cannot be a wall of gravel/cobble due to the physics of slope stability of non-cohesive porous media.

During the time between January to October 2011 when high flows were entraining injected gravel/cobble, the analysis predicted 2,005 tons of erosion in the upstream injection area (Table 11), meaning that ~40 % of the original injection material eroded and transport downstream. The highest flow recorded within this period was 19,530 cfs. The results of TCD analysis from December 2007 to October, 2011 suggest that 2,675 tons, or 47% of the total injected 5,000 tons, remained in the upstream area for use in spawning in autumn 2011 and possibly beyond.

A last step in interpreting the upstream adjusted DoD is inspection of the elevation change distributions, which can provide insight into how the topographic change was distributed through erosion and deposition for the three upstream epochs (Fig. 32, left). As expected, from December 2007 to January 2011 injection deposition dominated the

elevation change distribution with most deposition ranging from 0 - 2 feet. From this period until the October 2011 monitoring campaign erosion dominated the elevation change distribution, with most erosion being < 2 feet (Fig. 32, middle). The net effect of this is that from December 2007 to October, 2011 net deposition dominated the elevation change distribution (Fig. 32, right), as a significant amount of the injected material stayed in this section of river despite the high flows (Fig. 5).

Table 11. Upstream injection area volumes of erosion and deposition by epoch.

Period	Erosion (Short Tons)	Deposition (Short Tons)	Net (Short tons)
December 2007 to January 2011	0	4,010*	4,010*
January to October 2011	2,005	99	-1,906
December 2007 to October 2011	16	2,675	2,659

*it is inferred that ~990 tons of material was stored in the as-built state of the project in the unmappable rapid at the entrance of the injection site and ~10 tons never made it into the river and/or washed downstream beyond the mapped as-built survey. This is consistent with the high fill depth where mapping was able to begin, as the onset of fill cannot be a wall of gravel/cobble due to the physics of slope stability of non-cohesive porous media.
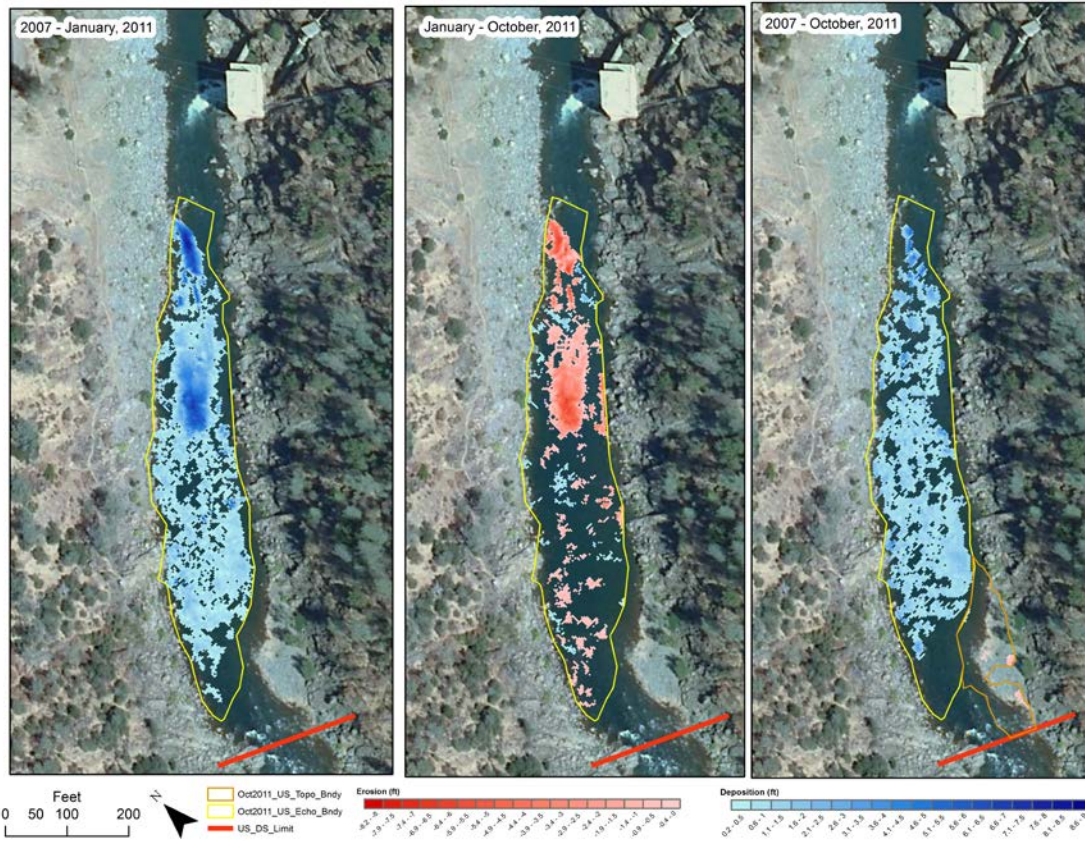
Figure 31. Upstream injection area patterns of erosion and deposition by epoch.
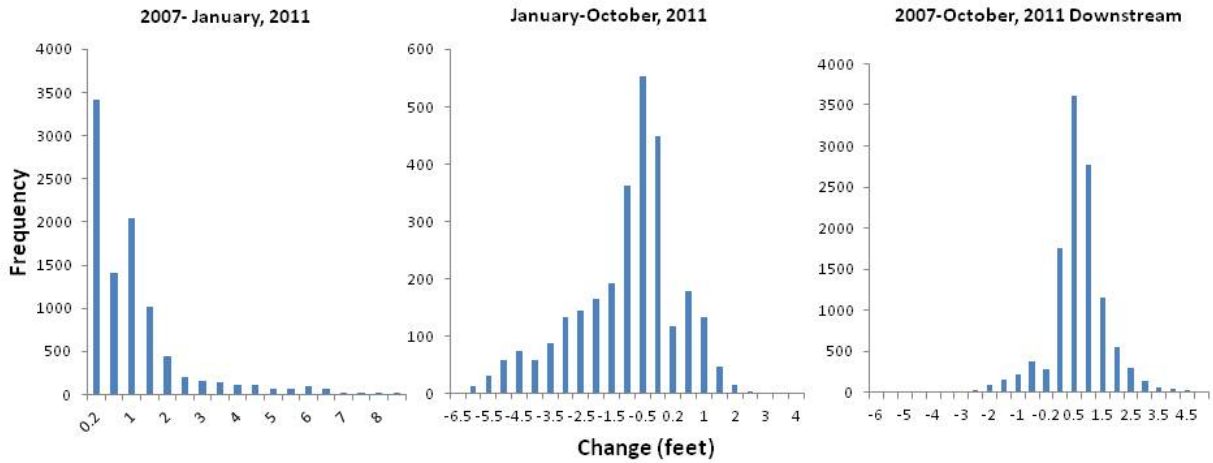
Figure 32. Elevation change histograms for the upstream epochs.

6.5.2. Downstream TCD

The purpose of the downstream TCD and sediment budget analyses was to determine where gravel/cobble form the injection site went down the river. The deepest deposit occurred between the large rapid downstream of the USGS gaging station and the house-sized boulder just downstream of the rapid (Fig. 15, middle; Fig. 33, far right). Widespread deposition occurred in deep areas throughout this region. There was one area of moderate net erosion at the second bed step (Fig. 19; Fig. 27; Fig. 33, left). This is inferred to be a result of convective acceleration around the bedrock outcrop there during the various high flow events in the 5-year epoch between surveys. Some of the erosional material scoured in this area may have re-deposited just downstream where the channel widens yielding no net change, or else some of that may have been exported to the Narrows Reach. As shown in Table 12, a volume of 698 tons of erosion and 3,606 tons of deposition was estimated for the downstream area. The net effect was deposition of 2,908 tons of gravel. Similar to the upstream area, most of the change was from deposition of 0.5 - 2.0 ft, but note that the tails of the elevation change distribution are fairly long, suggesting that topographic change occurred at a variety of scales (Fig. 34).

Table 12. Downstream area volumes of erosion and deposition.

Period	Erosion (Tons)	Deposition (Tons)	Net (tons)
December **2007** to **October 2011**	698	3,606	2,908
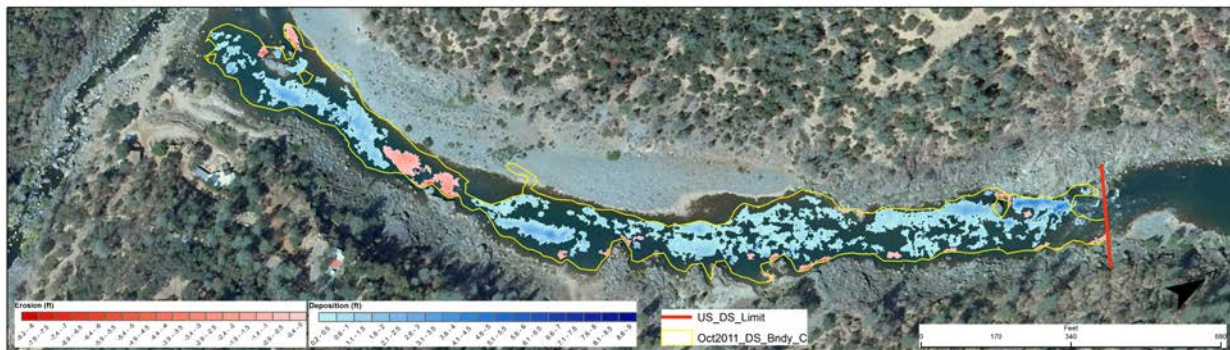
Figure 33. Spatial patterns of deposition and erosion for the downstream area for the one epoch investigated.
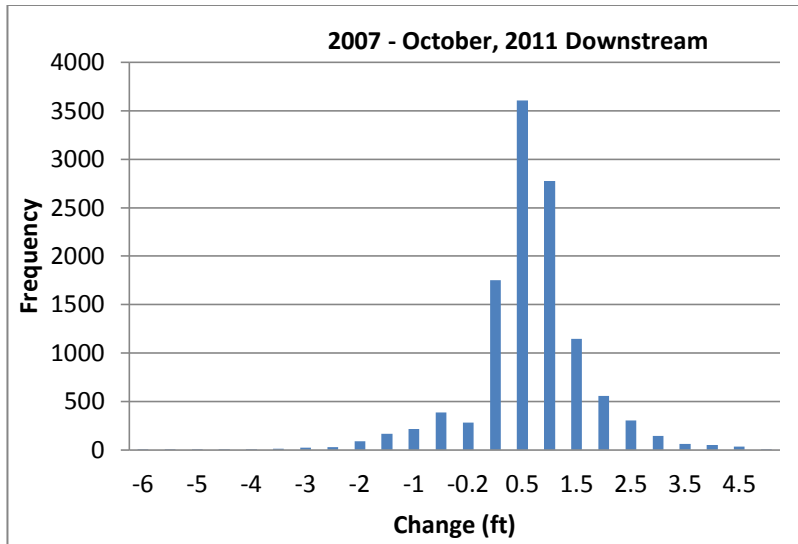
Figure 34. Elevation change histograms for the downstream scenario with +/-0.16 feet excluded.

6.5.3. Sediment Budget For 2010-2011 Project Fate

Beginning with ~5,000 tons of gravel/cobble injected into the river in the injection zone, there was a residual of 2,659 tons deposited in the upstream area above the main rapid in October 2011. That means 2,341 tons moved to the downstream area where an additional 698 tons were added by redistribution of locally eroded material. Together, that sums to a supply of 3,039 tons for the downstream area. A gross of 3,606 tons of depositional material was estimated from the final adjusted DoD, so that yields a mathematical surplus of 567 tons. In other words, there was 567 tons additional material found in the river through TCD than the ~5,000 tons placed during the gravel injection. Given the high topographic variability of the bedrock-shotrock riverbed and some uncertainty of the exact total injection input, a residual error of ~10% to the sediment budget is very reasonable.

The excess material might be explained by improved mapping and topographic representation of boulders in the October 2011 survey compared to the December 2007 survey. Surveying submerged boulders is difficult to control, because they cannot be seen and are often not evident until the map is made. Such features end up having a higher topographic variation in the raw DoD than in the combined LoD, so they end up in the final DoD after accounting for uncertainty. Even though a cutting-edge uncertainty analysis was included to diminish the effects of topographic variability in each survey and the propagation of that error, it is a difficult setting in which to assess change via any modern method.

A key outcome of the budget analysis is that there is no reason to think that any

measurable amount of injected sediment went downstream of EDR into the Narrows and beyond. Small pebbles were seen at the entrance to the Narrows Gateway rapid, but the amount observed was too little to exceed topographic uncertainty in the DEM differencing analysis and no substantial deposits were observed in a reconnaissance of the Narrows Reach. Thus, the injected material predominantly stayed in EDR despite a long duration of flooding. It is possible and expected that eventually the sediment will move out of the reach, and as called for in the GAIP, that amount will have to be accounted for by additional injection.

6.5.4. Channel Geometry and TCD

The amount of topographic change associated with water depth predictions can reveal whether or not deposition is occurring preferentially in areas that are favorable for spawning or alternately where it is excessively deep, which goes toward evaluating the mechanisms presented in Table 2. As a reference for shallower and deeper water, the depth raster for 862 cfs was used. Scatter plot analysis revealed that most deposition was distributed through a wide range of depths spanning 1-14 ft with somewhat higher amounts of deposition at about 2 -4 ft and 8-10 ft of water depth (Fig. 35). Erosion was relatively focused on areas that were between 6-8 ft of water depth. Neither deposition (R^2 = 0.002) or erosion (R^2 = 0.003) showed a statistically significant correlation with water depth. This confirms that the topographic controls on sediment dynamics are not a simple function of detrended bed elevation. Histograms of water depth for deposition and erosion simplify the presentation of the data and confirm that both occurred at a range of depths (Fig. 36). The important result is that deposition is not a simple function for water depth, but is more likely linked to the diverse scale-dependent mechanisms explained in Table 2.

The covariances of flow width at the three discharges versus VPN, detrended, standardized bed elevation versus VPN, and flow width vs detrended, standardized bed elevation show that 1) scale dependent controls on TCD are present as hypothesized, 2) this changes longitudinally in the river corridor, and 3) flow width explains a good amount of TCD, but not all change (Figs. 37-39). Note that by scale dependent it is meant that different relations between channel geometry variables as well as between those and VPN occur at different discharges. There are some locations where width and bed elevation each affect VPN independently and there are some where they work together, such as where they covary positively (wide plateaus and narrow troughs) or negatively (narrow plateaus and wide troughs) (Fig. 39). Bivariate R^2 values show that there are some interdependent fluctuations in covariances, but the more different the flow is, the more the pattern of co-dependence changes (Table 13). For example, the R^2 between covariances for widths at 862 and 5,000 cfs versus VPN is

very high, but that between covariances for widths at 862 and 21,100 cfs versus VPN is low.

From station 2,500 to ~ 2,000 VPN is positively associated with the 862 and 5,000 cfs flow but not the larger 21,100 cfs event as this section of the river has a steep hydraulic geometry rating curve where large flows transport sediment downstream (Fig. 37). At smaller flows this area is a relative expansion which is why there is a positive covariance for those flows. Recall the emergent gravel bar from the cover of this report, which is located approximately at station 2,000. The covariance of only the 862 cfs flow with VPN peaks at 1.7, while for the other two larger flows it is negative, which suggests that the expansion of flow width at larger flows was not a mechanism for TCD, but more complex hydraulic mechanisms or even simple obstruction forcing phenomenon may be responsible. For example, if the channel is constricted by an outcrop, then deposition may be preferentially occurring there due to highsiding on the upstream face of the outcrop or eddying out behind it. Downstream the river corridor towards Sinoro Bar relative wide areas are found at both of the two higher flows. For example, at stations 900 to 800 deposition was found in the channel, slightly more preferential to river left, and high covariance's greater than 2 standard deviations were found for all flows which suggests that this area is a relative expansion at all flows influencing TCD. A scale dependent mechanism of erosion was found at approximately station 600, where the TCD analysis showed pool scour associated with a bedrock outcrop. The covariance analysis supports this because there is a negative covariance for both the 5,000 and 21,100 cfs events, but not at 862 cfs, suggesting that this area is a relative contraction where scour would be focused at sediment mobilizing flows. Towards the downstream end of the reach at approximately station 170 there is a covariance greater than 4 (4 standard deviations) showing that at all flows this area is relatively wider and correlates positively with gravel stored in this area.

Overall, the complex behaviors observed in EDR demonstrate that topography is the dominant factor influencing sedimentary processes. Topography consists of patterns of variation layered on top of each other, like a piano chord consisting of multiple keys held down at the same time- each generates its own frequency and together they produce a harmony or discordance. The river behaves the same way, and the challenge is to deconstruct what the keys are and how the chord functions. That is what this suite of analyses has yielded.

Table 13. Coefficients of determination (R^2) between covariances to evaluate if width, bed, and VPN variations are interdependent. Values >0.25 (grey boxes) are statistically significant and physically meaningful relations.

Covariance	C(W5k,Z11std)	C(W21k,Z11std)	C(Z11,VPN)	C(W862,VPN)	C(W5,000,VPN)	C(W21,100,VPN)
C(W862,Z11std)	**0.426**	0.163	0.026	0.088	0.060	0.094
C(W5k,Z11std)		**0.654**	0.005	0.043	0.092	0.022
C(W21k,Z11std)			0.004	0.014	0.024	0.030
C(Z11,VPN)				0.0001	0.004	0.036
C(W862,VPN)					**0.282**	0.013
C(W5,000,VPN)						**0.445**
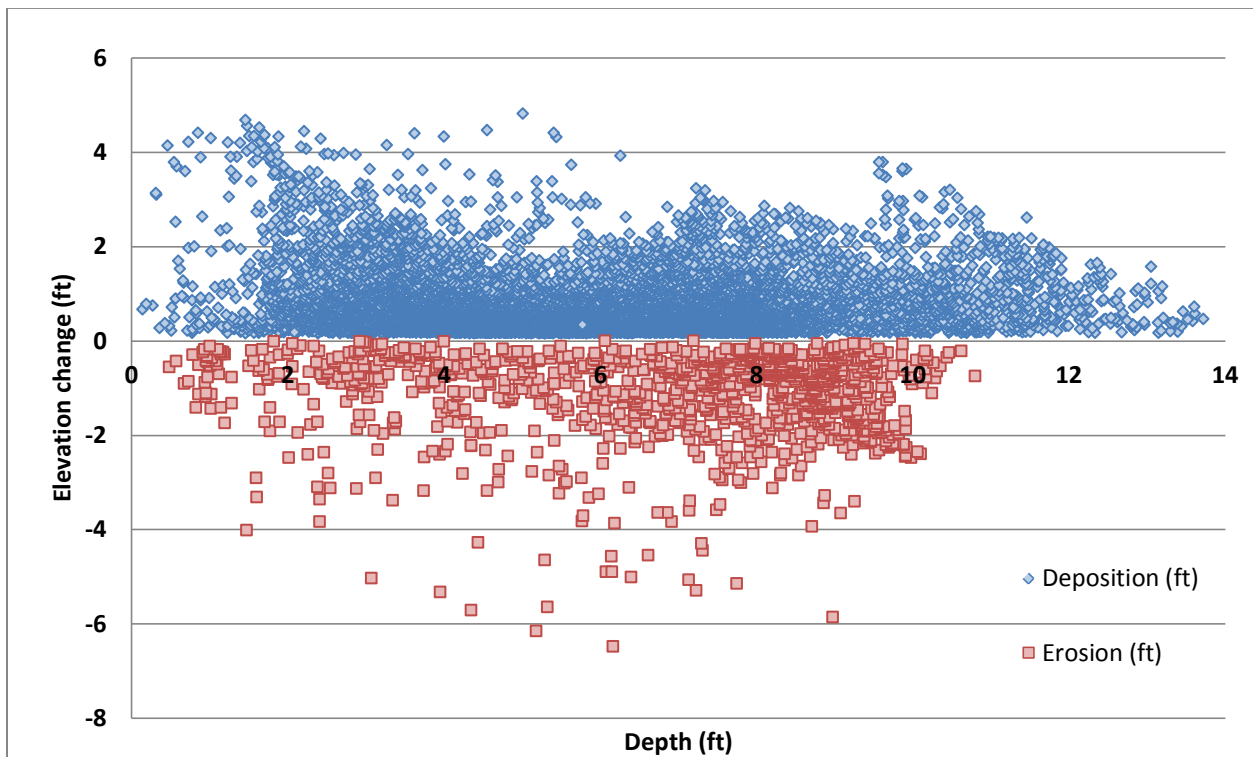
Figure 35. Topographic change for the 2007-October, 2011 period plotted against water depth at 862 cfs.
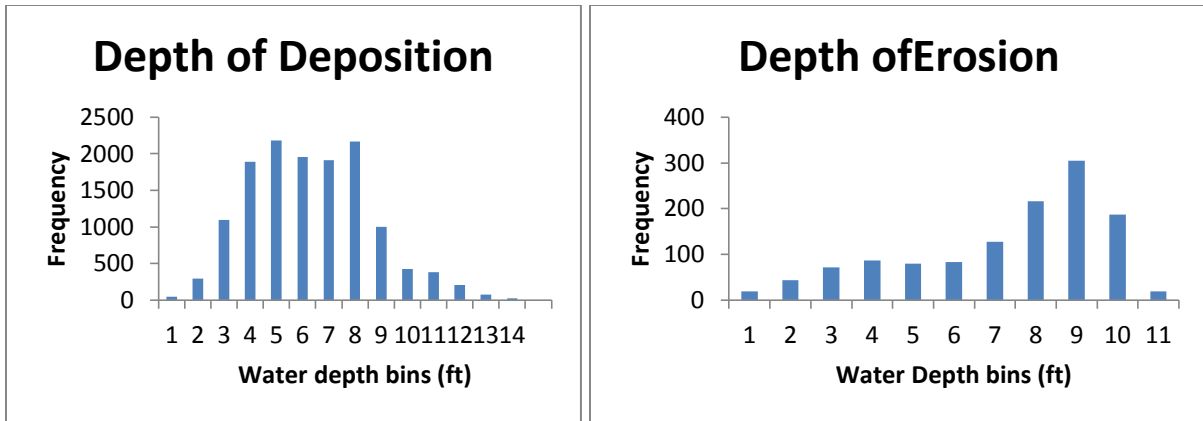
Figure 36. Histograms of depth associated with erosion and deposition. X-axis numbers are the right limit of each bin.
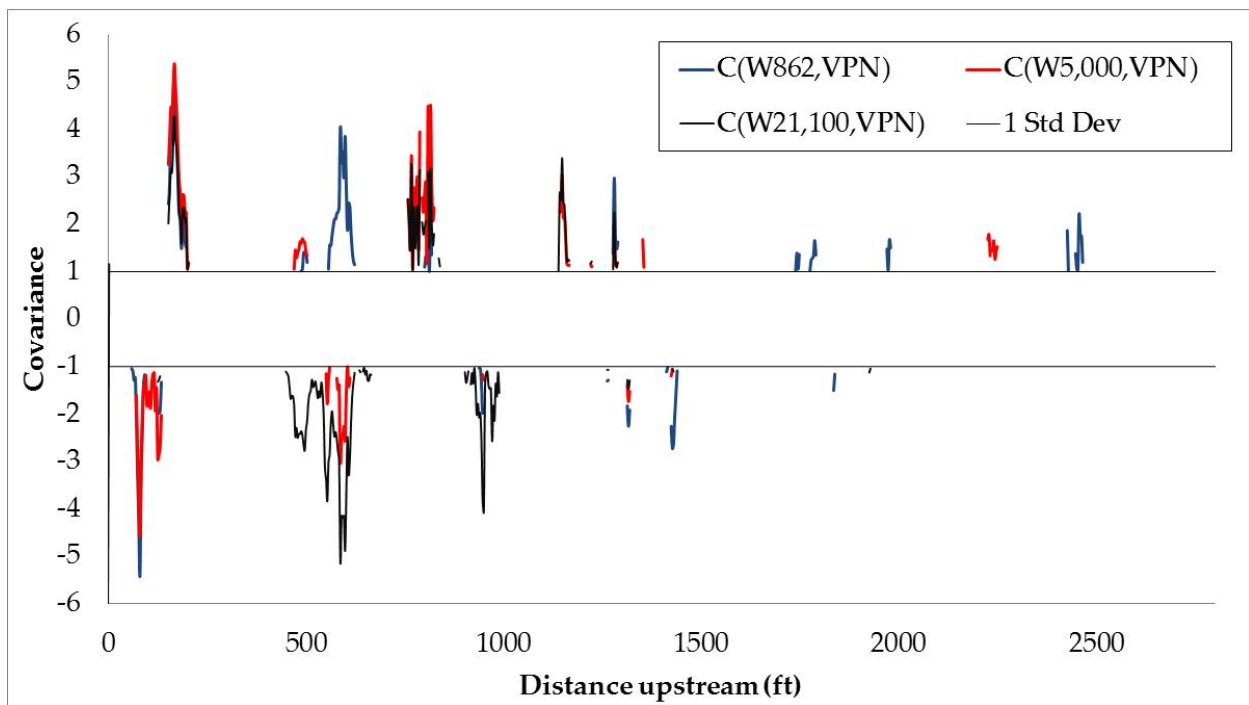
Figure 37. Covariance of 2D modeled flow width (W) at different discharges (862, 5,000, and 21,100 cfs) and VPN through river corridor. Only values with deviations greater than one standard deviation are shown. High positive values are locations where deposition occurs in expansions, while strongly negative values are locations where deposition occurs in constrictions.
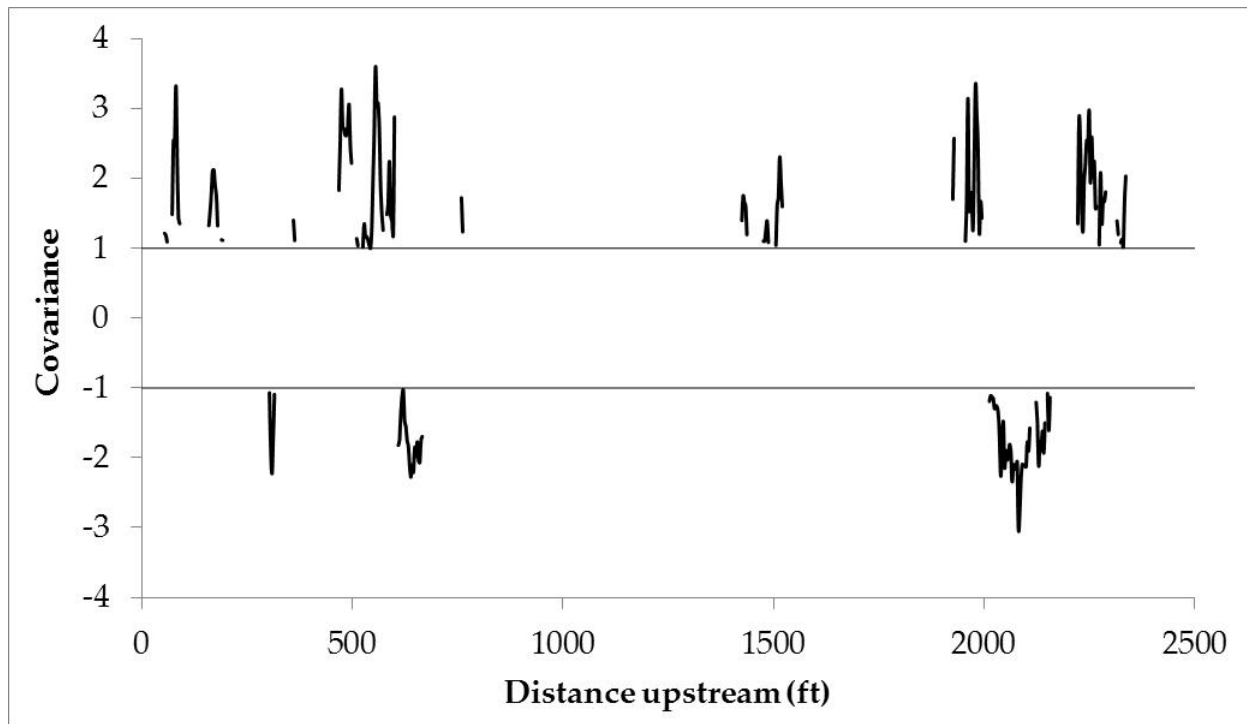
Figure 38. Covariance of detrended, standardized bed elevation (Z11std) and VPN through river corridor. Only values with deviations greater than one standard deviation are shown. High positive values are locations where deposition occurs on unusually high bedrock/shotrock plateaus, while strongly negative values are locations where deposition occurs in the deepest troughs.
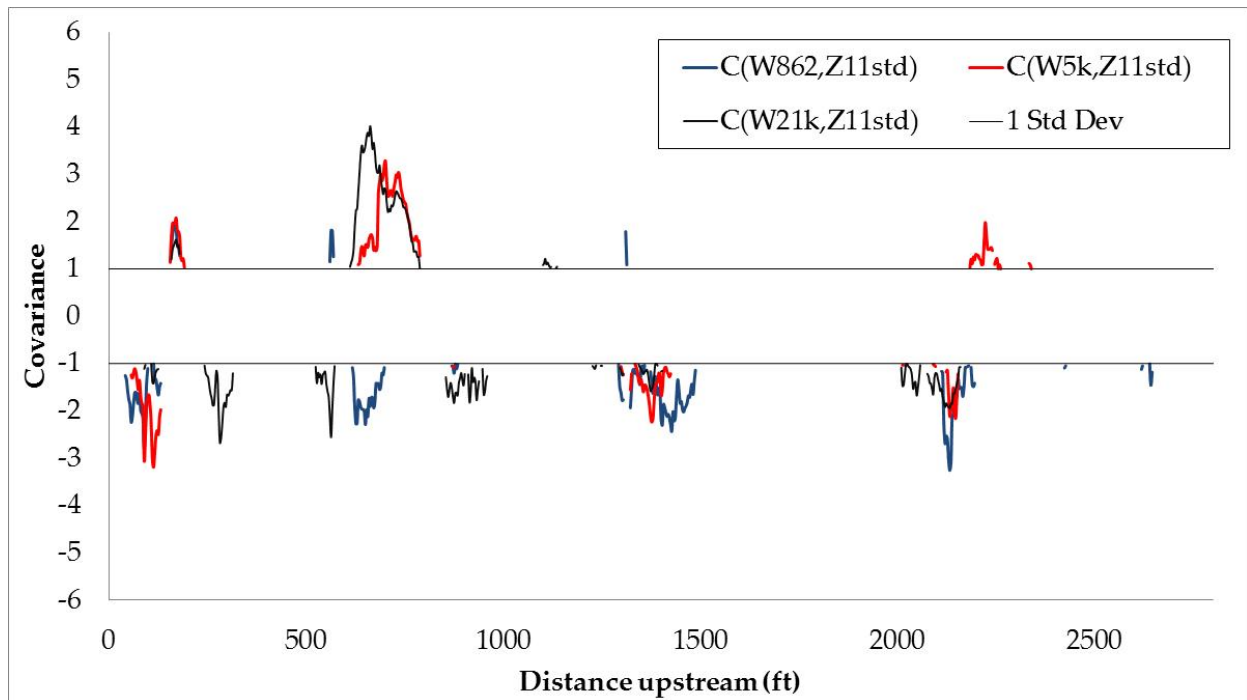
Figure 39. Covariance of 2D modeled flow width (W) at different discharges (862, 5,000, and 21,100 cfs) and detrended, standardized bed elevation (Z11std). Only values with deviations greater than one standard deviation are shown. High positive values are locations where there are wide plateaus. Strongly negative values are locations of constricted toughs.

6.5.5.   Gravel/Cobble Storage Mechanisms

Sediment transport and internal re-deposition was the overall response of the river to both high flows and gravel augmentation. Direct observation, blimp imagery, and topographic change detection of the spatial pattern of re-deposition all confirm that the mechanisms of sediment deposition proposed in section 2.1.1 occurred between January and October 2011. First, blanket filling of the bed within interstitial zones of bed roughness elements such as boulders, shot rock, and bedrock is occurring widespread in the downstream reach. Second and third, large bedrock and boulder protrusions promote deposition both upstream (i.e. "highsiding") and downstream (i.e. "eddying out"). The former was the dominant form of deposition where Chinook salmon spawning was observed; it occurred on the cobble bar just upstream of the big rapid and just upstream of the bedrock outcrop at the top of Sinoro Bar. The latter was evident in the eddies alongside the rapid and downstream of the house-size boulder just downstream of the rapid. As flow converges through the rapid eddy shedding from the rough bedrock boundary occurs pushing sediment outward out of the main zone of flow convergence into topographic nooks. Fourth, curvature of the channel

68

(especially at Sinoro Bar) appears to steer flow and sediment to the outer bend where the sediment gets caught up by the earlier three mechanisms within areas of bedrock variability on river left opposite Sinoro Bar. The bar itself was not sufficiently inundated to receive sediment on the inside of the bed and it is likely that most of its sediment "accommodation space" is full art this point anyway. Finally, at several locations the channel expands (in width and depth), which decreases velocity and causes a general tendency for deposition. Where flow moves straight through these expansions, there are long lines or bands of deposited material.

Erosion from the December 2007 baseline state was primarily limited to areas influenced by large bedrock protrusions that promote convective acceleration around them. The mechanisms for this have been researched and explained by Thompson (2001, 2006, 2007). The largest example of this is at the second bed step in the reach, which is opposite Sinoro Bar (Fig. 27). As constrictions in bedrock channels are agents of pool maintenance this is an expected outcome, but is also difficult to discern whether this change occurred before or after the January 2011 injection. Interestingly, it does appear that some incision occurred in Narrows Gateway from inspection of the new rating curve information but there is also some blanket fill deposition immediately upstream of this area.

It appears that selective filling nooks and crannies among boulders, shot rock, and bedrock fractures is widespread, but difficult to quantify. Another noteworthy point is that is does appear deposition occurred more so on river left before the rapid. At high flow the streamlines go to that side, pushing the sediment there as well. As a result, gravel/cobble gets pushed up against the pre-existing shot rock cobble bar there in sufficient depth to create spawning habitat. This is a positive sign that natural bar growth can occur even with modest amounts of injected gravel in some locations.

6.6.   Habitat Suitability Modeling

6.6.1.   GHSI Bioverification

Given that the majority of the reach still lacks gravel and cobble, the 2D model coupled with the Beak hydraulic HSCs predicted that there is still very little Chinook spawning habitat. Within the areas that gained gravel/cobble substrate, there was an overall small amount of habitat predicted to be available relative to the total wetted area (Fig. 40). At least 90% of the total wetted area was predicted to be non-habitat (GHSI=0) or low quality habitat for each of the six model runs. By excluding areas with GHSI=0 (domain that for this study must be considered as not available for spawning on the basis of no appropriate alluvium), it is possible to determine the distribution of available habitat

quality amongst bins with GHSI>0. Even without the non-available areas, the remaining domain lacks much high quality habitat (Fig. 41).

Comparing the locations of observed redds and the GHSI values there to the 2D model predicted GHSI values for the whole domain, areas predicted to be medium to high quality habitat using the Beak hydraulic HSCs were utilized by adult Chinook spawners preferentially to build redds. Recall that an electivity index (EI) > 1.2 indicates preference, while an EI between 0.5 – 1.2 indicates tolerance and an EI < 0.5 indicates avoidance. The EI analysis found that observed redds had a very strong preference for GHSI bins > 0.4, where for all flows the EI for these areas were >2, except for one that was 1.54 (Fig. 42). This is a similar outcome reported by Pasternack (2008) and in preliminary results for the entire LYR according to the RMT's 2D model study involving bioverification of the Beak hydraulic HSCs using the 2009-2010 and 2010-2011 redd datasets. The Beak HSC perform remarkably and consistently well as predicting the actual locations where Chinook spawn, even in an area where there was no spawning substrate prior to gravel injection and now there is spawning habitat both in terms of substrate and hydraulics. At four flows, the 0.2-0.4 GHSI bin had an EI > 1.2 and at two flows there were ~1. Elkins et al. (2007) reported that prior to habitat rehabilitation Chinook salmon on the lower Mokelumne River were observed to show a similar preference for low quality habitat, but that as rehabilitation progressed over two years, they abandoned that and exclusively used areas with GHSI >0.4. The interpretation from that study was that in the pre-project state, there simply was not enough habitat with GHSI >0.4 for all the fish to use, so they were forced into the marginal 0.2-0.4 GHSI areas. The same thing is likely happening here, because so far the gravel/cobble deficit for the reach is too great to yield enough medium and high-quality habitats for all the spawners to use exclusively. Overall, spawners did not simply use areas that had substrate, but specifically preferred areas where the depths and velocities met the stringent ranges specified by Beak Consultants, Inc. (1989). Consequently, the Beak hydraulic HSCs are now validated for use in all subsequent GAIP monitoring and assessment.
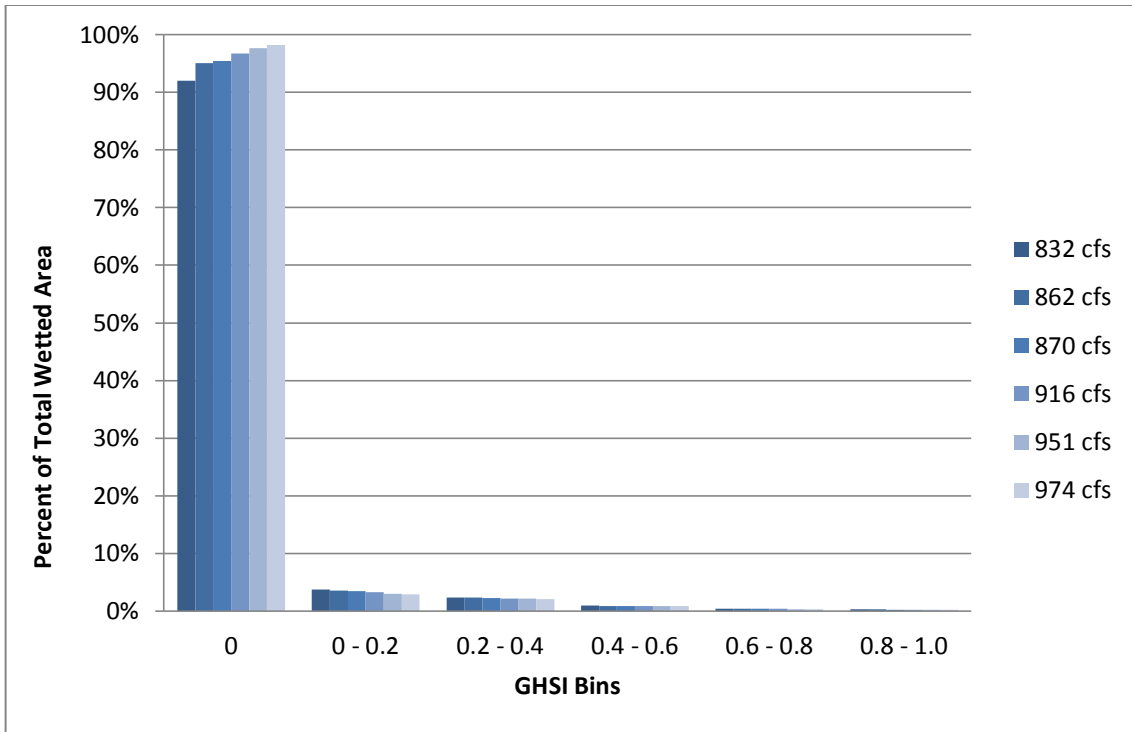
Figure 40. Model predicted GHSI by flow, including 0 values.
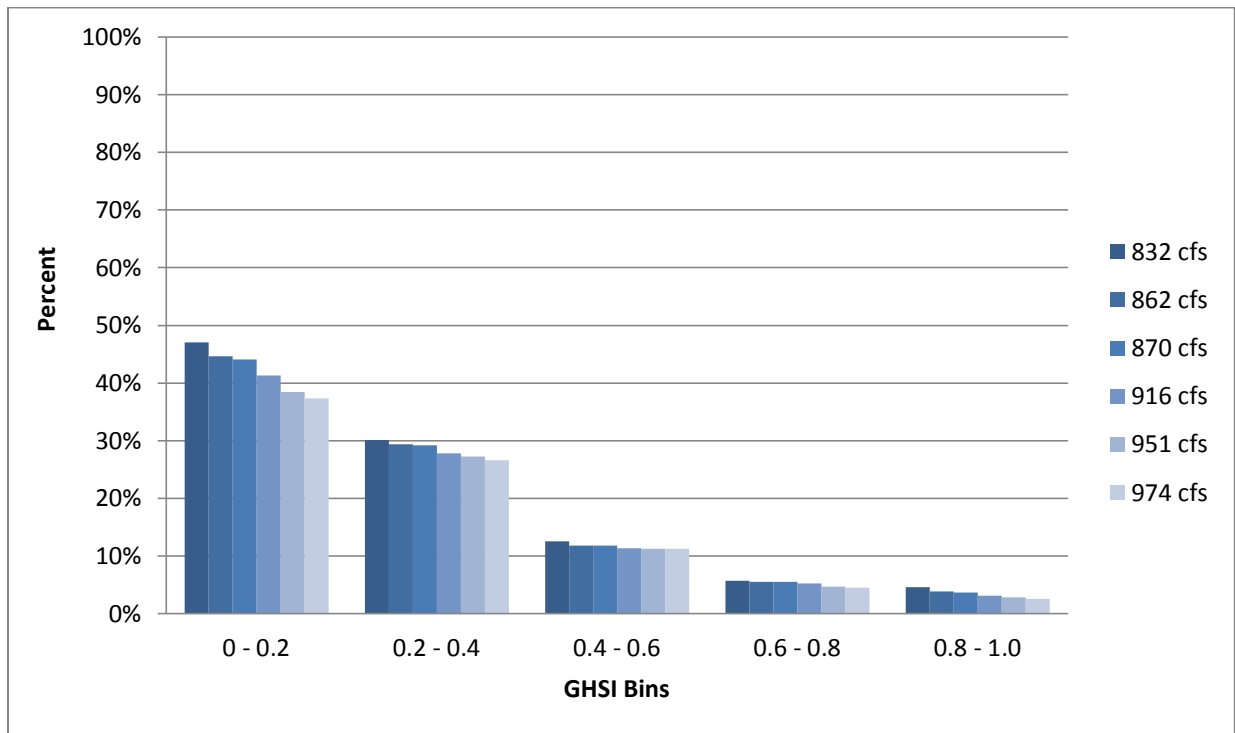
Figure 41. Percent of GHSI for each bin excluding areas of zero physical habitat.
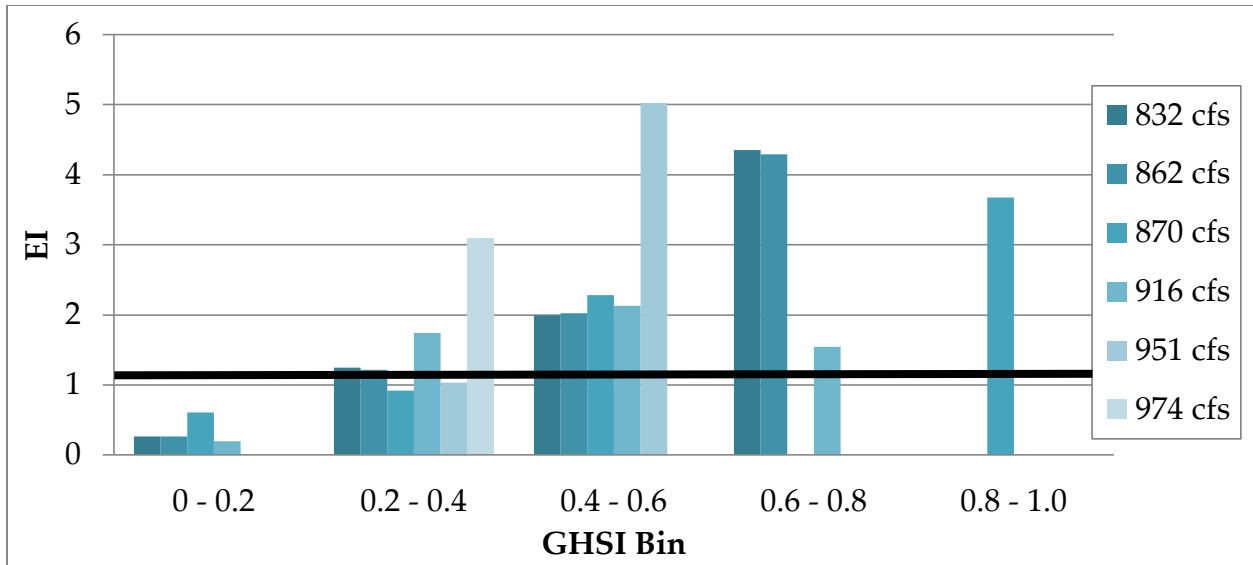
Figure 42. Electivity index (EI) by modeled discharge. Bars above thick black line were preferred by spawners. For the category of 0-0.2, that is excluding values of exactly 0. Therefore, the available area used in calculating EI excluded the vast area with an EI=0, because that would skew the results in exactly the way that makes the forage ratio invalid (i.e. yield such small areas for the non-zero GHSI bins that all GHSI bins would have a high EI).

6.6.2.   2D Model Chinook Spawning Habitat Predictions

To illustrate the overall patterns of DHSI, VHSI, HHSI, and GHSI a series of plots for the 862 cfs evaluation were made (Fig. 43). This discharge was chosen as representative of the other modeled discharges. It can be appreciated that for the DHSI and VHSI rasters, excessive depth limits spawning from a hydraulic perspective (Fig. 43, top); suitable velocity is widespread down the center of the channel (Fig. 43, second from top). In contrast, suitable depths are mostly in a thin band along the channel edges. In addition to depth, it appears that suitable substrate is also a limiting factor as the GHSI (which excludes non-alluvial areas) has a much smaller area than the HHSI accounting for hydraulics alone (Fig. 43). Thus, gravel augmentation is a necessary mitigation to managing physical habitat by causing (1) a reduction in depth by adding sediment storage and (2) providing suitable gravel/cobble substrate.

Analyzing close views of predicted GHSI patterns illustrates observed redds have clustered around patches of model predicted GHSI values > 0.4. For example, at 862 cfs it is evident that all observed redds occurred in areas where the model predicted spawning habitat to be present and to mostly have preferred GHSI values (Fig. 44). For most of the flows analyzed, redds were located in areas of at least low-quality habitat

showing a preference for higher quality habitat when available. In fact, most redds clustered around the loci of highest quality habitat predicted. While only one of six discharges modeled is shown here the overall patterns are nearly identical for these flows.

Two factors could contribute to why observed redds were not exactly on the highest possible predicted habitat. First, the cluster sites are so small in this initial phase of gravel augmentation that there simply is not enough high-quality habitat for all the spawners, so many have to use sub-optimal spots. Second, the mapping-grade Trimble GeoXT GPS units used for recording the geographic coordinates of redds has an accuracy of ~ 0.5 - 2 m (especially considering the blockage of line-of-site with satellites from being in a canyon), which is less than the precision needed for fairly testing the detailed accuracy possible with the 2D model.
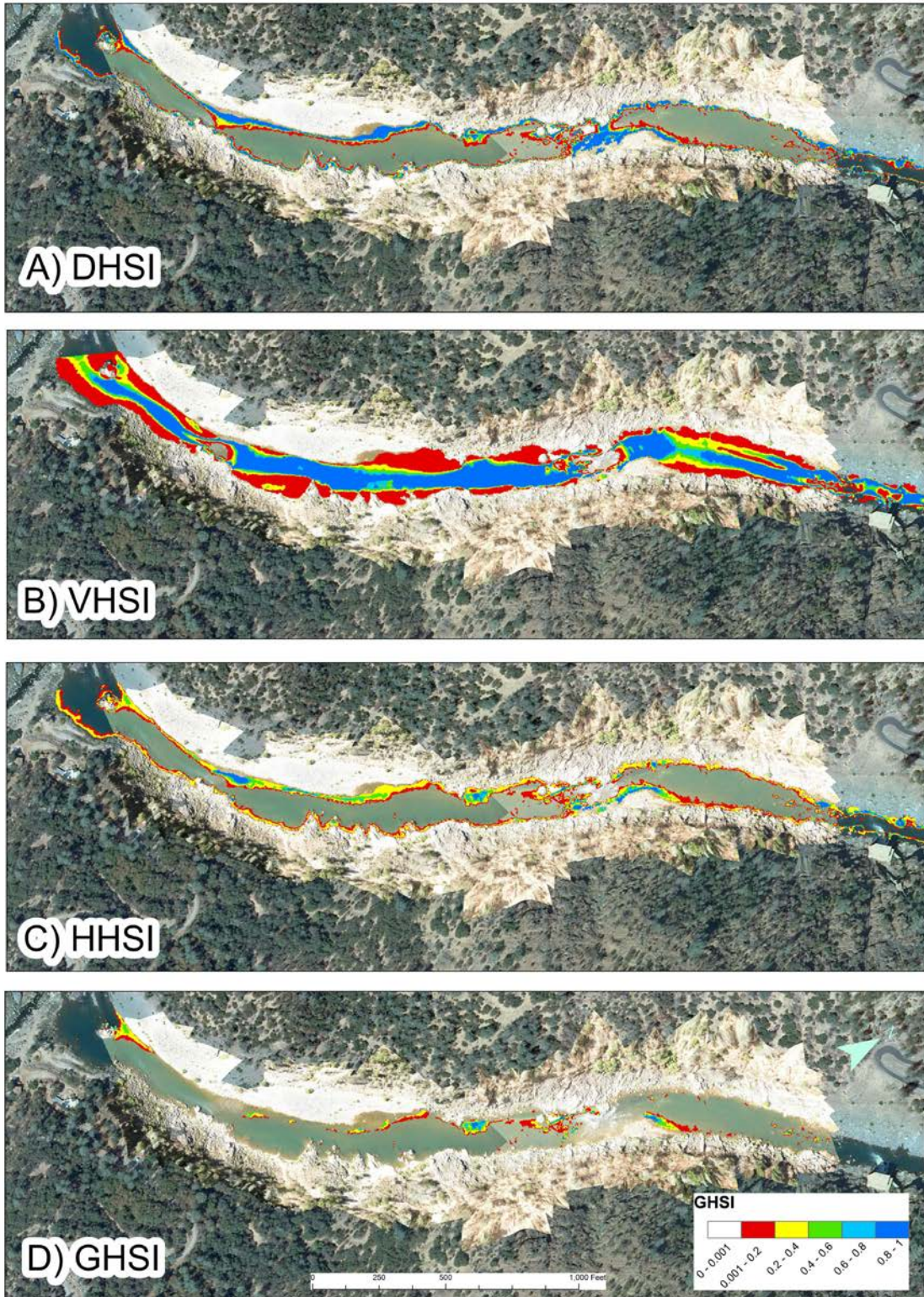
Figure 43. DHSI, VHSI, HHSI, and GHSI predicted by the 2D model for 862 cfs.
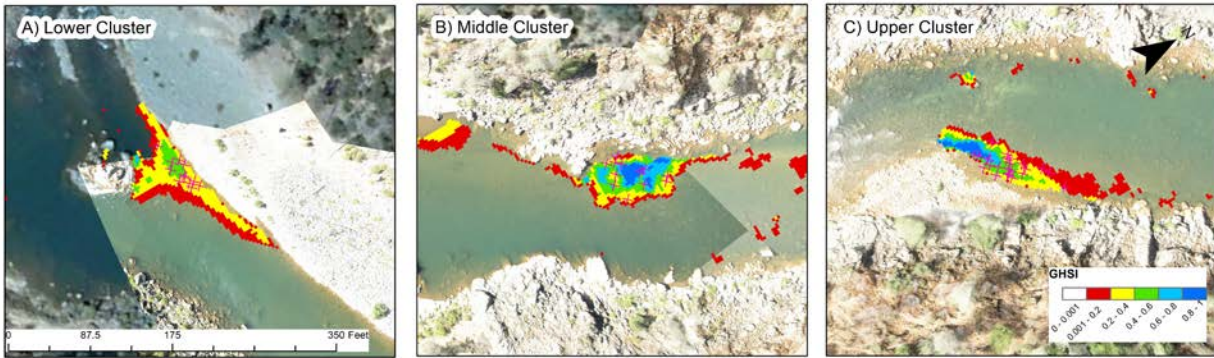
Figure 44. Close views of the GHSI raster for 862 cfs with observed redds shown as magenta colored crosses.

6.6.3. Observed Spawning use and Deposition

Previously in section 6.4, it was reported that all the redds occurred on some newly deposited gravel. The next step in evaluating the deposits was to ascertain how thick they were at the spawning clusters. This is important because for a salmon embryo to emerge from a created redd a number of physical and chemical conditions must be present, including but not limited to, a minimum amount of gravel for egg pocket burial. This can be evaluated by comparing the statistical properties of egg pocket depths with measured deposit thickness. For Chinook salmon, the mean depth of embryo egg pocket is typically about 12" (30.5 cm) (Evenson, 2001). As it turns out, only 10% of redds were made on gravels that met this requirement (Fig. 45). The results of this analysis suggest that while new gravel is being used, most of the deposits are not new material with depths exceeding that needed for average egg burial, which could impact embryo survival. The upper cluster had the deepest deposits that had redds, with a maximum thickness of 1.4' feet. The lower cluster had no new gravel deposits associated with the redds, although from our reconnaissance there were some new gravel in this area, albeit sparse and patchy. Based on these results, we conjecture that the new deposits are attracting the spawners, but may not be as thick as needed or desired for optimal embryo survival and fry production. Considering that this first injection only met ~8% of the gravel/cobble deficit for the reach, this outcome is not surprising. Substantially more of the deficit will have to be addressed before deep and resilient spawning sites are available at downstream locations.

75
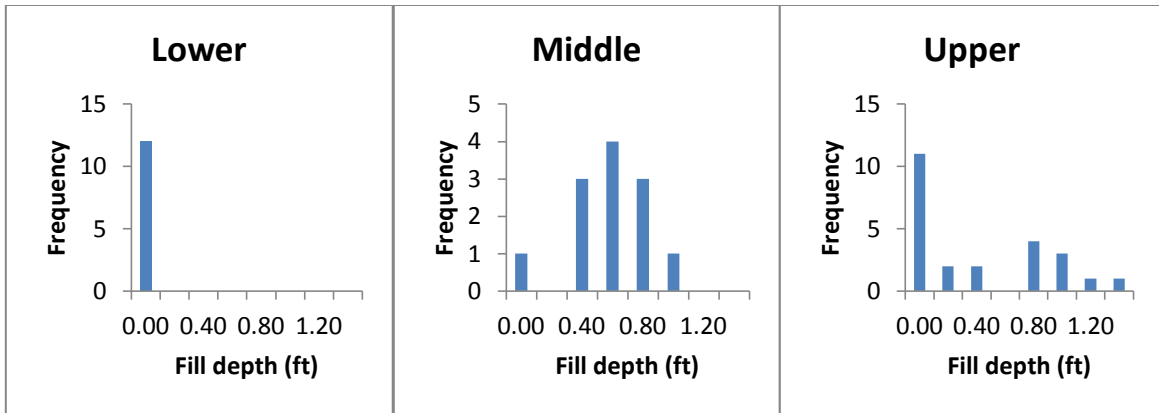
Figure 45. Histograms of deposition detectible using TCD with DoD uncertainty analysis associated with observed redd clusters. X-axis values are left edges of bins.
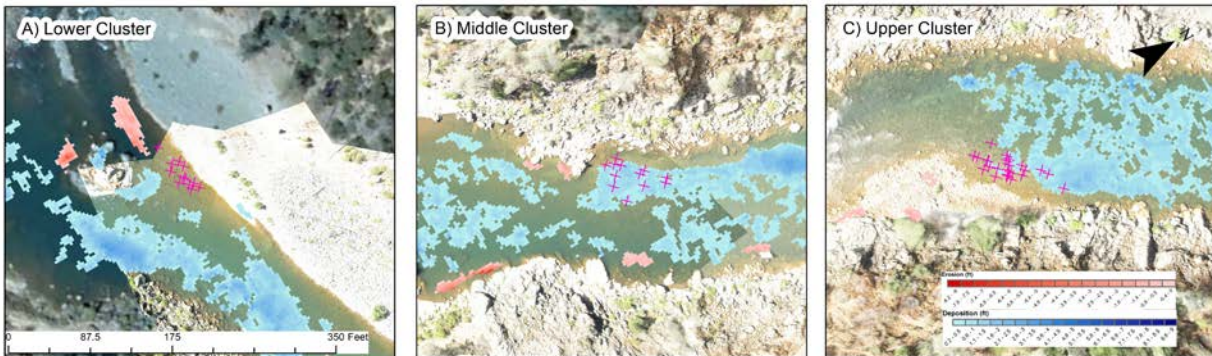
Figure 46. Close-up views of spawning redds (X's) with final adjusted DoD values shown (red is erosion, blue is deposition) for the a) lower, b) middle, and c) lower spawning clusters. Even though all redds occurred on injected sediment, in some locations the thickness was too low to be discernible using TCD and accounting for DoD uncertainty.

6.6.4. Redd proximity analysis

The next step was to test hypothesis 3 of the GAIP, which states that structural refugia in close proximity to spawning habitat should provide resting zones for adult spawners and protection from predation and holding areas for juveniles. As illustrated in Figure 43, deep pools for adult holding are widespread in proximity of all three clusters and are dominantly abundant throughout EDR. The primary resting and rearing refugia in close proximity to red clusters consisted of complex banks bedrock protrusions, boulders, and large cobble (Fig. 47). Bedrock and boulders were observed to provide

local shading. Little riparian vegetation was along the banks of the baseflow channel, which is not surprising considering the duration of flood flows in 2011. None of the clusters were associated with large streamwood, but there is abundant large streamwood in EDR further up the banks on both sides of the river that is outside the wetted width of spawning flows.
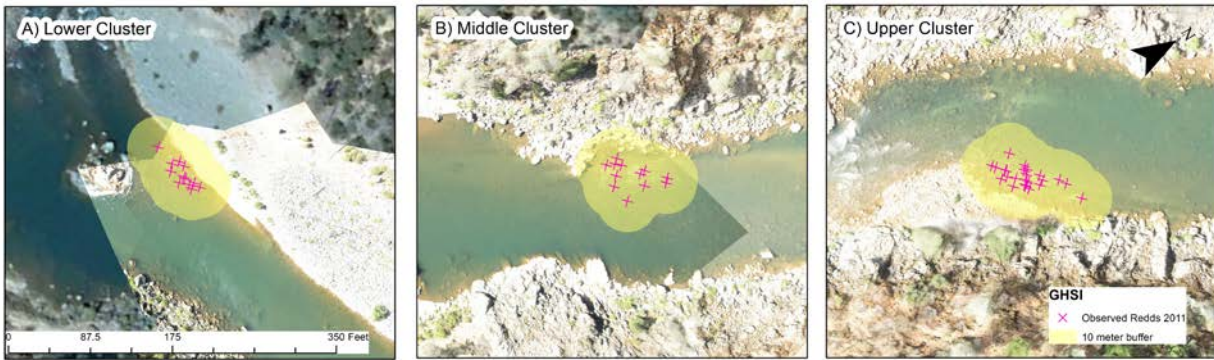
Figure 47. 10-m buffers around the redds in the three clusters.

7.0   GAIP Hypothesis Testing Evaluation

In this section succinct evaluations of the outcome of the 2011 gravel augmentation relative to the GAIP hypotheses are presented.

7.1.   Hypothesis 1 - Total Sediment Storage Should Be At Least Half of the Volume at the Wetted Baseflow

In the first GAIP-related gravel injection, ~8% of the estimated minimum deficit was addressed. Despite a wet year in 2011 with several floods, TCD was able to detect all of the injected material in EDR. There is no evidence that any measurable amount of injected material left EDR. The fact that TCD yielded a ~10% net surplus of sediment is not surprising given the roughness of the bedrock/shotrock topography. In both this evaluation as in the 2009 evaluation of the 2007 injection (Pasternack, 2009), it was found that some amount of sediment is infiltrating into the bed roughness. Because the GAIP's estimate of total volume inges on the 2007 topographic map, which does not fully capture the available roughness-scale storage capacity of the bed, the estimate based on the half-volume at wetted baseflow perhaos should be viewed as the minimum total deficit. No final conclusion about hypothesis 1 will be attaininable until enough sediment has been injected to yield sizable alluvial morphological units that are not hiding behind or highsiding in front of obstructions.

7.2. Hypothesis 2

7.2.1. Hypothesis 2a - SRCS Require Deep, Loose River Rounded Sediment for Spawning

River-rounded gravel and cobble were added to the EDR bedrock/shotrock river corridor. In years prior to adding any gravel, the corridor was devoid of salmon spawning. Chinook were observed attempting to spawn on bedrock. After a pilot gravel/cobble addition in 2007 and again after the GAIP-related addition in 2010-2011, Chinook were attracted to the new material and used it to construct redds. In the EDR since 2007, spawning only occurs on injected gravel/cobble. These are strong indications in support of the hypothesis. More than 10 times more sediment needs to be added before the full benefit will be attainable.

7.2.2. Hypothesis 2b - Spawning Habitat Should Be As Close To GHSI High Quality Habitat as Possible

This study found that 2D model predicted patches of medium and high quality GHSI were utilized by spawners in far greater occurrence than their areal availability, indicating a strong nonrandom preference. Low quality areas were preferred at some discharges, but not others, indicating that demand for spawning habitat far exceeds supply. Very poor quality areas were avoided by spawners as were non-habitat areas. These results bioverify the use of LYR habitat suitability curves produced by Beak Consultants, Inc (1989) for California Department of Fish and Game using the method of non-parametric tolerance limits. Every test of these HSC on the LYR has confirmed their strong predictive ability.

Rehabilitation of the lower Mokleumne River below Camanche Dam showed that as more medium and high quality habitat availability was provided, spawners shifted their usage pattern to avoid low quality habitat and only prefer medium and high quality habitat (Elkins et al., 2007). The same pattern is expected once enough gravel is added that the availability of medium and high quality habitats are not limited. It will take time to get enough sediment into the canyon to reach this potential.

Most importantly, the findings confirm that spawners do not merely require gravel addition, but that preferred depths and velocities are also requisite for spawning to occur. Many areas where floods deposited gravel as a blanket fill were simply too deep to be desired by Chinook spawners. Thus, it appears reasonable to continue to focus on using gravel addition to create habitat that is as close as possible to high quality GHSI as represented for the LYR.

7.3. Hypothesis 3 – Structural refugia in close proximity to spawning habitat should provide resting zones for adult spawners and protection from predation and holding areas for juveniles.

All observed redds were located within 10 m of structural refugia such as overhanging bedrock and large boulders. The redd clusters were within ~ 20 m of deep pools. In 2012 the RMT began conducting snorkel surveys of fry and juveniles in EDR. They have found plenty, and they have even found them upstream of the first red cluster, indicating that these small fish are able to move against the flow and find preferred areas upstream, if they wish. EDR has ample adult holding habitat and sufficient fry rearing habitat for its needs, so the key deficiency is spawning habitat. There is no reason to expect a steep, narrow canyon to be the primary rearing region for the fish produced there. Downstream slackwater, swale, and floodplain habitats are the regions of primary anticipated growth prior to outmigration.

7.4. Hypothesis 4a - Designs Should Promote Habitat Heterogeneity and Provide Habitat for All Species and Life stages

Presently there are no large alluvial deposits in EDR with homogenous hydraulics. Gravel addition is at too early of a stage to worry about excessive homogeneity of spawning riffles. There remains ample complexity of bedrock landforms along the banks and deep pools throughout the reach.

7.5. Hypothesis 5a - There are no mechanisms of riffle-pool maintenance in the EDR and it is not feasible in this section of the river

The presence of bedrock, lack of alluvium from Englebright Dam, and history of anthropogenic activities prohibit the presence of archetypal free-formed riffle pool units such as those found in the Lower Yuba River. Despite this, evidence of forced riffle-pool scour and maintenance associated with bedrock was observed in the EDR located ~600 feet upstream of the Narrows Gateway. It remains to be seen whether mechanical rehabilitation of Sinoro Bar, shot rock removal, and continual gravel augmentation makes this process more widespread within the EDR and whether this will maximize SRCS habitat and its stability.

7.6. Hypothesis 5b - Flows overtop Englebright Dam and erode placed sediments

Consistent with earlier 2D hydrodynamic modeling and site observations, high flows do have the ability to erode placed sediments and transport them through the EDR. The injected gravel was smaller than commonly found on the LYR, so erosion risk is

higher. However, no sediment was observed to leave EDR despite several floods of moderate duration. Eventually some sediment will leave the reach, but it should be possible to add enough gravel/cobble annually to keep up with losses and rebuild alluvial landforms. It would help if the sediment was not sized for the low-flow Stanislaus River, but was properly designed for the larger, steeper, and less flow-restricted LYR. Such a change to the gravel/cobble mix is underway for future additions.

8.0   Annual Volume and Placement Design

8.1.   Gravel Placement Design Development

Under the current augmentation implementation approach the contouring of gravel features at the injection site is problematic and of questionable value. First, the site is relatively inaccessibility to heavy equipment without significant disturbance that was deemed unacceptable in the Environmental Assessment. Second, the sluice pipe is rigid, heavy, and difficult to position. There is a strong preference by the operations contractor to inject as much material as possible into the fewest spots as possible and allow flow to redistribute the sediment in the form of a blanket fill. Innovations can be expected to increase the capabilities for more controlled gravel injection over time. Third, the gravel mixture contains too many fine sizes by design to promote landform development and stability, because it is based on standards from a very different and inappropriate river to use as a baseline reference. A new coarser mix has now been developed to replace that, but sluicing may have limited capacity to get in the larger structural cobbles that would help hold a landform together. That will be evaluated in the next placement project. Finally, even if an appropriate gravel/cobble mix could be perfectly placed according to a design, the fact is that the canyon is too narrow at the injection site to yield sustainable spawning riffles there that can survive right there in the face of floods. That is not saying that gravel/cobble injection in EDR as a whole is unsustainable, but just that the injection site itself is a transport corridor, not a depositional zone. The primary benefit of this injection location is that it promotes downstream distribution of the sediment throughout EDR, but that is also its limitation. Every effort will be made to place sediment there to obtain a temporary spawning landform for the first spawning season after injection (when injection is done in the summer), but there should not be expectations for the landform to persist. Once there is enough alluvium throughout EDR, this will be inconsequential as the injection site can serve purely as a location for gravel injection and then pre-existing spawning habitat landforms in the downstream sections of the river will be sustained by the injections.

8.2. Annual Injection Volume Assessment

The project is still in an early phase of rapid learning and adaptation. Several enhancements to the system and to the gravel mix are planned for the next project. It is necessary to determine how all the enhancements function to determine the final efficiency of the system with best practices.

Ultimately, gravel/cobble sluicing has maximum efficiency possible for EDR and once that is determined then the only way to add more gravel is to extend the period over which sluicing may be operated. Commonly, regulators limit gravel/cobble augmentation projects for anadromous salmonids in California to a narrow period of roughly July to mid September (sometimes less). For the EDR, when all injected sediment exports from the injection zone and moves downstream, there is no reason why gravel sluicing cannot occur any time year round. Regulatory agencies are most comfortable with the pre-specified period, but the first injection in 2010-2011 was outside that period and no one indicated any problems.

With a remaining deficit of at least 58,000 short tons, the minimum time to completion of erasing the reach's sediment deficit time with annual injections of 5,000 short tons is 12 years. If it is found to be feasible to inject 10,000 short tons per year, then the minimum remaining deficit could be addressed in 7 years (considering that 2012 is likely to be a 5,000 short ton addition). If efforts with 10,000 short tons are tested and found to be feasible either in the existing period or in an expanded period, then it might be appropriate to test a 15,000 short ton injection. However, that amount would very likely require an expanded period to be achievable, so that regulatory constraint would have to be addressed first. If the sequence of injection was 5,000 in 2012, 10,000 in 2013, and then 15,00 thereafter, then the deficit could be addressed in 5 years.

9.0   Lessons Learned

9.1.   Gravel Sluicing Operations

Prior to performing the 2010-2011 gravel/cobble injection there was substantial uncertainty about the potential effectiveness of the gravel sluicing method for a moderately sized, remote canyon. A key outcome of the project was that gravel sluicing can work just fine in this setting. During the first two weeks participants were highly creative in problem-solving myriad minor glitches. The sluice pipe did clog and break from time to time, but as a whole the system was resilient and effective. After the project was done, many ideas were developed to make further improvements, and these ar eebing implemented in the second effort that is forthcoming. For example, Seam W. Smith provided a lsit of the following sluicing enhancements to be used in the

future to alleviate the likelihood and frequency of clogs, among other things (the text below is modified paraphrasing from his email):

a. Positioning the Rock Hopper much further down the sluice pipe at the switchback in the road where the sluice pipe leaves the road and heads down the steep slope to the river. This is anticipated to significantly increase overall sluicing efficiency by:
    a. Limiting the friction wear sections of the pipeline to the lower section from the re-positioned Hopper at the lower bend to the River.
    b. Increasing the gradient of the rock delivery end of the system thereby eliminating 99 % percent of all rock jams that occurred on the upper moderate gradient section. (The faster the rock moves through the system along with higher flow velocity, the better)
b. Condensing the crew closer together will make down time more productive. For example, when adding pipe sections in-stream, the Rock Hopper tender can quickly add additional support to River Crew.
c. Re-positioned Rock Hopper Tender in full view of River Crew will provide safe communications and vantage point in identifying problems before they occur.
d. The Rock Hopper system will also need to undergo a few changes to accommodate operation from the lower bend location:
    a. Removing the 6-Inch "Y" section for direct connect to the 8-Inch Certa-Lok™ Yelomine pipe.
    b. Installing an 8-Inch inline Bray Series 31 H Valve with shut-off stem positioned adjacent to the Hopper cat-walk.
    c. Installing an 8-Inch anti-siphon valve at the top of the hill adjacent to pipe road crossing apparatus.
e. Several miscellaneous river specific rigging issues are being improved
    a. Making available more metal tripods to hold the pipe on shore and in the river
    b. Using a strong cableway across the river to support rafts and possibly even a raft barge/bridge. These will float over the swift current and hold the sluice pipe in place there. The barge would enable the River Crew to walk across the flow and quickly adjust the location of the outflow.

9.2.   Enhanced Yuba-specific Gravel Mix

The original gravel specification for the GAIP (and the preceding 2007 pilot injection)

dates back to discussions among participants of the Lower Yuba River Technical Working Group in 2006 that resulted in the recommendation made by the USFWS to adopt the gravel mix from the lower Stanislas River for use on the lower Yuba River (Table 14). The mix includes a high fraction (> 42.5%) of sizes <32 mm. Prior to the 2010-2011 project, there was insufficient information to conclude whether this mix design was appropriate or not. However, by now substantial evidence has led to the conclusion that the Stanslas mix design is not appropriate for the LYR and should be discontinued.

Two key studies provide a new scientific understanding pointing toward significantly larger sizes being necessary in the mix design. The first is Moir and Pasternack (2010), which reported that Chinook salmon spawning in Tumbuctoo Bend on the LYR have elastic preferences for spawning sizes that are quite wide and hinge strongly on the available hydraulics. That study found that the median size of utilized substrates ranged between 58-94 mm, with D_{84} (the size that 84% of substrate is finer than) values ranging between 121-182 mm. The median size range of redd tailspills at these sites was 29-80 mm. Most interestingly, substrate size use showed strong interdependence with velocity. Chinook used smaller substrates when current was slow and larger substrates when it was fast. More recently, the RMT conducted a riverwide weekly census of utilized spawning substrate sizes at Chinook redds during the spawning season in 2009-2010 and 2010-2011. These data confirm the results of Moir and Pasternack (2010) for the whole river and show that the LYR needs a coarser mix than that designed for the Stanslas. Specifically, whereas the Stanslas mix design has >42.5 % of material < 32 mm, census-wide observations on the LYR found that in fact only 19 % of material was < 32 mm (Table 15). At the other end of the spectrum, the Stanslas mix design includes only 2.5 % of the material as sizes >102 mm and 0 % > 127 mm, while on the LYR spawning sites had >11 % of material > 126 mm.

Although there is a strong regional scientific consensus that a predominance of large cobbles can result in excessive porosity allowing embryos to wash away, the Stanislaus mix design goes too far in completely eradicating the structural framework sizes necessary to holding alluvial landforms together. The LYR is a gravel/cobble-bed river, not a gravel-bed river. Like the use rebar in concrete as a reinforcing agent, large cobbles in an alluvial landform help hold the mix together. Also, large cobbles break up the log-velocity profile near the bed, yielding refugia against the current, and maintain proposity necessary for fry rearing and reoxygenation of egg pockets in the substrate.

Observations of the deposits in EDR since 2007 have found that the sediment merely fractionates into two populations by the mechanisme of hydraulic sorting, so the notion that the Stanislas mix stays together has been proven incorrect. Spawning observed in 2008-2011 on the seidment injected in 2007 has been entirely on the residual large size

fraction of cobbles left behind just downstream of the injection area at Narrows II. The finer fraction of gravel washed down throughout the reach. For the 2010-2011 injection, grain size results found that once again the substrate fractionated and is hydraulically sorting downstream, but at least this time the quantity injected meant that deposits yielded large enough landforms for some Chinook spawning. Still, the substrate sizes of these deposits are significantly smaller than preferred throughout the LYR.

Despite the usage of large cobbles and small boulders at spawning sites in the LYR, it is not feasible to put particles >128" through the gravel sluice. In discussion with Sean W. Smith (the gravel-sluicing contractor), a new mix design was developed to reflect Yuba-preferred spawning conditions while still being achievable with gravel sluicing (Table 16). The size fraction of < 32mm gravels has been reduced to the same 20% as observed on the river. Meanwhile, the majority of the material will be in the gravel/cobble size range of 32-90 mm. Finally, an effort will be made to put in up to 30 % of sizes 90-128 mm.

Because the new mix design involves coarser particles, there is uncertainty about gravel-sluice performance. Operational performance was good during the 2010-2011 injection, and numerous enhancements to sluicing are underway that should significantly increase efficiency and help accommodate the abundance of larger particles. Nevertheless, it would be wise to take a cautious approach during the initial loads and then gain experience with coarsening the mix operationally. A strategy for this has been developed in contractual language for the next gravel injection.

Table 14. Original gravel/cobble mix design in the GAIP.

Size class (mm)	Size class (in)	% retained	Fractional %
102-127	4 to 5	0 - 5	2.5
51-102	2 to 4	15 - 30	20
25-51	1 to 2	50 - 60	35
19-25	¾ to 1	60 - 75	15
13-19	½ to ¾	85 - 90	15
6-13	¼ to ½	95 - 100	10
<6	< ¼	100	2.5
*Based on Stanislaus River expert opinion			

Table 15. Observed 2010-2011 LYR redd substrate composition.

Size class (mm)	Size class (in)	% retained	Fractional %
>256	>10	0.87	0.87
128-256	5 to 10	11.15	10.28
90-128	3.5 to 5	41.34	30.19
32-90	1.25 to 3.5	81.31	39.97
2-32	0.08 to 1.25	99.47	18.16
<2	<0.08	100	0.53

Table 16. Planned 2012 gravel/cobble mix design.

Size class (mm)	Size class (in)	% retained	Fractional %
90-128	3.5 to 5	30	30
32-90	1.25 to 3.5	80	50
19-32	¾ to 1.25	88	8
13-19	½ to ¾	96	8
6-13	¼ to ½	100	4

9.3. Gravel/Cobble Sourcing

Scientific requirements and concerns for sourcing of gravel and cobble for the GAIP was never formally addressed in the GAIP. That occurred because sourcing was previously discussed by participants of the Lower Yuba River Technical Working Group in meetings in 2006 and a consensus was reached by all involved, including agency staff at USFWS, NMFS, and CDFG. However, since then staff have changed and a broader community has become concerned with a variety of geomorphic and sedimentary issues in the EDR. As a result, it is important to clarify gravel/cobble sourcing.

The lower Yuba River valley has hundreds of millions of tons of hydraulic mining alluvium, which is composed of all sizes of sediment from clay to boulder. Apart from a few remnant sedimentary high terraces that pre-date hydraulic mining and a very small contribution from Dry Creek downstream of Virginia Ranch Dam, virtually all sediment in the LYR corridor is hydraulic mining alluvium. Therefore gravel/cobble supply for the GAIP that is going to come from within the basin is going to come from hydraulic mining alluvium.

Much land in the river corridor is owned by commercial suppliers of aggregate. Individual commercial suppliers can extract hundreds of thousands to millions of ton of alluvium per year for different commercial purposes. To gain an understanding of the

suitability of the hydraulic mining alluvium as a starting source for further processing to obtain the final gravel/cobble mixture for the GAIP, it is helpful to read statements from the commercial suppliers in the LYR (without endorsing any):

"Teichert's Hallwood Plant has actively operated in the Yuba Gold Fields since 1953 and offers examples of modern active gravel mining techniques, equipment, and award-winning active and complete mine reclamation." (http://reclaimingthesierra.org/teichert-materials/)

"SRI operates year round, and mines some of the world's finest aggregate from the Yuba Gold Fields in Yuba County. The chemical and physical characteristics of the Yuba Gold Fields resource enables us to manufacture multi-functional products. One of the most unique aspects of this reserve is the full spectrum size range (diameters) of quality aggregate, and the wide variety of reserves available from a single source… we conduct our own state-of-the-art washing, screening, drying, grading, and packaging operations" (http://www.sri-sand.com/)

To be perfectly clear, there is no intent to scoop up raw hydraulic mining alluvium and dump it "as is" into EDR. The raw LYR alluvium is the starting source, but then the material must be washed, screened, and graded according to common best practices for gravel augmentation and as required by water quality permitting and other regulatory requirements. It has been demonstrated in this study that Chinook spawners intensively use the injected sediment. There appears to be no aversion of spawners to utilize the injected mix.

10.0 Conclusions

The purpose of this study was to evaluate the status of the EDR and the efficacy of past gravel injections into the EDR with regard to making progress toward meeting the geomorphic and ecological goals stated in the GAIP. By design, ~5,000 short tons of gravel and cobble was to be added into the EDR just downstream of the Narrows 1 powerhouse, filling no more than 8 % of the reach's coarse sediment deficit. Gravel sluicing was a successful method of gravel/cobble addition with extremely low environmental impact compared to other methods. It is recommended that gravel sluicing be continued as the preferred method to implement the GAIP, with new enhancements to the method being tested as oppportunities arise.

During and after injection was completed, there were several overbank floods, including peaks of 19,000, 11,400, 19,500, 13,700, 11,200, and 8,000 cfs. December 2010 was the 6th wettest month out of the 103-year precipitation record at the Colgate powerhouse upstream. In June and July 2011, an overbank flood had a sustained duration of one month (Fig. 5). Consequently, there was no opportunity to evaluate Chinook spawning utilization at the injection zone and ample opportunity to evaluate

sediment transport dynamics and creation of Chinook spawning habitat downstream.

Analysis of sediment distribution in a remote canyon is not easy, but this study used state-of-the-art methods of topographic change detection account for uncertainty in digital elevation models and the propagation of that uncertainty through DEM differencing. According to the resulting sediment budget, all of the measurable amount of gravel/cobble injected in the EDR stayed in the EDR, despite the moderate flood peaks and long flood durations. It is likely that the sediment will transport out of the reach eventually, which is why the GAIP calls for adding sediment annually to match losses after the initial sediment deficit is eradicated.

This study found that the mechanisms of sediment deposition in the EDR canyon are myriad as hypothesized in Table 2. In this initial injection, local hiding spots consisting of bedrock/shotrock nooks and crannies absorbed some sediment, larger obstructions captured some sediment in their upstream stagnation zone and their downstream eddy zone, and flows of different magnitudes interacted with stage-dependent channel geometric variables to steer sediment into different depositional locations. Covariance analysis proved useful at illuminating the relative roles of detrended riverbed undulations as well as channel and valley width undulations in determining where sediment deposited. At this time there are still ample locations in EDR for sediment to be stored, so continued implementation of the GAIP is recommended.

Despite the initial nature of the injection and its small total volume, gravel/cobble did deposit downstream where none existed before and Chinook spawners utilized those new landforms. This is the same outcome as occurre din the smaller 2007 gravel/cobble pilot injection. Bioverification analysis with 2D modeling and CDFG/Beak habitat suitability curves revealed that Chinook spawners heavily utilized and preferred medium and high quality hydraulic habitat on those depositional landforms (Fig. 42). There were many more spawners seeking to utilize those sites than there was space to meet their demand, demonstrating the importance of continued gravel addition.

Chinook spawning habitat is something that occurrs on top of alluvial landforms, and for the lower Yuba River the ones that are preferred more than random likelihood are riffles, riffle transitions, and runs (RMT, unpublished analysis). When gravel is injected into a reach and distributed downstream, the potential for creating such features depends on the volume added compared against the sediment deficit as well as the topographic structure of the channel. In this initial injection, no more than 8 % of the gravel deficit was met, so there is no reason to expect that a large amount of habitat would be created. Landform creation and spawning habitat utilization is a highly nonlinear phenomenon in terms of the amount of utilization that occurs per unit of gravel added (Elkins et al., 2007), because a small addition on top of a degraded alluvial landform will yield dramatically more habitat than a large addition at the bottom of a

deep bedrock pool that is non-habitat. Consequently, appropriate caution must be used in devising utilization metrics and extrapolating in time or space. Calculating the number of spawners served per ton of gravel added and extrapolating from that ratio is scientifically invalid.

Overall, gravel/cobble injection by gravel sluicing is working in that the sediment is getting added to the channel, it is moving downstream and creating landforms in the river, it is staying in the canyon for now (helping to reduce the sediment deficit), the hydraulics over the created landforms includes medium and high quality habitat that is preferred for spawning more than random likelihood, and Chinook spawners are making use of that habitat. Section 7.0 draws on the data and analyses to report on the outcomes of GAIP hypothesis testing. At this time there is no need to modify the GAIP, as the results of the study support the hypotheses. Annual gravel/cobble addition should continue as permitted and the interim outcomes monitored until the sediment deficit is eradicated. At that point, the long-term plan in the GAIP should commence.

11.0 References

Barker, J.R., Pasternack, G.B., Bratovich, P., Massa, D., Wyrick, J.R., Johnson, T.R. submitted. Rapid, Abundant Velocity Observation to Validate Million-Element 2D Hydrodynamic Models. Journal of Hydrology.

Brown, R. A. and Pasternack, G. B. 2008. Engineered channel controls limiting spawning habitat rehabilitation success on regulated gravel-bed rivers. Geomorphology 97:631-654.

Brown, R. A. and Pasternack, G. B. 2009. Comparison of Methods for Analyzing Salmon Habitat Rehabilitation Designs For Regulated Rivers. River Research and Applications 25:745-772.

Campos, Casey And D Massa.2012. Redd Monitoring And Mapping In The Englebright Dam Reach Of The Lower Yuba River, Ca. Summary Report September 12, 2011 – December 19, 2011. Prepared For The U. S. Army Corps Of Engineers. February 28, 2012

Carley, J. K., Pasternack, G. B., Wyrick, J. R., Barker, J. R., Bratovich, P. M., Massa, D. A., Reedy, G. D., Johnson, T. R. submitted. Accounting for uncertainty in topographic change detection between contour maps and point cloud models. Geomorphology.

Elkins, E. E., Pasternack, G. B., and Merz, J. E. 2007. The Use of Slope Creation for Rehabilitating Incised, Regulated, Gravel-Bed Rivers. Water Resources Research 43,

W05432, doi:10.1029/2006WR005159.

Heritage, G.L., Milan, D. J., Large, R.G., Fuller, I.C. 2009. Influence of survey strategy and interpolation model on DEM quality. Geomorphology 112, 334-344.

Ivlev, V.S. 1961. Experimental ecology of the feeding of fishes. Yale University press, New Haven, CT.

Lowe, D.G. 2004. Distinctive image features from scale-invariant keypoints. International Journal of Computer Vision 60 (2), 91-110.

MacWilliams, M. L., Wheaton, J. M., Pasternack, G. B., Kitanidis, P. K., Street, R. L. 2006. The Flow Convergence-Routing Hypothesis for Pool-Riffle Maintenance in Alluvial Rivers. Water Resources Research 42, W10427, doi:10.1029/2005WR004391.

Pasternack, G. B. 2011. 2D Modeling and Ecohydraulic Analysis. Createspace: Seattle, WA.

Pasternack, G. B., Wang, C. L., and Merz, J. 2004. Application of a 2D hydrodynamic model to reach-scale spawning gravel replenishment on the lower Mokelumne River, California. River Research and Applications 20:2:205-225.

Pasternack, G. B., Gilbert, A. T., Wheaton, J. M., Buckland, E. M. 2006. Error Propagation for Velocity and Shear Stress Prediction Using 2D Models For Environmental Management. Journal of Hydrology 328:227-241.

Pasternack, G. B. 2009. Current Status of an On-going Gravel Injection Experiment on the Lower Yuba River, CA. Prepared for the U.S. Army Corps of Engineers.

Pasternack, G. B. 2010. Gravel/Cobble Augmentation Implementation Plan (GAIP) for the Englebright Dam Reach of the Lower Yuba River, CA. Prepared for the U.S. Army Corps of Engineers.

Pasternack, G. B. and A.E. Senter. 2011. 21st Century instream flow assessment framework for mountain streams. California Energy Commission, PIER. CEC-500-XXXX-XXX.

Pasternack, G. B., Fulton, A. A., and Morford, S. L. 2010. Yuba River analysis aims to aid spring-run Chinook salmon habitat rehabilitation. California Agriculture 64:2:69- 77.

Sawyer, A. M., Pasternack, G. B., Merz, J. E., Escobar, M., Senter, A. E. 2009. Construction constraints on geomorphic-unit rehabilitation on regulated gravel-bed rivers. River Research and Applications 25:416-437.

Thompson, D.M., 2001. Random controls on semi-rhythmic spacing of pools and riffles in constriction-dominated rivers. Earth Surface Processes and Landforms 26, 1195–

1212.

Thompson, D.M., 2006. The role of vortex shedding in the scour of pools. Advances in Water Resources 29, 121–129.

Thompson, D.M., 2007. Turbulence characteristics in a shear zone downstream of a channel constriction in a coarse-grained pool. Geomorphology 83, 199–214.

Wheaton, J. M., Pasternack, G. B., and Merz, J. E. 2004. Spawning Habitat Rehabilitation - 1. Conceptual Approach & Methods. International Journal of River Basin Management 2:1:3-20.

Wheaton JM, Brasington J, Darby SE and Sear D. 2010a. Accounting for Uncertainty in DEMs from Repeat Topographic Surveys: Improved Sediment Budgets. Earth Surface Processes and Landforms. 35 (2): 136-156. DOI: 10.1002/esp.1886

Wheaton JM, Brasington J, Darby SE, Merz JE, Pasternack GB, Sear DA and Vericat D‡. 2010b. Linking Geomorphic Changes to Salmonid Habitat at a Scale Relevant to Fish. River Research and Applications.26: 469-486. DOI: 10.1002/rra.1305.

Van Asselt, M. B. A., and J. Rotmans. 2002. Uncertainty in integrated assessment modeling—from positivism to pluralism. Climatic Change 54:75–105.